이학박사학위논문

# Molecular Identification of Voltage-gated $K^+$ Channels Responsible for Electrophysiological Characteristics in Hypothalamic Paraventricular Nucleus Neurons

## 시상하부 뇌실곁핵 세포의 전기생리학적 활성을 조절하는 전압의존성 $K^+$ 통로의 분자생물학적 특성

**2014년 8월**


서울대학교 대학원

협동과정 뇌과학전공

이 슬 기

**Doctoral Thesis**

# Molecular Identification of Voltage-gated $K^+$ Channels Responsible for Electrophysiological Characteristics in Hypothalamic Paraventricular Nucleus Neurons

**Seul Ki Lee**

Academic advisor: Pan Dong Ryu, DVM, PhD

Interdisciplinary Program in Brain Science
Graduate School
Seoul National University

August 2014

# Molecular Identification of Voltage-gated $K^+$ Channels Responsible for Electrophysiological Characteristics in Hypothalamic Paraventricular Nucleus Neurons

시상하부 뇌실곁핵 세포의 전기생리학적 활성을 조절하는 전압의존성 $K^+$ 통로의 분자생물학적 특성

지도교수 류 판 동

이 논문을 이학박사학위논문으로 제출함
**2014년 4월**

서울대학교 대학원
협동과정 뇌과학전공
이 슬 기

이슬기의 이학박사학위논문을 인준함
**2014년 6월**

| | | |
|---|---|---|
| 위 원 장 | 황 인 구 | (인) |
| 부위원장 | 류 판 동 | (인) |
| 위 원 | 홍 성 종 | (인) |
| 위 원 | 최 성 우 | (인) |
| 위 원 | 이 소 영 | (인) |

# ABSTRACT

The hypothalamic paraventricular nucleus (PVN) comprises anatomically and functionally distinct neuronal populations. The A-type $K^+$ current ($I_A$) is involved in their different electrophysiological properties, but the molecular identity responsible for these differences remains unknown. Accordingly, I hypothesized that voltage-gated $K^+$ (Kv) channels encoding $I_A$ are molecular components underlying the determination of electrophysiological characteristics, and compared expressions of Kv channel subunits between distinct neuronal populations in the PVN, using single cell analysis (single cell reverse transcription-polymerase chain reaction [RT-PCR] or single cell real-time RT-PCR).

Results revealed that several Kv channel subunits were expressed in type I and type II PVN neurons which are electrophysiologically distinct. However, the expression density of Kv4.2 and Kv4.3 was significantly higher in type I than in type II neurons. These two subunits were also expressed in the presympathetic neurons, which project to the rostral ventrolateral medulla (RVLM; PVN-RVLM), but were differentially regulated during heart failure: Kv4.2 was up-regulated whereas Kv4.3 was down-regulated. In contrast, estrogen replacement into ovariectomized female rats down-regulated Kv4.2 mRNA levels, but did not affect Kv4.3 in the PVN-RVLM neurons. Estrogen also diminished $I_A$ density. These estrogenic effects occurred specifically in the dorsal cap parvocellular subdivision where vasopressin is remarkably sparse.

Taken together, Kv4.2 and Kv4.3 are important molecular components

underlying the determination of electrophysiological characteristics of different cell types and the modulation of neuronal properties of the presympathetic neurons. The finding of the differential and selective regulations of these two subunits under different pathophysiological conditions suggests that Kv4.2 and Kv4.3 play different roles independently of each other in the coordination of responses of the PVN to various types of stimuli.

---

Keyword: single cell analysis, hypothalamic paraventricular nucleus, voltage-gated $K^+$ channel, A-type $K^+$ current, electrophysiological characteristic, gene expression

**Student Number : 2008-20475**

# CONTENTS

# LIST OF FIGURES

**CHAPTER III**



**CHAPTER IV**

# LIST OF TABLES

# ABBREVIATIONS

| | |
|---|---|
| **ACSF** | Artificial cerebrospinal fluid |
| **CRH** | Corticotropin-releasing hormone |
| **Ct** | Threshold cycle |
| **CTB** | Cholera toxin subunit B |
| **DC** | Dorsal cap subdivision |
| **Dyn** | Dynorphin |
| **E2** | 17β-estradiol |
| **Enk** | Enkephalin |
| **ER-β** | Nuclear estrogen receptor subunit β |
| **GHRH** | Growth hormone-releasing hormone |
| **HF** | Heart failure |
| **$I_A$** | A-type $K^+$ currents |
| **Kv channel** | Voltage-gated $K^+$ channel |
| **Kv4.2-ir** | Kv4.2-immunoreactivity |
| **Kv4.3-ir** | Kv4.3-immunoreactivity |
| **MI** | Myocardial infarction |
| **OT** | Oxytocin |
| **OVX** | Ovariectomy |
| **PaPo** | posterior parvocellular subdivision |
| **PaV** | Ventral parvocellular subdivision |
| **PBS** | Phosphate-buffered saline |

| | |
|---|---|
| **PFA** | Paraformaldehyde |
| **Pm** | Posterior magnocellular subdivision |
| **PVN** | Paraventricular nucleus |
| **RT-PCR** | Reverse transcription-polymerase chain reaction |
| **RVLM** | Rostral ventrolateral medulla |
| **Sst** | Somatostatin |
| **TEA** | Tetraethylammonium |
| **TRH** | Thyrotropin-releasing hormone |
| **TTX** | Tetrodotoxin |
| **VP** | Vasopressin |
| **3V** | Third ventricle |
| **4-AP** | 4-aminopyridine |

# BACKGROUND

### *The PVN consists of heterogeneous cell populations*

The PVN is an important site for the integration of neuroendocrine and autonomic functions (Swanson and Sawchenko, 1980) and thus consists of heterogeneous cell populations that are morphologically, anatomically, and functionally distinct. Magnocellular cells project to the posterior pituitary gland and secret oxytocin or vasopressin. Parvocellular cells are subdivided into two subpopulations: neuroendocrine cells project to the median eminence and control hormone secretion from the anterior pituitary gland while preautonomic cells project to the brain stem and spinal cord, including the intermediolateral column, and control the autonomic nervous system (Armstrong et al., 1980; Swanson and Sawchenko, 1980; Swanson and Sawchenko, 1983).

These different neuronal populations are well characterized by their distinct electrophysiological properties. When PVN neurons were hyperpolarized and then incrementally depolarized, magnocellular neuroendocrine cells, which are categorized as “type I”, displayed transient outward rectification while parvocellular neuroendocrine cells, “type II”, did not (Luther and Tasker, 2000). Some parvocellular cells evoked a low-threshold spike (LTS) that was not observed in type I neurons. An LTS has been shown to be a characteristic of parvocellular preautonomic cells and is closely related to T-type $Ca^{2+}$ currents which are particularly encoded by voltage-gated $Ca^{2+}$ channel subunits, Cav3.1 (Lee et al., 2008; Luther et al., 2002).

Luther and Tasker (2000) demonstrated that transient outward rectification, which is exclusively apparent in type I neurons, is correlated with transient A-type $K^+$ current ($I_A$) based on the observation that $I_A$ was reduced to a similar degree as delay in the onset of the first action potential, which was generated by transient outward rectification, and that the amplitude of $I_A$ was larger in type I than type II. However, the key molecules underlying the distinct characteristics between type I and type II remain unknown.

### *Transient A-type $K^+$ currents in the PVN*

Electrophysiological properties of neurons, including resting membrane potential, input resistance and action potential waveform, are determined by the expression and properties of a variety of ion channels (Hille, 2001). Voltage-gated $K^+$ (Kv) channels, which are activated by depolarization and are selective for $K^+$ ions, have roles in the repolarization of the action potential and in regulating neuronal excitability (Rogawski, 1985; Rudy, 1988). These Kv currents are classified into two types of currents: a transiently activating and rapidly inactivating A-type ($I_A$) and a slowly activating and non-inactivating delayed rectifier ($I_K$) (Rudy, 1988). Both currents were observed in the PVN (Luther and Tasker, 2000). Specifically, $I_A$ is responsible for distinct electrophysiological properties distinguishing cell types of the PVN (Luther and Tasker, 2000), regulates action potential waveform and firing activity of presympathetic PVN neurons (Sonner and Stern, 2007), and is involved in neuronal modulation of the PVN caused by cardiovascular diseases, such as hypertension (Sonner et al., 2008).

### *Kv channels underlying $I_A$ in the PVN*

Kv currents were encoded by a macromolecular protein complex of Kv channels comprising Kv α subunits together with accessory subunits and regulatory proteins that influence channel stability, localization, and properties (Carrasquillo and Nerbonne, 2013; Coetzee et al., 1999). The Kv α subunit is the primary subunit for the tetrameric channel structure, which is composed of six transmembrane domains, the pore domain (P-loop), the voltage sensor, and the amino- and carboxyl-terminal cytoplasmic domains, and play critical roles in ion selectivity and voltage sensitivity (Birnbaum et al., 2004). A variety of Kv channel α subunits have been cloned and characterized (Gutman et al., 2005). These subunits form a homo- or heteromultimeric complex within the same subfamily with sequence homology, and these different combinations of subunits produce diverse and cell-specific Kv currents (Covarrubias et al., 1991; Rudy, 1988). Among those, Kv4.x and Kv1.4 are the major subunits encoding $I_A$ and other Kv1 subunits generate $I_A$ when assembled with Kvβ1 subunits that confer rapid inactivation (Heinemann et al., 1996; Rettig et al., 1994; Serodio et al., 1994; Serodio et al., 1996). Kv4.2 and Kv4.3 are of particular interest as a primary correlate for $I_A$ in brain because of their wide and abundant expressions and differential distributions according to neuronal types (Serodio and Rudy, 1998).

Some Kv1 and Kv4 subunits have been identified in the PVN (Chung et al., 2001; Sonner and Stern, 2007; Sonner et al., 2011). Studies have shown that Kv1.4 and Kv4.3 are expressed in presympathetic PVN neurons and have suggested that these subunits mediate $I_A$ in this neuronal population (Sonner and Stern, 2007; Sonner et al., 2011). Kv1.2 was detected in unclassified PVN neurons

(Chung et al., 2001). However, an extensive expression profile of Kv channel subunits related to $I_A$ in the PVN has not been reported, indicating that more diverse Kv channel subunits that can contribute to $I_A$ in the PVN remain unidentified. In the case of the identified Kv channel subunits, Kv1.2, Kv1.4, and Kv4.3, the relationship of these subunits with $I_K$ or $I_A$ also remains to be determined.

Kv channels, which are responsible for the electrical behavior of neurons, are well known to be modulated in response to internal and external physiological alternations. An increase or decrease in their expressions on cell membrane and significant changes in their activation and inactivation properties alter neuronal excitability, thereby influencing signal integration and outputs of the neurons. Accumulating studies have shown modulations of Kv channels by pathophysiological stress caused by cardiovascular diseases, such as hypertension and heart failure, in the peripheral system as well as in the central regulatory system (Gao et al., 2010; Kaprielian et al., 1999; Li et al., 2008; Sonner et al., 2011). Other studies have also shown that Kv channels are regulated by circulating hormones, such as estrogen and thyroid hormone, in several organs including brain, heart, and uterus (Arroyo et al., 2011; Eghbali et al., 2005; Nishiyama et al., 1998; Roepke et al., 2007; Song et al., 2001).

However, the modulation of Kv channels in the PVN is rarely reported in spite of evidence that firing activity of PVN neurons is remodeled in pathophysiological stress and that $I_A$ is one of the major $K^+$ currents detected across the PVN, regulating neuronal activity (Luther et al., 2000; Luther and Tasker, 2000; Sonner and Stern, 2007; Sonner et al., 2008). Accumulating studies have

demonstrated that the PVN is under hormonal regulation by examining alternations in neuronal activity and stress responses of the PVN following estrogen replacement or estrus cycles (Akaishi and Sakuma, 1985; Buller and Day, 2000; Gerrits et al., 2005; Kisley et al., 2000). In addition, there is an abundant expression of nuclear estrogen receptor β subunits in PVN, suggesting estrogen-mediated gene regulation (Stern and Zhang, 2003). However, estrogenic effects on Kv channels in the PVN have not been examined.

### *Single cell analysis*

$I_A$ in the PVN is correlated with electrophysiological properties and modulations of neuronal excitability, but little is known about the molecular identity of Kv channels underlying $I_A$; the reason for this is most likely due to heterogeneous cell composition of the PVN. The PVN is basically classified into eight distinct subdivisions, which are anatomically and functionally different (Swanson and Kuypers, 1980). However, within the same subdivision, differently characterized cells intermingle (Hallbeck et al., 2001; Simmons and Swanson, 2009). Therefore, it might be difficult to completely isolate anatomically or functionally specific cells from the PVN for molecular work.

To overcome this difficulty, I adapted single cell analysis using the cytoplasm extracted from a single cell (Liss et al., 1999; Liss, 2002). Single cell analysis has several advantages as previously described (Griffith et al., 2006): 1) amenability to a number of applications, such as electrophysiological recording, that are useful for examining the correlation of gene expression of interest with functional properties in an individual cell; 2) high sensitivity to detect even a single

copy of an mRNA target sequence by amplification; 3) simplicity with high efficiency of data turnaround and low labor intensive; 4) reproducibility; 5) quantifiability for estimating the relative abundance of a transcript; 6) stability by using cDNA templates through RT; and 7) precision of the expression profile data can be obtained from a distinct cell population, which prevents misinterpretation caused by the mixing of other cell populations. In addition, single cell analysis allows for multiple genes of interest to be examined spontaneously and independently in a single cell; co-expression of up to 10 different genes can be examined in an identical cell.

However, there are also limitations. First, the efficiency of PCR is very critical for target detectability so that if the efficiency is not close to optimal, some transcripts cannot be detected (Griffith et al., 2006). Therefore, finding optimal PCR conditions close to 100% efficiency for each target is required (Pfaffl, 2001; Zhang et al., 2009). Second, a small amount of templates obtained from a single cell requires a high number of cycles of PCR amplification, which increases the potentiality of false positive. To avoid error by an amplification of non-specific products, the specificity of all PCR products should be confirmed with their sizes or melting temperatures. In addition, to check contamination from the genomic DNA, negative controls should be ascertained by running RT without the reverse transcriptase for every PCR set.

### *Hypothesis and purpose*

In view of the role of $I_A$ in the electrophysiological differences between distinct cell subtypes and in the remodeling of neuronal excitability of a specific cell type

of the PVN in addition to the large molecular diversity of Kv channels, I hypothesized that specific Kv channels, most potentially Kv1 and Kv4 which are known as major encoders for $I_A$, are primarily or differentially expressed in the PVN and are involved in the determination of electrophysiological characteristics of neurons and modulations of neuronal properties by environmental stimuli. Accordingly, I aimed to identify the Kv channels responsible for different electrophysiological properties between distinct cell types (Chapter I) and to examine changes in the expression of the specific Kv channels following pathophysiological conditions, such as heart failure (Chapter II), and estrogen replacement (Chapter III). I also studied differences in the distribution of neuropeptides among subnuclei of the PVN (Chapter IV). For these works, I performed single cell real-time RT-PCR in combination with whole cell patch-clamp recording or retrograde tracing.

# CHAPTER I

# Single cell analysis of Kv channels that determine neuronal types of rat PVN neurons

# ABSTRACT

The hypothalamic paraventricular nucleus (PVN), a site for the integration of both the neuroendocrine and autonomic systems, has heterogeneous cell composition. These neurons are classified into type I and type II neurons, based on their electrophysiological properties. In the present study, I investigated the molecular identification of Kv channels, which determine a distinctive characteristic of type I PVN neurons, by means of single cell RT-PCR, along with slice patch clamp recordings. In order to determine the mRNA expression profiles, firstly, the PVN neurons of male rats were classified into type I and type II neurons, and then, single cell RT-PCR and single cell real time RT-PCR analysis were performed using the identical cell. The single cell RT-PCR analysis revealed that Kv1.2, Kv1.3, Kv1.4, Kv4.1, Kv4.2, and Kv4.3 were expressed both in type I and in type II neurons and several Kv channels were co-expressed in a single PVN neuron. However, I found that the expression densities of Kv4.2 and Kv4.3 were significantly higher in type I neurons than in type II neurons. Taken together, several Kv channels encoding $I_A$ are present both in type I and in type II neurons, and among those, Kv4.2 and Kv4.3 are the major Kv subunits responsible for determining the distinct electrophysiological properties. Thus these two Kv subunits may play important roles in determining PVN cell types and regulating PVN neuronal excitability. This study further provides key molecular mechanisms for differentiating type I and type II PVN neurons.

# INTRODUCTION

The hypothalamic paraventricular nucleus (PVN) is an important integrating site of hormone secretion and regulation of the autonomic nervous system (Swanson and Sawchenko, 1980). PVN neurons are composed of heterogeneous cell groups, including magnocellular and parvocellular cells (Armstrong et al., 1980; Swanson and Kuypers, 1980). Magnocellular neurosecretory cells and parvocellular neurosecretory cells are responsible for hormone secretion from the posterior pituitary and the anterior pituitary gland, respectively, and parvocellular preautonomic neurons projecting to the autonomic centers in the brain stem and spinal cord underlie the regulation of autonomic nervous system outflow (Blair et al., 1996; Coote, 1995; Kannan et al., 1988; Patel and Zhang, 1996; Porter and Brody, 1985; Porter and Brody, 1986).

PVN neurons have been well-classified based on their electrophysiological properties. Type I neurons, putative magnocellular neurons, express transient outward rectification, whereas type II neurons, putative parvocellular neurons, do not show the transient outward rectification and some of the type II neurons exhibit an LTS that is not found in type I neurons (Hoffman et al., 1991; Luther and Tasker, 2000; Tasker and Dudek, 1991). The transient outward rectification, which was distinguished by a delay in the onset of the first action potential, is known to be associated with $I_A$ (Luther and Tasker, 2000).

Previously, three types of $K^+$ currents such as $I_A$, slowly activating and non-inactivating delayed rectifier, and slowly activating and inactivating $K^+$ current have

been recorded in PVN neurons (Luther and Tasker, 2000; Sonner and Stern, 2007). Particularly, $I_A$ has been reported to exert a strong influence on repetitive firing patterns by altering the interspike interval and action potential repolarization, as well as the postsynaptic responsiveness (Rogawski, 1985; Rudy, 1988). Also, $I_A$ was determined to influence the action potential waveform and firing activity in PVN neurons projecting to the RVLM (Sonner and Stern, 2007).

The electrophysiological differences between type I and type II neurons may be due to the differential expression of ion channels; specifically, Kv channels encoding $I_A$. However, extensive differential identification of Kv channels in the PVN neurons has not yet been completely reported. Several subunits of Kv channels were identified in PVN neurons. Kv1.4 and Kv4.3 were identified in presympathetic PVN neurons (Sonner and Stern, 2007), and Kv1.2 immunoreactivity was detected in the PVN (Chung et al., 2001). However, the direct comparison of Kv channel expression profiles between type I and type II neurons was not performed.

Using the combined method of current-clamp recording with single cell RT-PCR and immunohistochemistry, I examined the differential expression profiles of Kv1.x and Kv4.x, which are known to be involved in generating $I_A$ (Jerng et al., 2004; Shibata et al., 2000) between type I and type II PVN neurons. Additionally, I analyzed the relationship of Kv subunits expression with a delay in the onset of the first action potential and performed single cell real-time RT-PCR to compare the expression density of each Kv channel subunit between type I and type II PVN neurons.

# MATERIALS AND METHODS

### *Animals*

Male Sprague-Dawley rats (n=61, 4-5 wks old) were purchased from Orient Bio Inc. (Kyonggi-do, Korea). The rats were maintained under a 12 hr light/dark cycle (lights on at 9:00 A.M.) and given free access to food and water until sacrifice. For the surgical procedure, anesthesia was induced by an intraperitoneal injection a mixture of Tiletamine and Zolazepam (Zoletil 50, 50 mg/kg; Virbac Lab, Carros Cedex, France) and xylazine (Rompun®, 12.5 mg/kg; Bayer Korea, Ansan, Korea). All animal experiments were performed in accordance with the guidelines of the Institutional Animal Care and Use Committee of Seoul National University and approved by the Institute of Laboratory Animal Resources of Seoul National University (SNU-100713-7).

### *Hypothalamic slice preparation*

Hypothalamic brain slices were prepared according to the methods described previously (Han et al., 2002; Han et al., 2010; Stern, 2001). The brains were immediately removed under anesthesia and immersed in oxygenated (95% $O_2$; 5% $CO_2$) ice-cold artificial cerebrospinal fluid (ACSF). Two or three coronal hypothalamic slices (300 μm) were caudally cut to the optic chiasm with a vibrating tissue slicer (Vibratome 1000 plus, Vibratome Company, St. Louis, MO, USA). The slices were incubated in oxygenated ACSF for at least 1 hr at 32 °C until recordings. The recordings were made at 30~32 °C. The ACSF for current

clamp experiments contained (in mM): 126 NaCl, 26 $NaHCO_3$, 5 KCl, 1.2 $NaH_2PO_4$, 2.4 $CaCl_2$, 1.2 $MgCl_2$, and 10 glucose.

### *Electrophysiological recording*

The PVN neurons were identified under the upright microscope (BX50WI, Olympus, Tokyo, Japan) with differential interference contrast and recorded in the whole cell current clamp mode. Patch pipettes were pulled from borosilicate glass capillaries of 1.7 mm diameter and 0.5 mm wall thickness. The pipette internal solution contained (mM): 135 K-gluconate, 5 KCl, 20 HEPES, 0.5 $CaCl_2$, 5 EGTA, and 5 MgATP. The pH was adjusted to 7.2 with KOH. Healthy looking neurons were selected for recording and were approached with the aid of a three dimensional hydraulic micromanipulator (Narishige Co., Tokyo, Japan). The open resistance of the pipette ranged from 3 to 6 MΩ, and a tight giga-ohm seal was obtained in the selected neuron. Electrical signals were recorded by an Axoclamp 2B amplifier (Axon Instruments, Foster City, CA, USA). Current or voltage signals were filtered at 1 kHz and digitized at 10 kHz using an analog-digital converter (Digidata 1320A, Axon Instruments) and pClamp software (Version 9.0, Axon Instruments). Membrane input resistance was obtained from the relations of the hyperpolarizing pulses (~60 pA). The resting membrane potentials were corrected for the liquid junction potential (~14.3 mV). The current clamp recording was used to classify cell types of PVN neurons. The serial depolarizing current pulses for 250 ms were applied after a hyperpolarizing pre-pulse to near -100 mV for 250 ms in a whole cell configuration (Figure 1A). In response to depolarizing from a hyperpolarizing membrane potential, PVN neurons displaying a delay in onset of

the first action potential were classified as type I neurons, whereas PVN neurons not displaying a delay as type II neurons.

4-aminopyridine (4-AP), a A-type $K^+$ channel blocker (Rudy et al., 1988), was obtained from Sigma-Aldrich (St. Louis, MO, USA) and was applied to the bath solution (ACSF) at the appropriate concentration.

### *Single cell RT-PCR*

Single cell RT-PCR was carried out as previously described with minor modifications (Di et al., 2003; Glasgow et al., 1999; Lee et al., 2008). I first classified PVN neurons into two cell types as type I or type II neurons by whole cell patch-clamp recording, and performed post-hoc PCR analysis by extracting the cytoplasm of the classified cell. The cytoplasm of the single neuron was pulled into a patch pipette with negative pressure under visual control, taking care not to contain the nucleus.

The cytoplasm in the pipette was again dissipated into a prepared microtube containing 5 μl of nuclease free water (Qiagen, Valencia, CA, USA) and then immediately moved into -70 °C deep-freezer. The RT for single cell cDNA preparations was carried out with High Capacity cDNA Reverse Transcription Kits (Applied Biosystems, Foster City, CA, USA) according to the manufacturer's manual.

PCR amplification was induced with a fraction of the single cell cDNAs as a template. The mixture of PCR reaction contained (in μl): 1 of 10 μM each forward and reverse primer, 10 of 2x Taq polymerase master mix buffer (GoTaq Green Master Mix, Promega, Madison, WI, USA), and 2~4 of the cDNA template.

PCR conditions were as follows: pre-denaturation at 94 ℃ for 5 min, 50 cycles of denaturation at 94 ℃ for 40 sec, annealing at 60 ℃ for 40 sec, extension at 72 ℃ for 1 min, and a final extension at 72 ℃ for 7 min. The primer pairs used in the experiments are presented in Table 1. All primers were synthesized by Bioneer (Daejeon, Korea). Final PCR product was electrophoresized in 1.8% agarose gel containing ethidium bromide to visualize its band. All the PCR products were purified using a PCR purification kit (Qiagen) and the purified products were sequenced to confirm the amplified sequences. Negative controls for checking contamination from the genomic DNA were ascertained by running RT without the reverse transcriptase for every set.

### *Single cell real-time RT-PCR*

All procedures before real-time PCR amplification were carried out in the same way as described in single cell RT-PCR. Single cell real-time PCR was performed using single cells harvested from the slices by means of the StepOnePlus System (Applied Biosystems) with SYBR Green detection. Primers for rat Kv1.2, Kv1.3, Kv4.2, and Kv4.3 were designed using Primer Express 2.0 (Applied Biosystems) and synthesized in Cosmo Genetech (Kyonggi-do, Korea). Primer sequences are presented in Table 2. The real-time PCR reactions contained (in μl): 2 of cDNA template, 0.4 of 10 μM each forward and reverse primer, 0.4 of 50x Rox dye and 10 of 2x SYBR master mix (SYBR premix Ex Taq; Takara Bio Inc., Shiga, Japan) and 6.8 of nuclease free water. PCR conditions were as follows: pre-denaturation at 95 ℃ for 10 sec, 50 cycles of denaturation at 95 ℃ for 5 sec and annealing at 60 ℃ for 31 sec, and dissociation stage programmed in the system for melt curve

**Table 1. Primer sequences for single cell RT-PCR.**

| Target (Acc. No.) | Sequence | Product size (bp) |
|---|---|---|
| Kv1.1 (X12589) | 5'- GCGCTACTTTGACCCTCTGA-3'<br>5'-AGTGCGACTCAGCTTCTTCC-3' | 857 |
| Kv1.2 (M74449) | 5'-GAGATGTTTCGGGAGGATGA-3'<br>5'-GATGAAGAAAGGGTCGGTGA-3' | 303 |
| Kv1.3 (X16001) | 5'-TCGAGACACAGCTCAAGAC -3'<br>5'-GTATTCGAAGAGCAGCCA-3' | 335 |
| Kv1.4 (M32867) | 5'-TCCCATGATCCTCAAGGAAG-3'<br>5'-AAAGCTGGGACGGTTCCTAT-3' | 471 |
| Kv4.1 (M64226) | 5'- GGCTACACCCTCAAGAGCTG-3'<br>5'-ATACTGCAGGAAGGCATTGG-3' | 402 |
| Kv4.2 (S64320) | 5'-ACCCCTGATCACTCTTGTGAC-3'<br>5'-AGAGCACTCTCTCCTGTATTGT-3' | 522 |
| Kv4.3 (U42975) | 5'-GCTGGGTAGCACAGAGAAGG -3'<br>5'-GTGTCCAGGCAGAAGAAAGC-3' | 498 |
| OT (NM_012996) | 5'-CTTGGCCTACTGGCTCTGAC-3'<br>5'-GGGCAGGTAGTTCTCCTCCT-3' | 216 |
| VP (NM_016992) | 5'-CCTCACCTCTGCCTGCTACTT-3'<br>5'-GGGGGCGATGGCTCAGTAGAC-3' | 463 |
| CRH (NM_031019) | 5'-AACTCAGAGCCCAAGTACGTTGAG-3'<br>5'-TCACCCATGCGGATCAGAATC-3' | 354 |
| TRH (NM_013046) | 5'-GGTGCTGCCTTAGACTCCTG-3'<br>5'-TTCTTCCCAGCTTCTTTGGA-3' | 372 |

**Table 2. Primer sequences for single cell real-time RT-PCR.**

| Target (Acc. No.) | Sequence | Product size (bp) |
|---|---|---|
| Kv1.2 (NM_012970) | 5'-TGACATTGTGGCTATCATCCCTTA-3'<br>5'-CGTCCTCTGGCTTCTCAGCT-3' | 68 |
| Kv1.3 (NM_019270) | 5'-GCCGTGGTAACCATGACAACT-3'<br>5'-GCCCACAATCTTGCCTCCTA-3' | 72 |
| Kv4.2 (NM_031730) | 5'-ACAAACGAAGGGCACAGAAGA-3'<br>5'-CATGTAGGCATTTGCACTTCCA-3' | 77 |
| Kv4.3 (NM_031739) | 5'-AACGCAGGGCACAGAAGAAG-3'<br>5'-GGCATTGGAGCTCCCTGTT-3' | 68 |
| β-actin (NM_031144) | 5'-GACCCAGATCATGTTTGAGACCTT-3'<br>5'-CACAGCCTGGATGGCTACGTA-3' | 61 |

analysis for PCR product specificity. Negative controls to check contamination from the genomic DNA were ascertained by running RT without the reverse transcriptase. The threshold cycle (Ct) values for transcripts were calculated using StepOne Software 2.0 (Applied Biosystems). All samples were run in duplicate. Ct values that showed a different Tm or two peaks were all discarded.

Quantifying the relative difference in target gene expression between type I and type II neurons was analyzed by the $2^{-\Delta\Delta Ct}$ method (Livak and Schmittgen, 2001). Primer efficiencies for each target and reference gene were calculated using the equation $E=10^{[-1/slope]}$ to apply the $2^{-\Delta\Delta Ct}$ method to the relative quantification in gene expression (Livak and Schmittgen, 2001; Pfaffl, 2001; Sonner et al., 2011; Zhang et al., 2009).

### *Immunohistochemistry*

Rats were anesthetized and perfused transcardially with 100 ml of 0.01 M PBS followed by 200-300 ml of 4% paraformaldehyde in 0.1 M phosphate buffer (PB; pH=7.4). The brain was removed and placed in 30% sucrose solution until it sank. Then, the brains were frozen in a deep-freezer for 24 hrs. The frozen brain was cut into 30 μm thicknesses using a sliding microtome (Leica, Nussloch, Germany). Slices were collected in the plate filled with 0.01 M PBS and then incubated in PBS mixed with 0.3% Triton X-100 and 5% normal donkey serum for 2 hrs at room temperature for blocking, followed by incubation for 1 hr at room temperature and for 48 hrs at 4 ℃ with primary antibody. Antibodies for Kv1.1, Kv1.2 and Kv4.3 were obtained from Chemicon (Temecula, CA, USA) and those for Kv1.3, Kv1.4, Kv4.1, and Kv4.2 were from Alomone Laboratories (Jerusalem,

Israel) and used in dilution 1:100 to 1:200 for the experiment. Slices were rinsed in PBS 5 times and incubated again for FITC-conjugated donkey anti-rabbit secondary antibody (1:500; Jackson ImmunoResearch Laboratories, West Grove, PA, USA) in PBS for 2 hrs at room temperature. Slices were washed, mounted onto slides and visualized using a combination of fluorescence illumination (BX51, Olympus, Tokyo, Japan) and video microscopic analysis (DP71, Olympus). For the specificity of the antibody, antibodies were pre-incubated with the provided peptides as control and treated according to the same procedure as above.

# RESULTS

### *Electrophysiological properties of type I and type II PVN neurons*

To classify cell types of PVN neurons, the serial depolarizing current pulses for 250 ms were applied after a hyperpolarizing pre-pulse to near -100 mV for 250 ms in a whole cell configuration (Figure 1A). In response to depolarizing from a hyperpolarizing membrane potential, type I PVN neurons exhibited a delay in onset of the first action potential which is well defined as the main characteristic of type I neurons (Luther and Tasker, 2000). Figure 1B presents the location of the recorded neurons for each type I and type II cell. Type I neurons located mostly in the posterior magnocellular division and partly in the medial parvocellular division and along the ventral boundary line of the PVN region. Type II neurons were intense in the medial parvocellular division of the PVN. Some neurons generating LTS in response to the same protocol were excluded from the present study because the PVN neurons expressing LTS were characterized as preautonomic cells and T-type $Ca^{2+}$ (Cav) channels underlying an LTS interplay with $I_A$ in PVN neurons (Anderson et al., 2010; Lee et al., 2008; Sonner et al., 2011). The delay time was determined as the duration from the point of initiating the depolarizing pulse to the peak of the first action potential (Figure 1C *inset*). A significant difference in delay time of the first action potential in type I and type II is demonstrated in Figure 1C (76.7±2.4 ms in type I neurons; 22.2±1.0 ms in type II neurons, $P<0.01$). The resting membrane potential of type I ($n=48$) and type II ($n=43$) neurons was -60.5±0.8 mV and -61.0±0.8 mV, respectively (non significant). The input resistance

**Figure 1. Classification of PVN neurons by electrophysiological properties. A**, Type I neurons were characterized by a delay in the onset of the first action potential, which was not found in type II neurons. **B**, Type I neurons were mainly located in the posterior magnocellular division and partly in the ventral border and the medial parvocellular division, while type II neurons were concentrated in the medial parvocellular division. **C,** Delay time as a distinct electrophysiological property between type I and type II neurons. Significant difference of delay time was found between type I and type II PVN neurons. The measurement of delay time ($\Delta t$) based on the duration from input of depolarizing current (-105 pA) to the peak of the first action potential *(inset)*. **D,** Reduction of delay of the first action potential by 5 mM 4-AP. **E**, Dose-dependent inhibition of a delayed onset by 4-AP. Values are means ± SE. * $P<0.05$, ** $P<0.01$ by Student's *t*-test.

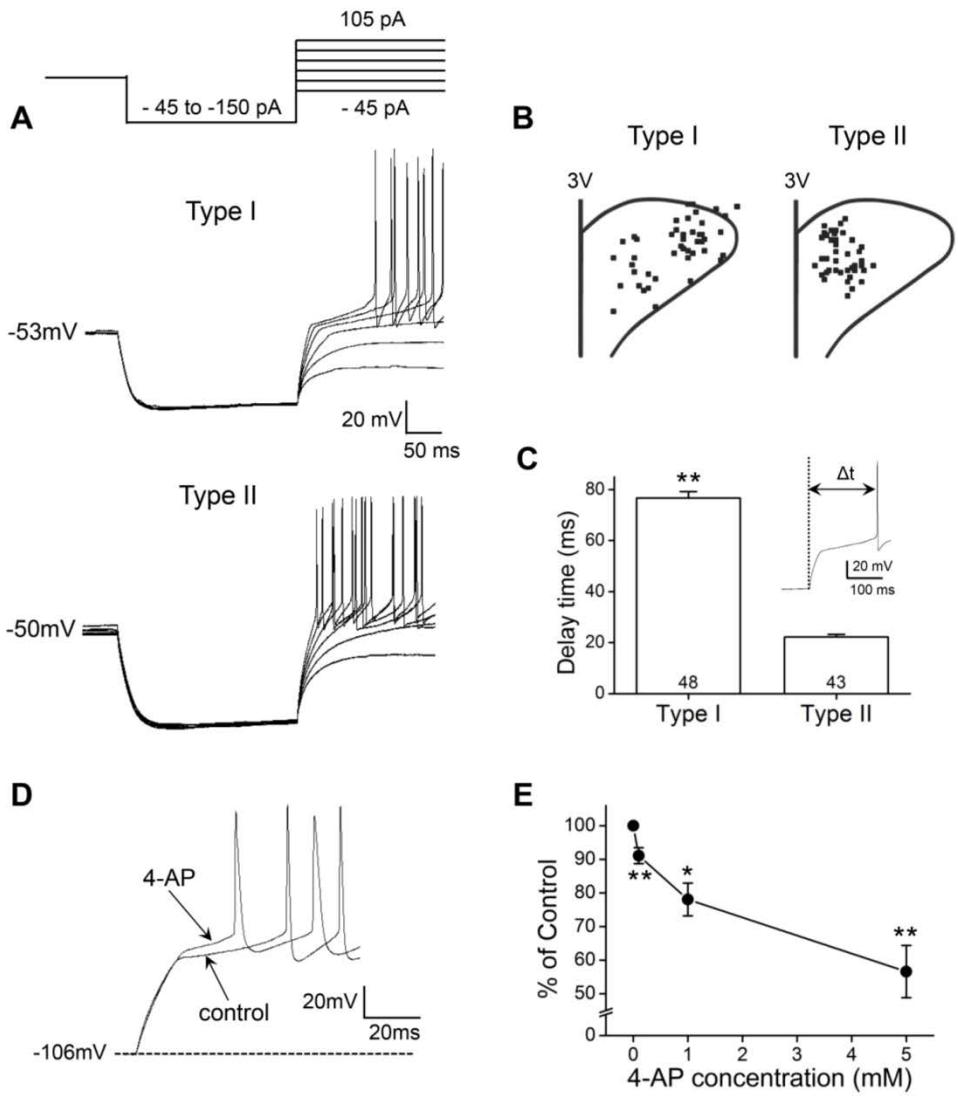
A
105 pA
- 45 to -150 pA
- 45 pA
Type I
-53mV
20 mV
50 ms
Type II
-50mV
B
Type I
Type II
3V
3V
C
Delay time (ms)
80
60
40
20
0
**
Δt
20 mV
100 ms
48
43
Type I
Type II
D
4-AP
control
20mV
20ms
-106mV
E
% of Control
100
90
80
70
60
50
0
**
*
**
0
1
2
3
4
5
4-AP concentration (mM)

was significantly different between type I and type II neurons (549.4±33.5 MΩ in type I neurons; 349.4±19.8 MΩ in type II neurons, $P<0.01$). Modulation of delay time on the onset of the first action potential by 4-AP, a $K^+$ channel blocker, was investigated in type I PVN neurons. Delay was recorded before and after application of 4-AP. Consistent with the previous report (Luther and Tasker, 2000), 4-AP dramatically reduced the delay time of the first action potential in a dose-dependent manner (91.1 ± 2.4% for 0.1 mM, 78.0 ± 4.9% for 1 mM, and 56.6 ± 7.8% for 5 mM; Figure 1D, E).

### *Expression of peptides in type I and type II PVN neurons*

In order to identify the types of peptides expressed in the PVN, the peptide's mRNA expression was examined in the cells analyzed in the present experiments. The peptides known to be mainly expressed in PVN, such as oxytocin (OT), vasopressin (VP), corticotropin-releasing hormone (CRH), and thyrotropin-releasing hormone (TRH), were included. Most PVN neurons (70%, 33/47) expressed these four peptides. Approximately 81% (21/26) of type I neurons and 57% (12/21) of type II neurons were positive for peptide expression. Type I neurons (Figure 2A) expressed exclusively OT and VP, whereas type II neurons (Figure 2B) expressed various peptides, including OT, VP, CRH, and TRH. In type I neurons, VP was most frequently detected (90%, 19/21) and OT was expressed in 57% (12/21) of the cells. The co-expression frequency of OT and VP was 48% (10/21) in type I neurons. CRH and TRH were not detected in type I neurons. Interestingly, type I neurons exhibiting non-peptides expression displayed a significantly longer delay (123.2 ± 27.6 ms, $n$=5), than type I expressing OT, VP,

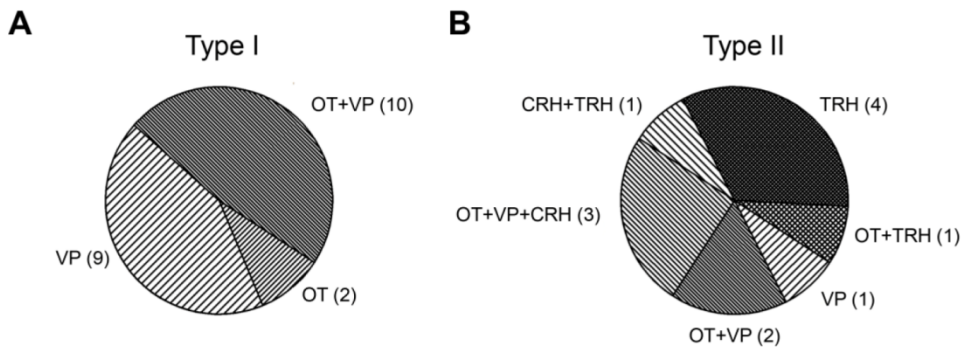


**Figure 2. Peptide expressions in type I and type II PVN neurons.** Peptide mRNA detection frequency was illustrated for type I (A) and type II (B) PVN neurons. The pie graphs represent the percentage of cells positive for individual peptides and their combination in the total number of cells expressing peptides (21 in type I and 12 in type II). The numbers in parentheses refer to the number of positive cells.

or co-expressing OT and VP (70.6 ± 2.7 ms, $n$=21) ($P$<0.01). In type II neurons, OT, VP, and TRH had the same detection frequency (50%, 6/12) and CRH showed a lower frequency (33%, 4/12). Co-expression of OT and VP was observed in type II neurons (42%, 5/12). Furthermore, co-expressions of OT and TRH or CRH and TRH were also detected but at low frequencies (8%, 1/12). Interestingly, co-expression of three different peptides, OT, VP, and CRH was evident in type II neurons (25%, 3/12).

### *The detection frequency of Kv1 and Kv4 mRNA expressions in type I and type II PVN neurons*

Since the Kv1 and Kv4 subfamilies have been suggested as candidates for encoding $I_A$ (Baldwin et al., 1991; Serodio and Rudy, 1998; Timpe et al., 1988), four different Kv1 subfamilies (Kv1.1, Kv1.2, Kv1.3, and Kv1.4) and three different Kv4 subunits (Kv4.1, Kv4.2, and Kv4.3) were included for single cell RT-PCR analysis. Since the cDNA template from a single cell was not sufficient for all the Kv channel subfamilies to be examined, three to five of the targets were selected randomly in every set, which led to a different total cell number in each target. The results from single cell RT-PCR are illustrated in Figure 3. Kv1.2 (26% [22/85] in type I neurons; 37% [28/76] in type II neurons), Kv1.3 (23% [17/73] in type I neurons; 51% [34/67] in type II neurons), Kv1.4 (15% [6/39] in type I neurons; 28% [11/40] in type II neurons), Kv4.1 (16% [6/38] in type I neurons; 11% [4/38] in type II neurons), Kv4.2 (27% [21/78] in type I neurons; 29% [20/68] in type II neurons), and Kv4.3 (56% [48/85] in type I neurons; 32% [24/75] in type II neurons) were detected both in type I and in type II neurons (Figure 3A). Kv1.1

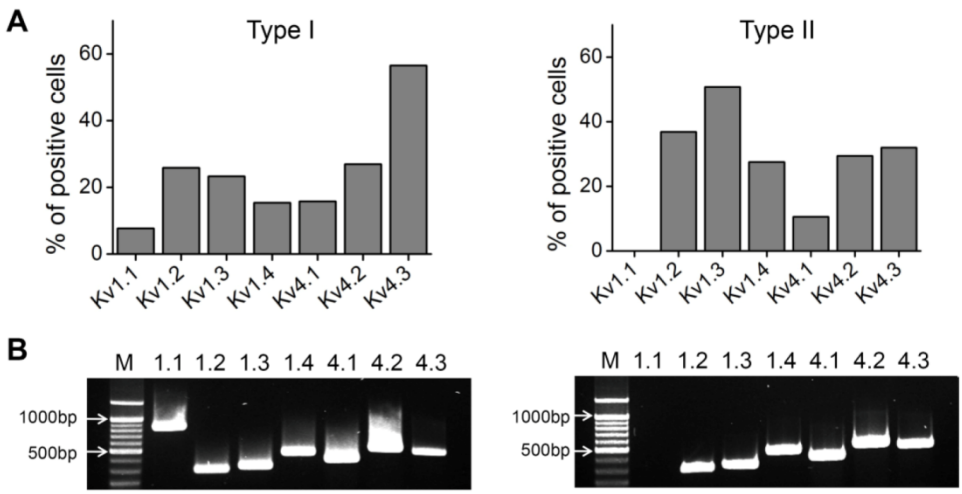


**Figure 3. mRNA expressions of Kv1 and Kv4 subunits in PVN neurons using the single cell RT-PCR. A**, The bar graphs indicate the percentage of cells expressing each Kv subunit. Most of type I and type II PVN neurons express mRNAs encoding Kv1.2, Kv1.3, Kv1.4, Kv4.1, Kv4.2, and Kv4.3. Kv1.1 was expressed only in type I neurons, not in type II neurons. **B**, Gel images represent expressions of Kv1 and Kv4 subunits in type I and type II neurons.

was detected only in type I neurons (8% [3/39]), but not in type II neurons (0% [0/40]). The sensitivity of the primer pair for Kv1.1 was ascertained by its positive detection in a single hippocampus neuron (data not shown). Figure 3B illustrates representative gel images for each Kv channel subunit. When the proportion of positive and negative for each Kv channel was compared between type I and type II neurons, Kv1.3 and Kv4.3 were significantly different (Fisher's exact test; Figure 4), suggesting that the number of Kv1.3-expressing neurons was larger in type II neurons as compared to type I neurons and, in contrast, that of Kv4.3-expressing neurons was larger in type I neurons as compared to type II neurons. Other Kv channel subunits examined (Kv1.1, Kv1.2, Kv1.4, Kv4.1, and Kv4.2) were statistically equivalent in both type I and in type II PVN neurons.

### *Protein expressions of Kv channels in the PVN neurons*

Immunohistochemistry was performed to confirm the protein expression of Kv1 and Kv4 in the PVN neurons. The representative fluorescence images of Kv1.1 (A1, *N*=3), Kv1.2 (B1, *N*=4), Kv1.3 (C1, *N*=3), Kv1.4 (D1, *N*=3), Kv4.1 (E1, *N*=3), Kv4.2 (F1, *N*=3), and Kv4.3 (G1, *N*=3) in PVN neurons are illustrated in Figure 5. Immunoreactivities for Kv1.2, Kv1.3, Kv4.1, Kv4.2, and Kv4.3 were widely observed within the PVN, indicating that apparent protein expressions of these Kv channel subunits in the PVN. The higher magnified images were included in Figure 5A2-G2. Figure 5A3-G3 show the negative controls obtained through pre-incubation with the peptides provided, supporting the specificities of antibodies used.

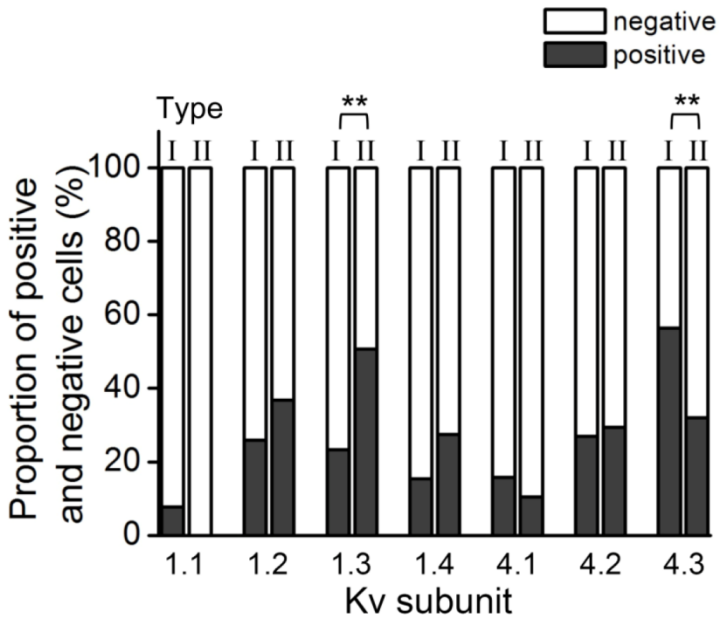


**Figure 4. Proportion of Kv channel expressing (positive) and non-expressing (negative) cells in type I and type II PVN neurons**. The data was analyzed with Fisher's exact test. The proportion of Kv1.3- expressing cells was higher in type II than in type I neurons, whereas that of Kv4.3- expressing cells was higher in type I than in type II neurons (**$P$<0.01).

**Figure 5**. **Protein expressions of Kv1 and Kv4 subunits in PVN neurons.** The confocal images showing Kv1.1 (A1, *N*=3), Kv1.2 (B1, *N*=4), Kv1.3 (C1, *N*=3), Kv1.4 (D1, *N*=3), Kv4.1 (E1, *N*=3), Kv4.2 (F1, *N*=3), and Kv4.3 (G1, *N*=3) immunoreactivities (scale bar= 100 μm). The higher magnified images were shown to better depict the immunoreactive patterns (A2-G2; scale bar= 50 μm). The negative controls (A3-G3; scale bar= 100 μm) were obtained through pre-incubation of respective peptides provided. 3V, third ventricle.

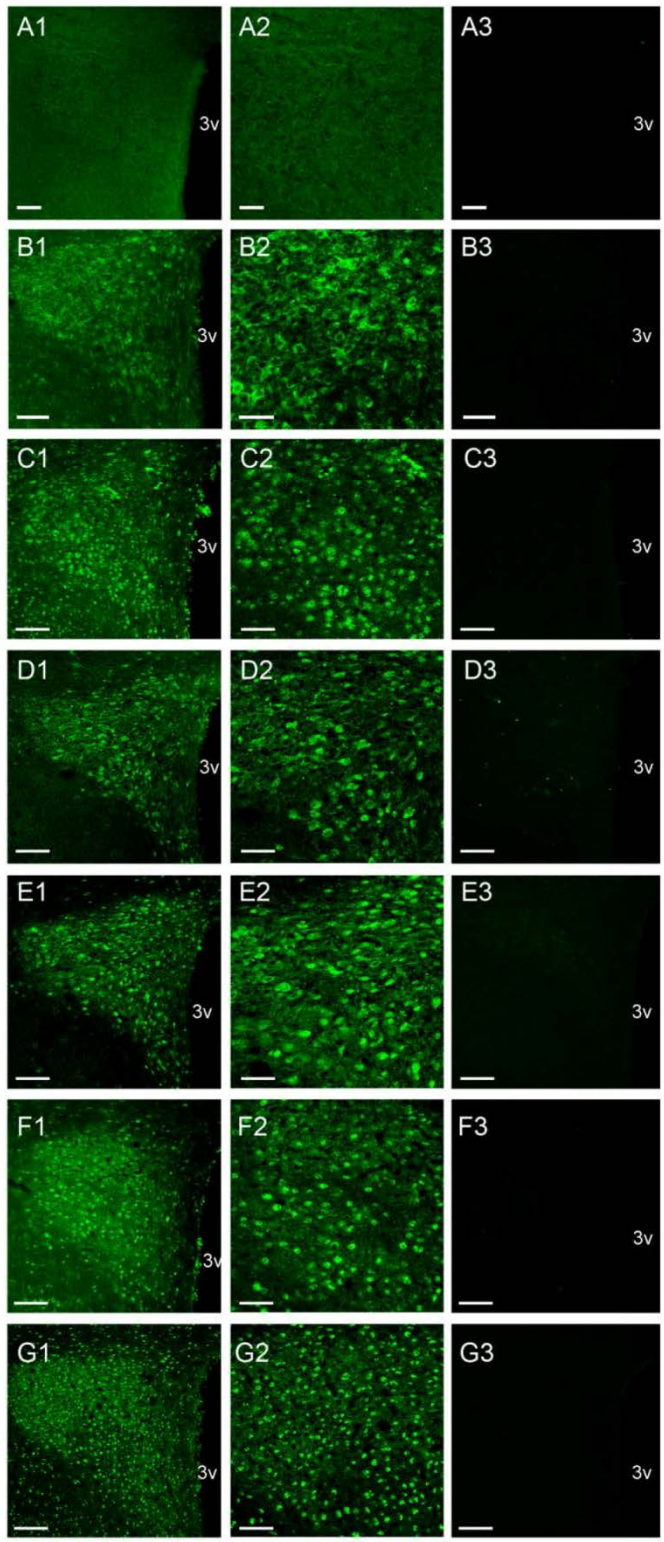
A1
3v
A2
A3
3v
B1
3v
B2
B3
3v
C1
3v
C2
C3
3v
D1
3v
D2
D3
3v
E1
3v
E2
E3
3v
F1
3v
F2
F3
3v
G1
3v
G2
G3
3v

### *Co-expression of Kv channel subunits in type I and type II PVN neurons*

Single cell PCR analysis revealed that individual PVN type I and type II neurons expressed multiple Kv channel subunits. Among those cells, as shown in Figure 6, most cells expressed a single Kv channel subunit; 47% (35/74) in type I neurons, 44% (28/63) in type II neurons. However, co-expressions of different Kv channel subunits were also detected (Guan et al., 2006). Co-expression of two different Kv channel subunits was detected in 34% (25/74) and 27% (17/63) of type I and type II neurons, respectively. Co-expression of three different Kv channel subunits was detected in 18% (13/74) and 21% (13/63) of type I and type II neurons, respectively. Even in a small proportion of the cells, co-expression of four different Kv channel subunits was also detected (1% [1/74] in type I neurons; 8% [5/63] in type II neurons).

Since in both type I and II neurons, co-expressions of Kv channel subunits were frequently detected, I analyzed which Kv channel subunits were involved in these co-expression patterns. The rank order of the Kv channel subunits' co-expression is listed in Table 3. The percentage was calculated from the number of cells expressing each Kv channel subunit in the total number of cells targeted. In type I cells, the expression frequency of one Kv channel subunit, Kv4.3 (25%, 21/85), was higher than that of the co-expression of two different Kv channel subunits (Table 4). In type I cells expressing two different Kv channel subunits, Kv4.2 + Kv4.3 (22% [17/78]) > Kv1.3 + Kv4.3 (16% [10/63]) > Kv1.3 + Kv4.2 (13% [8/63]) were expressed in that order. In type II cells expressing one of the Kv channel subunits, Kv1.3 (12% [8/67]) was mostly expressed (Table 5); however, this was at a lower frequency than those expressing two different Kv channel

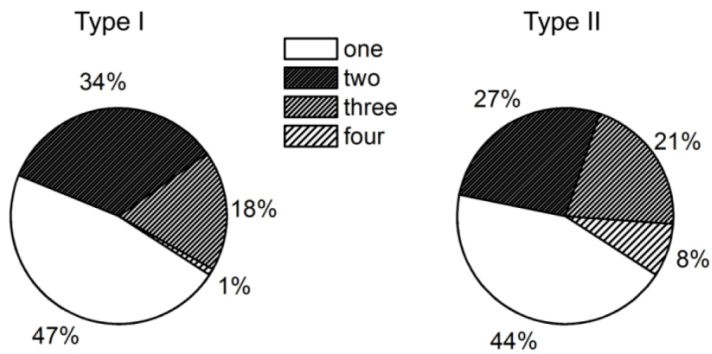


**Figure 6. Co-expression of Kv channels in type I and type II PVN neurons.** The pie graphs represent the percentage of cells expressing a single Kv channel subunit or of those co-expressing more than two different Kv channel subunits in the total number of cells expressing Kv channel subunits (74 in type I and 63 in type II).

**Table 3. Ranking of the detection frequency in co-expressions of Kv1 or Kv4 in PVN neurons.**

| | Type I | | Type II | |
|---|---|---|---|---|
| Ranking | Kv channel | % | Kv channel | % |
| 1 | Kv4.3 | 25 | Kv1.2+Kv1.3 | 25 |
| 2 | Kv4.2+Kv4.3 | 22 | Kv1.3+Kv4.2 | 22 |
| 3 | Kv1.3+Kv4.3 | 16 | Kv1.3+Kv4.3 | 20 |
| 4 | Kv1.3+Kv4.2 | 13 | Kv1.2+Kv4.2 | 19 |

**Table 4. Percentage of co-expressed Kv channel subunits in type I neurons**

| Kv subunit | 1.1 | 1.2 | 1.3 | 1.4 | 4.1 | 4.2 | 4.3 |
|---|---|---|---|---|---|---|---|
| 1.1 | 0 (0/39) | 0 (0/39) | 0 (0/32) | 2.6 (1/39) | 3.4 (1/29) | 4.5 (1/22) | 3.4 (1/29) |
| 1.2 | | 8.2 (7/85) | 9.0 (7/78) | 2.6 (1/39) | 3.4 (1/29) | 7.4 (6/81) | 9.3 (7/75) |
| 1.3 | | | 2.7 (2/73) | 0 (0/27) | 0 (0/17) | 12.7 (8/63) | 15.9 (10/63) |
| 1.4 | | | | 2.6 (1/39) | 3.6 (1/28) | 4.5 (1/22) | 6.9 (2/29) |
| 4.1 | | | | | 2.6 (1/38) | 9.4 (3/32) | 5.3 (2/38) |
| 4.2 | | | | | | 2.6 (2/78) | 21.8 (17/78) |
| 4.3 | | | | | | | 24.7 (21/85) |

**Table 5. Percentage of co-expressed Kv channel subunits in type II neurons**

| Kv subunit | 1.1 | 1.2 | 1.3 | 1.4 | 4.1 | 4.2 | 4.3 |
|---|---|---|---|---|---|---|---|
| 1.1 | 0 (0/40) | 0 (0/40) | 0 (0/33) | 0 (0/40) | 0 (0/27) | 0 (0/21) | 0 (0/28) |
| 1.2 | | 9.2 (7/76) | 25.4 (17/67) | 10.0 (4/40) | 3.7 (1/27) | 19.3 (11/57) | 10.9 (7/64) |
| 1.3 | | | 11.9 (8/67) | 16.1 (5/31) | 5.3 (1/19) | 21.8 (12/55) | 20 (11/55) |
| 1.4 | | | | 7.5 (3/40) | 7.4 (2/27) | 4.8 (1/21) | 3.6 (1/28) |
| 4.1 | | | | | 0 (0/38) | 3.1 (1/32) | 2.6 (1/38) |
| 4.2 | | | | | | 4.4 (3/68) | 14.7 (10/68) |
| 4.3 | | | | | | | 9.3 (7/75) |

subunits, in which Kv1.2 + 1.3 (25% [17/67]) > Kv1.3 + Kv4.2 (22% [12/55]) > Kv1.3 + Kv4.3 (20% [11/55]) > Kv1.2 + Kv4.2 (19% [11/57]) were detected in that order (Table 3). The data for type I and type II neurons are presented in detail in Table 4 and Table 5, respectively. These results indicate that multiple Kv channel subunits co-exist in type I and type II PVN neurons but the co-expression pattern is different between the two types.

### *Comparison of Kv channel mRNA expression patterns according to the presence of neuropeptides in type I and type II PVN neurons*

I analyzed the mRNA detection frequency of Kv1.2, Kv1.3, Kv4.2, and Kv4.3, which were frequently detected compared to other Kv channel subunits (Figure 3), along with the expression of four peptides, OT, VP, CRH, and TRH. Cells expressing none of these four peptides were designated as 'none'. Type I neurons expressed exclusively OT or VP, but not CRH or TRH (Figure 2A). As shown in Figure 7A, in type I neurons expressing OT or VP, Kv4.3 was the most frequently detected (78% [7/9] and 75% [9/12], respectively). Kv4.2 (33% [3/9] in OT neurons; 33% [4/12] in VP neurons) and Kv1.2 (22% [2/9] in OT neurons; 25% [3/12] in VP neurons) followed in succession. Kv1.3 was not detected in type I neurons expressing OT or VP, but Kv1.3 was detected in those neurons expressing none of the four peptides (50% [1/2]). In contrast, Kv4.2 was detected in both type I neurons expressing OT and VP, but was not detected in type I cells which do not contain the peptides examined.

Type II PVN neurons expressed four peptides, OT, VP, CRH, and TRH (Figure 2B). In type II neurons expressing peptides, Kv1.3 was the most frequently

**Figure 7. mRNA expressions of peptides and Kv channels in type I and type II PVN neurons.** The mRNA detection frequencies of Kv1.2, Kv1.3, Kv4.2, and Kv4.3 in type I and type II neurons were illustrated along with the expression of four peptides. **A,** Kv4.3 had a high frequency of detection in type I neurons expressing peptides. The expression pattern of Kv channels subunits was similar in OT and VP neurons. Note that no CRH or TRH neurons were detected in type I neurons and no Kv1.3 was detected in peptide-expressing type I neurons. **B,** Kv1.3 had a high frequency of detection in type II neurons expressing peptides even though this also occurred in those not expressing peptides. The expression pattern of Kv channel subunits was different in each peptide-expressing type II neuron. The numbers in parentheses and in bar graphs refer to cell numbers positive for each peptide and each Kv channel subunit, respectively.

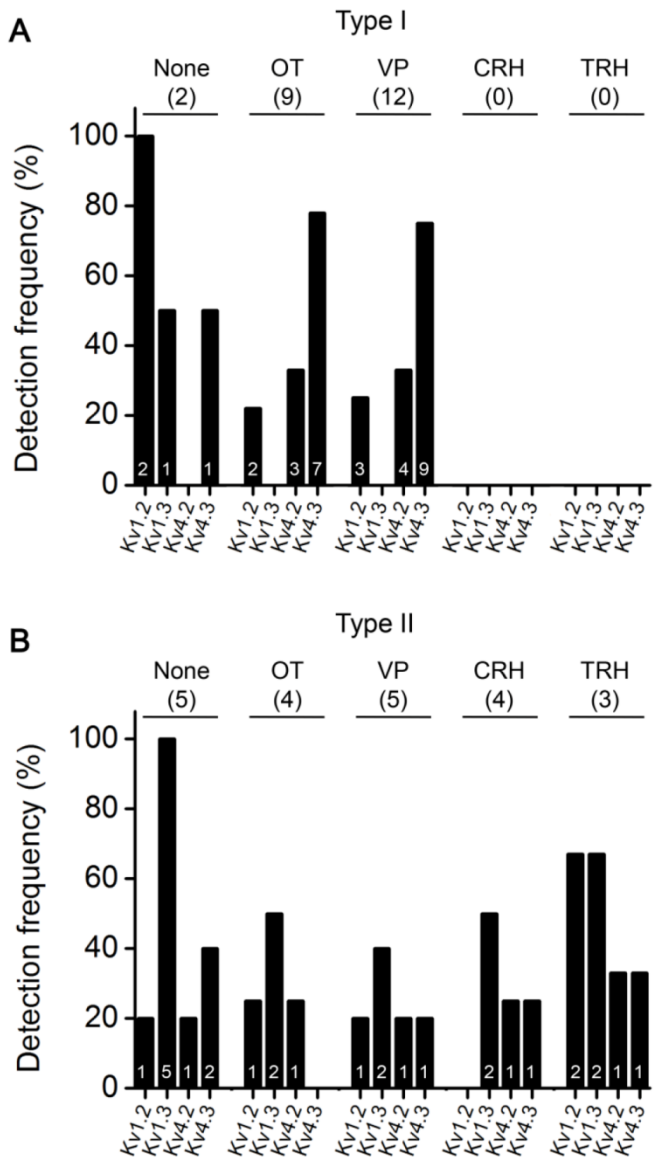
A
Type I
None (2)
OT (9)
VP (12)
CRH (0)
TRH (0)
Detection frequency (%)
100
80
60
40
20
0
2 1 1 2 3 7 3 4 9
Kv1.2 Kv1.3 Kv4.2 Kv4.3
B
Type II
None (5)
OT (4)
VP (5)
CRH (4)
TRH (3)
Detection frequency (%)
100
80
60
40
20
0
1 5 1 2 1 2 1 1 2 1 1 2 1 1 2 2 1 1
Kv1.2 Kv1.3 Kv4.2 Kv4.3

detected (67% [2/3] in TRH neurons; 50% [2/4] in both OT and CRH; 40% [2/5] in VP; Figure 7B). However, the expressions of other Kv channel subunits were different among the neurons expressing each peptide. The OT-expressing type II neurons did not express Kv4.3 and the CRH-expressing neurons did not express Kv1.2.

### *The relative quantification of Kv1 and Kv4 mRNA expressions in type I and type II PVN neurons*

In order to compare the mRNA expression density of Kv1.2, Kv1.3, Kv4.2, and Kv4.3 at the single cell level in type I and type II PVN neurons, single cell real-time RT-PCR was performed. Figure 8 demonstrates that the primers for each Kv channel subunit and PCR conditions were suitable for single cell real-time RT-PCR analysis (Zhang et al., 2009) since they have appropriate efficiencies (99% for Kv1.2, 101% for Kv1.3, 98% for Kv4.2, 101% for Kv4.3, and 100% for β-actin [data not shown]) in the range embracing a single cell detection. The primer efficiency was calculated from the slope value for each primer (*insets* in Figure 8) according to the equation $E=10^{[-1/slope]}$ (Pfaffl, 2001). The melting curve also demonstrated that a specific product was amplified both in brain tissue and in a single cell.

The relative quantification using the $2^{-\Delta\Delta Ct}$ method (Livak and Schmittgen, 2001) revealed that the expression density of Kv4.2 and Kv4.3 were significantly higher in type I PVN neurons compared to type II neurons by 3.7±0.9 and 4.3±1.1 folds, respectively ($P<0.05$, Figure 9). The expression density of Kv1.2 and Kv1.3 were higher in type I neurons compared to type II neurons by 1.7±0.6 and 1.5±0.6

**Figure 8. Real-time PCR assay for Kv1.2 (A), Kv1.3 (B), Kv4.2 (C) and Kv4.3 (D) transcripts from brain tissue (upper) and a single cell (lower) using SYBR Green detection method.** Amplification plots in a logarithmic scale (left) and melt curve (right) were obtained from the StepOne software system. Standard curve (*inset*) was plotted with serial dilutions of rat brain tissue cDNA ($10^0$ to $10^4$). The melt curves illustrated one peak, which means that primers produced a single PCR product. These conditions enable primers to be applicable to single cell real-time PCR analysis since the Ct value detected from a single cell (lower) was in range of Ct values from dilution of brain tissue (upper).

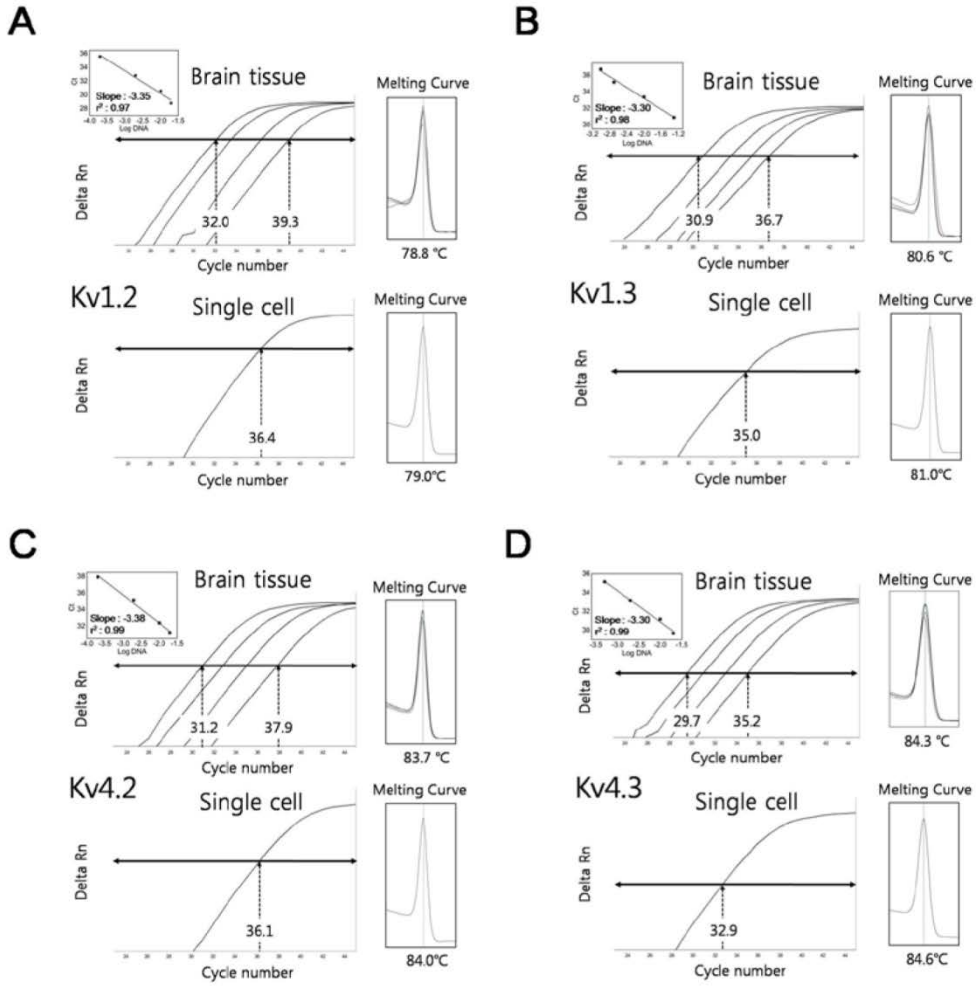
A
Brain tissue
Slope : -3.35
r² : 0.97
Log DNA
Delta Rn
32.0
39.3
Cycle number
Melting Curve
78.8 ℃
Kv1.2
Single cell
36.4
79.0℃
B
Brain tissue
Slope : -3.30
r² : 0.98
30.9
36.7
80.6 ℃
Kv1.3
35.0
81.0℃
C
Brain tissue
Slope : -3.38
r² : 0.99
31.2
37.9
83.7 ℃
Kv4.2
36.1
84.0℃
D
Brain tissue
Slope : -3.30
r² : 0.99
29.7
35.2
84.3 ℃
Kv4.3
32.9
84.6℃

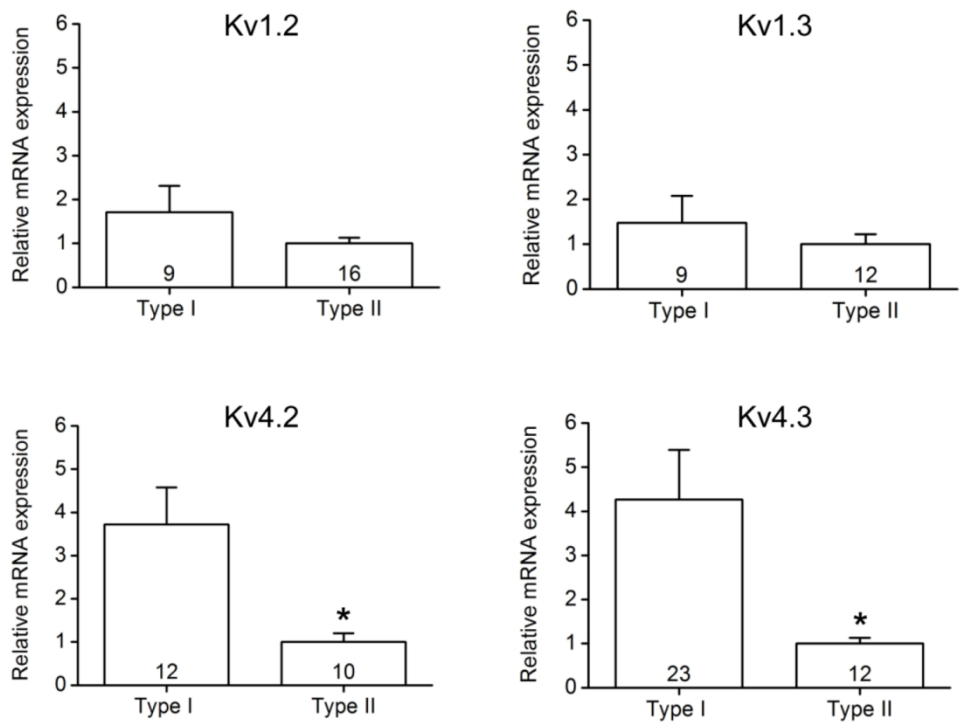


**Figure 9. Relative quantification of mRNA expressions of Kv channel subunits between type I and II neurons.** The mRNA densities of Kv1.2, Kv1.3, Kv4.2, and Kv4.3 expression were compared between type I and type II PVN neurons using single cell real-time RT-PCR. SYBR Green detection method and the $2^{-\Delta\Delta Ct}$ analysis were used for the relative quantification. The relative mRNA expression densities of Kv4.2 and Kv4.3 in type I neurons were significantly higher compared to type II neurons. Bar graphs represent the means ± SE (*$P$<0.05). Numbers in the bar represent total cell numbers examined.

folds, respectively; however, there was no significant difference ($P$>0.05). These results suggest that the relative mRNA density of Kv4.2 and Kv4.3 are important in determining the electrophysiological properties of type I and type II PVN neurons.

### *Delay time and co-expression of Kv channel subunits in type I PVN neurons*

I analyzed the relationship of co-expression of Kv channel subunits with delay time in the onset of the first action potential in type I PVN neurons. As shown in Figure 10A, the co-expression of Kv4 and Kv1 extended the delay time to 83.1±3.4 ms, as compared to the expression of either Kv4 (70.7±4.2 ms) or Kv1 (67.5±6.6 ms; one-way ANOVA with fisher LSD *post hoc*, $P$<0.05).

To investigate which Kv1 subunit affects delay time the most, I compared the delay time between the neurons expressing only Kv4 and the neurons expressing Kv4 and Kv1.x together. As shown in Figure 10B, cells expressing Kv4 with Kv1.3 significantly extended the delay (88.4±6.2 ms) compared to those expressing only Kv4 (70.7±4.2 ms). In the analysis of only Kv1 expression and co-expression with the Kv4.x, cells expressing Kv1 with Kv4.2 or Kv4.3 showed significantly longer delay (85.0±4.7 ms and 81.9±3.4 ms, respectively) than those expressing only Kv1 (67.5±6.6 ms, Figure 10C). These results indicate that co-expression with Kv1.3, Kv4.2, and Kv4.3, rather than single expression of Kv1 or Kv4, facilitates the delay in the onset of the first action potential in type I PVN neurons.

**Figure 10. Relation between delay time and Kv channel expression in type I PVN neurons. A**, PVN neurons expressing Kv1 and Kv4 together demonstrated longer delay time in the onset of the first action potential than the cells expressing Kv1 or Kv4 only. **B**, Co-expression of Kv4.x with Kv1.3 significantly extended the delay time in type I cells compared to cells expressing Kv4.x only. In comparison, expression of Kv4 with Kv1.1, Kv1.2, and Kv1.4 did not show significant difference in delay time. **C**, Co-expression of Kv1.x with Kv4.2 or Kv4.3 significantly extended the delay time in type I cells compared to cells expressing Kv1.x only. In comparison, expression of Kv1.x with Kv4.1 did not show significant difference in delay time. The bar graphs represent the means ± SE of the delay time. The numbers in the bar graphs represent the number of positive cells. * $P<0.05$ by one-way ANOVA with fisher LSD *post hoc* test.

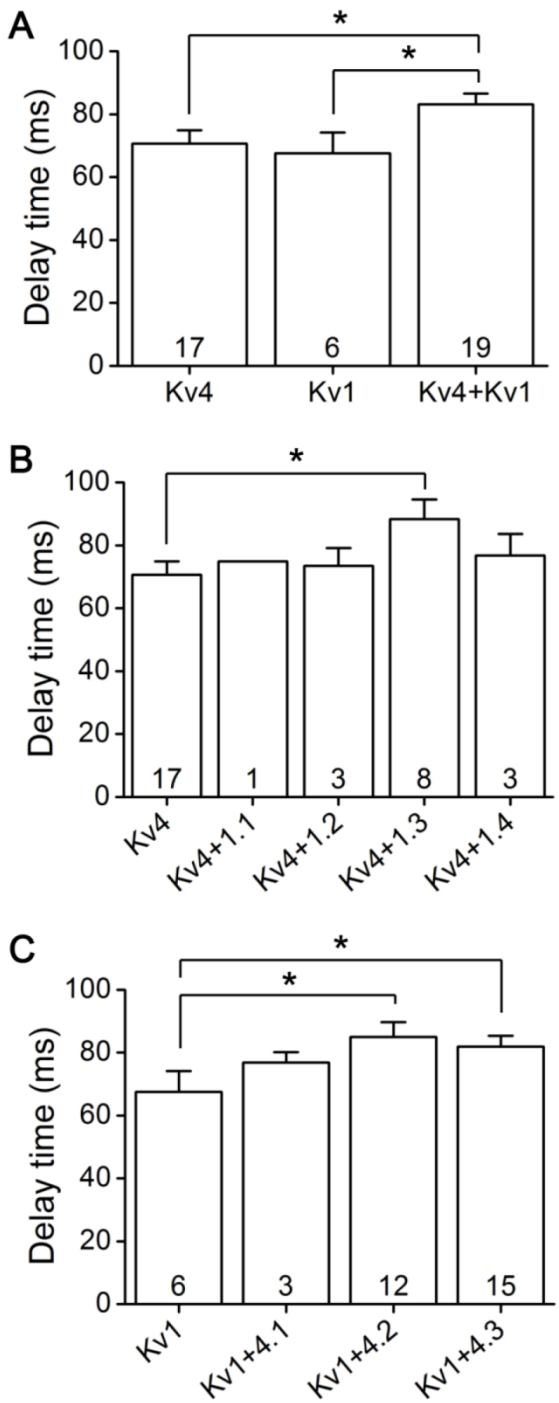
A
*
*
Delay time (ms)
100
80
60
40
20
0
17
6
19
Kv4
Kv1
Kv4+Kv1
B
*
Delay time (ms)
100
80
60
40
20
0
17
1
3
8
3
Kv4
Kv4+1.1
Kv4+1.2
Kv4+1.3
Kv4+1.4
C
*
*
Delay time (ms)
100
80
60
40
20
0
6
3
12
15
Kv1
Kv1+4.1
Kv1+4.2
Kv1+4.3

# DISCUSSION

The present study aimed to identify the Kv channels subunits that underlie different electrophysiological properties determining cell types of the PVN, by comparison of Kv channel expression profiles and expression density between type I and type II PVN neurons. Since PVN neurons are composed heterogeneously, even adjacent neurons display completely different function, which requires single cell analysis in studying PVN neurons. Thus, single cell RT-PCR and single cell real-time PCR analysis were performed to identify the differential profile of Kv channel expression and expression density between type I and type II PVN neurons.

In this study, I excluded the type II PVN neurons possessing LTS characteristics, which are known as pre-autonomic neurons. It has been identified that type II neurons displaying LTS express T-type $Ca^{2+}$ channels, specifically Cav3.1 (Lee et al., 2008). In addition, it has been recently verified that Cav channels and Kv channels influence their activities each other (Sonner et al., 2011) by direct physical coupling (Anderson et al., 2010). Consequently, the neurons I recorded and collected for this study were expected to be in the range of neuroendocrine magnocellular type I neurons and neuroendocrine parvocellular type II neurons. Immunohistochemical analysis has shown that magnocellular oxytocinergic and vasopressinergic neurosecretory cells correspond to electrophysiologically-characterized type I neurons (Hoffman et al., 1991). Similarly, type I PVN neurons examined in this study expressed mainly OT and VP, suggesting that they are correlated with the previously known magnocellular

neurosecretory neurons. However, type I neurons expressing neither OT nor VP were also observed. Previously, type I PVN neurons have been reported to consist of two distinct subsets of cells, weakly-rectifying and strongly-rectifying neurons, which are classified according to the absence or presence, respectively, of a hyperpolarizing notch in response to depolarizing current pulses injected at a hyperpolarized membrane potential (Luther et al., 2000). In this report, strongly-rectifying neurons displayed a more pronounced transient outward rectification and a longer delay to the first spike than weakly rectifying neurons. In this study, type I neurons exhibiting non-peptides expression displayed a significantly longer delay (123.2 ± 27.6 ms) than type I neurons expressing OT, VP, or OT/VP combination (70.6 ± 2.7 ms), suggesting that they could correspond to the strongly-rectifying neurons. This finding supports that electrophysiologically or biochemically distinct subtypes exist in type I PVN neurons.

Regarding type II neurons, they have been electrophysiologically characterized by the absence of a delay in the onset of the first action potential and the presence of an LTS (Luther and Tasker, 2000). These neurons were also subdivided into neurosecretory and non-neurosecretory cells depending on the absence or presence, respectively, of an LTS generated by a depolarizing pulse following a hyperpolarizing pulse (Luther et al., 2002). According to the immunohistochemical study, neuroendocrine CRH and TRH neurons are densely located in the dorsal zone of the medial parvocellular division and neuroendocrine VP and OT neurons are also detected in this area (Simmons and Swanson, 2009). These previous reports support that type II neurons examined in this study are closely related to neuroendocrine parvocellular neurons, based on the PVN region

where they were found and their characteristic of the absence of both a delayed onset and an LTS. Some ‘none’ cells negative for four peptides were detected in type II neurons. These neurons can be thought to have none of four peptides, or only a very small amount of the four peptides (below the limit of detection). Otherwise, they could be other peptides-expressing cells such as growth hormone-releasing hormone, somatostatin, and dopamine (Simmons and Swanson, 2009) which are reported to be expressed in the PVN.

Previous studies have revealed the expression of some Kv channel subunits in the PVN using immunohistochemistry (Chung et al., 2001; Sonner and Stern, 2007). Chung et al. (2001) examined the spatial localizations of Kv channels in the rat brain following transient focal ischemia. They found the increased expression of Kv1.2 in several brain regions, including PVN following ischemic insults. Sonner and Stern (2007) have studied the functional role of $I_A$ in PVN neurons projecting to RVLM, in which the immunoreactivities of Kv1.4 and Kv4.3 were observed. However, comprehensive comparison of specific Kv channel subunits responsible for differential electrophysiological properties between type I and type II PVN neurons is presently unknown.

In the present study, the mRNA expressions of Kv1.2, Kv1.3, Kv1.4, Kv4.1, Kv4.2, and Kv4.3 were observed in both types of PVN neurons. Kv1.1 was only detected in type I PVN neurons, not in type II PVN neurons, even though the occurrence of Kv1.1 was rare in type I PVN neurons. I also conducted immunohistochemical assays to confirm protein expressions for these Kv channel subunits. All Kv channel subunits’ immunoreactivities were observed within PVN. However, it was difficult to distinguish the spatial difference for Kv channel

subunits between the magnocellular division and the parvocellular division in the PVN, where type I and type II neurons, respectively, were mainly found. The reason could be due to the distribution characteristic of type I neurons, not exclusively restricted to the magnocellular division, but expanded throughout the PVN, as previously suggested (Luther et al., 2000).

Comparison of mRNA detection frequencies of Kv channels in this study suggests that the expression by itself may not be the critical factor in determining the electrophysiological properties of the PVN neurons. Therefore, I compared the expression densities of four different Kv channel subunits (Kv1.2, Kv1.3, Kv4.2, and Kv4.3) that showed recognizable detection rates in both type I and type II PVN neurons. Single cell real-time PCR analysis revealed a significant difference in mRNA levels of Kv4.2 and Kv4.3. Along with the frequency of the expression of Kv4.2 and Kv4.3 in the PVN neurons, these results suggest that both Kv4.2 and Kv4.3 are expected to be most contributive to the delay time of the first action potential in type I PVN neurons.

Kv channels can exist as tetrameric forms (MacKinnon, 1991), and this heteromerization gives rise to a variety of possible channel combination possessing different electrophysiological properties (Christie et al., 1990; Po et al., 1993). Based on the co-expression analysis (Figure 6), I suggest that various combinations of Kv channels may exist in type I and type II PVN neurons. In addition, the co-expression of Kv4 with Kv1.x, especially Kv1.3, facilitates the delay in the onset of the first action potential. These results suggest that fine-tuning mechanisms exist for determining the characteristics of type I neurons. Since various combinations of Kv channels are present in both type I and type II PVN neurons, there could be

delicate regulatory mechanisms that modulate the function of those neurons by regulating each Kv channel subunit expressed in each cell.

Since the PVN neurons were expected to be in the range of neurosecretory cells, I examined mRNA expressions of four peptides - OT, VP, CRH, and TRH - known to be primarily expressed in PVN neurons. Results revealed that a majority of type I neurons expressed VP and, to lesser extent, OT, and type II neurons displayed all four peptides in a variety of expression pattern. Regarding type I neurons, VP was expressed at a higher frequency than OT. There could be bias of sampling since the type I neurons examined in this study were mainly located in the posterior magnocellular division where VP neurons were found more than OT neurons (Simmons and Swanson, 2009). The type II neurons expressed a variety of peptides, but it is possible that other peptides not examined here exist in this type of neurons.

In addition, for insight into the correlation between the peptide phenotype and Kv channel subunit expression, I examined mRNA expressions of the Kv channel subunits in each of OT, VP, CRH, and TRH neurons (Figure 7). Surprisingly, Kv1.3 was not detected in type I neurons expressing OT or VP. However, it should be noted that sample size of neurons expressing none of four peptides is very small ($n$=2) because these neurons were very rarely detected. However, it is possible that ‘none’ cells shown in type I neurons could be a different subtype of the type I PVN neurons as the expression profile of Kv channels and delay time of the first action potential are distinct, compared with OT- or VP-expressing neurons. In type II neurons expressing peptides, the OT-containing type II neurons did not express Kv4.3 and the CRH-containing neurons

did not express Kv1.2.

At this point, the physiological relationship between OT or VP neurons and Kv channels is not yet clear, but the Kv channel subunits may be closely related to the roles of OT or VP. Regarding hypothalamic magnocellular neurosecretory neurons, OT and VP neurons have different exciting patterns for their optimal peptide release into neurohypophysis (Poulain and Wakerley, 1982). It has been demonstrated that diverse $K^+$ channels such as $Ca^{2+}$ activated $K^+$ channels (BK and SK channels) are involved in the neuronal activities of OT and VP neurons (Ohbuchi et al., 2010). Together, $I_A$ and $Ca^{2+}$ activated $K^+$ currents may exert an important role in regulating neuronal excitabilities of hypothalamic neuroendocrine neurons, ultimately, peptide release. Therefore, further studies on the functional relationship between the peptide phenotype and diverse $K^+$ channels, including Kv channel subunits, are required in the future.

Modulations of Kv channel expression, specifically Kv4.2 and Kv4.3, by extracellular factors such as hormones, growth factors, angiotensin II, and glutamate would be able to alter the electrophysiological characteristics of PVN neurons regulating firing frequency. It is very well established that $K^+$ channel gene expression is dynamically regulated (Levitan and Takimoto, 1998). Expression of Kv4.2 is regulated by estrogen and during pregnancy (Farkas et al., 2007; Suzuki and Takimoto, 2005). Angiotensin II suppressed $I_A$ in the magnocellular neurons of PVN by a direct action at AT1 receptors in the PVN (Li and Ferguson, 1996), and down-regulated Kv4.3 mRNA and protein expressions in neonatal rat cardiac myocyte, as a stimulator of cardiac myocyte hypertrophy (Zhang et al., 2001). $I_A$ was reduced by metabotropic glutamate receptor (group I receptor) activation in

the hypothalamic supraoptic nucleus (Schrader and Tasker, 1997). It has been demonstrated that $I_A$ density and intrinsic pacemaker frequency in dopaminergic substantia nigra neurons were highly correlated with the expression number of Kv4.3 (Liss et al., 2001). Therefore, those changes that occur in the PVN possibly affect excitability of the PVN neurons similar to other neuronal cells reported previously (Farkas et al., 2007; Roepke et al., 2007). In general, firing patterns of neurons are modulated by different expression levels of a variety of ion currents, especially $K^+$ currents (Baxter and Byrne, 1991; Llinas, 1988; Rudy, 1988). Similarly, the function of the PVN neurons controlling hormone secretion and autonomic outputs can be altered through modulation of firing patterns (Bicknell and Leng, 1981; Dutton and Dyball, 1979; Poulain and Wakerley, 1982).

Recently, it has been shown that the mRNA expression level of Kv4.3 was decreased in the RVLM-projecting PVN neurons in hypertensive rats along with increased expression of Cav3.1 encoding T-type $Ca^{2+}$ currents (Sonner et al., 2008; Sonner et al., 2011). In addition, Kv4.3 expression was down-regulated in the RVLM in rats with chronic heart failure (Gao et al., 2010). Also several Kv channels can be affected by hypoxia or ischemia condition (Chung et al., 2001). Thus, Kv channel regulation by various chemicals or in certain pathophysiological instances may provide the regulation mechanism of neuronal excitability in the PVN neurons. Further studies are warranted to evaluate the relation of Kv4.2 and/or Kv4.3 expression to the firing activities and, as a result, the change of the function of the PVN neurons in various circumstances. In addition, the function of Kv channels and Cav channels influence each other in hypertensive rats, at least through Kv4.3 and Cav3.1. These Kv4 and Cav3 channels make signaling complex

in regulating neuronal activity (Anderson et al., 2010; Sonner et al., 2011). Thus, the findings suggest that Kv4.2/ Kv4.3 (Kv4.2/Kv4.3 alone or in combination with other ion channels) in PVN neurons may be involved in regulation of neuronal activity, such as firing frequency in certain physiological and pathophysiological conditions.

Considering the dynamic regulation of Kv channel expression in neuronal cells (Levitan and Takimoto, 1998), this vibrant control of Kv channel expression could be related to the plasticity of PVN neurons by the Kv channel expression modifiers. Moreover, the result of the reduction in delay time of the first action potential by 4-AP (Kv channel blockers) suggests that type I PVN neurons may be converted to type II-like neurons. Previously, it has been demonstrated that elimination of Kv4.2 resulted in a delay in latency and suppression of excitability in cerebellar granule cells (Shibata et al., 2000). Therefore, these results suggest that characteristics of PVN neurons which are electrophysiologically defined as type I and type II could be interchangeable depending on the expression pattern, molecular composition, and expression density of certain Kv channel subunits. This could be another cellular plasticity mechanism, in addition to changes in synapses in PVN neurons, which is closely related to the adaptive function of neuroendocrine cells (Armstrong et al., 2002; Wamsteeker and Bains, 2010).

# CONCLUSIONS

Several Kv channel subunits exist both in type I and in type II PVN neurons and some of the Kv channels are co-expressed in a single PVN neuron. Among Kv channels expressed in PVN neurons, Kv4.2 and Kv4.3 are major contributors to distinct electrophysiological characteristics of type I PVN neurons. In addition, Kv4.x combinations with Kv1.x exert a synergistic effect on the delay time of type I PVN neurons. This would provide a molecular basis on studying specific Kv channel subunits for intrinsic electrophysiological properties. Moreover, this molecular diversity of Kv channels in the PVN neurons may provide the fine-tuning regulatory mechanisms of PVN neurons in controlling endocrine and autonomic systems.

# CHAPTER II

# Differential regulation of Kv4 channel subunits in rat presympathetic PVN neurons after myocardial infarction

# ABSTRACT

The hypothalamic paraventricular nucleus (PVN), the integrating center of neuroendocrine and autonomic functions, contains the presympathetic neurons, which control cardiovascular sympathetic outflow by projecting to the RVLM (PVN-RVLM). The modulation of neuronal excitability of the PVN-RVLM neurons during heart failure has been established, but little information is available at the molecular level. Here, this immunohistochemical study examined the regulation of Kv4.2 and Kv4.3, Kv channel subunits contributing to neuronal excitability, in the PVN-RVLM neurons of male rats following heart failure (8 weeks after coronary ligation). Results revealed that relatively less expressed Kv4.2 was up-regulated and dominantly expressed Kv4.3 was down-regulated in heart failure. These differential regulations reduced the remarkable difference between Kv4.2 and Kv4.3 expressions shown in the sham group. This finding that differentially expressed Kv4 subunits were differentially regulated suggests the possibility of distinct functions of Kv channel subunits and of the molecular dissection of Kv currents in the PVN-RVLM neurons.

# INTRODUCTION

The hypothalamic paraventricular nucleus (PVN) is an important integrating site in neuroendocrine and autonomic regulation (Swanson and Sawchenko, 1980). Of the neurons involved in autonomic regulation, the presympathetic neurons, which centrally control sympathetic nerve activities, project to the RVLM or to the spinal cord or send collaterals to both sites (Badoer, 2001; Chen and Toney, 2010; Pyner and Coote, 2000; Yang and Coote, 1998). Specifically, the PVN-RVLM neurons play a critical role in the regulation of cardiovascular sympathetic tone. The modulation in their neuronal excitabilities occurs during cardiovascular diseases, such as hypertension and heart failure (HF), and the altered excitability contributes to the sympathoexcitation observed in these pathological conditions (Allen, 2002; Dampney, 1994; Han et al., 2010; Sonner et al., 2008; Xu et al., 2012).

The Kv channels play important roles in controlling neuronal excitability in the brain. Kv4.2 and Kv4.3, the major subunits encoding $I_A$, which are characterized by rapid activation and inactivation, have been dominantly found in PVN where these subunits are considered to be the major molecular candidates responsible for characterizing electrophysiologically distinct subpopulations of the PVN (Lee et al., 2012). Recent studies using retrograde tracing have shown that Kv4.2 and Kv4.3 are expressed in the PVN-RVLM neurons and are significantly modulated by altered physiological conditions (Lee et al., 2013a; Sonner and Stern, 2007; Sonner et al., 2011). In relation to cardiovascular diseases in particular, Kv4.3 was down-regulated and $I_A$ was diminished in the PVN-RVLM neurons in

hypertensive rats, which suggests that a reduction in Kv4.3-mediated $I_A$ contributes to the elevated neuronal excitability of the PVN-RVLM neurons and finally to sympathoexcitation following hypertension (Sonner et al., 2011). Regarding HF, accumulating electrophysiological studies have revealed the elevated neuronal excitability of the PVN-RVLM neurons and sympathoexcitation following HF (Gao et al., 2010; Han et al., 2010; Xu et al., 2012), but little is known about the molecular modulation of Kv4, a major Kv channel subfamily expressed in the PVN-RVLM neurons.

In the present study, I hypothesized that Kv4.2 and Kv4.3 would be modulated in the PVN-RVLM neurons following HF, and I briefly explored expression changes of Kv4.2 and Kv4.3 using immunohistochemistry combined with retrograde tracing. Most recent studies have found that the PVN-RVLM neurons have subdivisionally discrete biochemical properties and display differential Kv4 modulation according to the subdivisions (Lee et al., 2013a; Lee et al., 2013b). Accordingly, I also examined the molecular regulation of Kv4.2 and Kv4.3 in each of the major subdivisions for PVN-RVLM neurons.

# MATERIALS AND METHODS

### *Animals*

Male Sprague-Dawley rats (5 wks old) were used (Orient Bio Inc., Kyonggi-do, Korea). The rats were maintained under a 12 hr light/dark cycle (lights on at 9:00 A.M.) and given free access to food and water until sacrifice. All surgical procedures were performed after anesthesia induced by an intraperitoneal injection of Zoletil (25 mg/kg) and xylazine (10 mg/kg). The experimental protocols were performed in accordance with the guidelines set by the Institutional Animal Care and Use Committee of Seoul National University and were approved by the Institute of Laboratory Animal Resources of Seoul National University (SNU-110221-4).

### *Rat model with myocardial infarction*

Rats were randomly assigned to either the sham-operated (sham) group or the myocardial infarction-operated (MI) group. The MI was induced by a ligation of the left coronary artery as previously described (Han et al., 2010) with a minor modification. The sham was equally processed but without the ligation. All animals were sacrificed 8 weeks after surgery. To assess the degree of myocardial infarction, hearts were isolated, weighed, and stored in 10% neutral-buffered formaldehyde for measurement of the infarct size for all animals. The heart was cut into four serial sections (2 mm thickness), and the infarct size was measured as the ratio of the infarction to the left ventricular circumference from each section using Image J

software (version 1.47). The MI rats that showed infarct sizes < 30% were excluded from this study.

### *Retrograde tracing*

Four or five days before sacrifice, a retrograde-transported fluorescent tracer, cholera toxin subunit B (CTB, Alexa 555-conjugated; Molecular Probes, Eugene, OR, USA) was injected unilaterally (~100 nl) into the RVLM, as described previously (Han et al., 2010; Lee et al., 2008), in order to identify the PVN neurons projecting to the RVLM. The coordinates were 13.5 mm caudal, 1.9 mm lateral, and 8.0 mm ventral, on average, from the bregma. To verify the RVLM injection site, serial medulla slices (100 μm thickness) were examined for all animals. Injections were located ventral to the nucleus ambiguus, within ~1 mm caudal to the facial nucleus.

### *Immunohistochemistry*

Eight weeks after coronary ligation, rats were anesthetized and perfused transcardially with 0.01 M phosphate-buffered saline (PBS, 150 ml) followed by 4% paraformaldehyde (PFA, 200-300 ml). Brains were removed, post-fixed in 4% PFA overnight at 4 ºC, and placed in 30% sucrose solution until the sample sank. Sections (30 μm) were cut using a sliding microtome, rinsed in PBS, and incubated in a solution of PBS with 0.1% Triton X-100 and 5% normal donkey serum for 2 hrs at room temperature. Sections were then incubated in the primary antibody solutions for Kv4.2 or Kv4.3 (rabbit polyclonal, 1:200 and 1:250, respectively;

Alomone Laboratories, Jerusalem, Israel) for 1 hr at room temperature and for 48 hrs at 4 ºC. Sections were rinsed in PBS and incubated in secondary antibody solutions (FITC-conjugated donkey anti-rabbit secondary antibody, 1:500; Jackson ImmunoResearch Laboratories, West Grove, PA, USA) for 2 hrs at room temperature. After washing, sections were mounted on glass slides and examined using confocal laser scanning microscopy (LSM 710; Zeiss, Oberkochen, Germany). The specificity of the antibody was assessed by a pre-incubation with peptides provided by the manufacturer.

# RESULTS

### *Confirmation of the rat myocardial infarction model*

Heart weight and infarct size were measured 8 weeks after coronary ligation or sham surgery. As shown in Figure 1A, gross examination of the heart transverse sections revealed a remarkable scar and thinning in the left ventricular wall (arrowhead) in the MI but no apparent damage in the sham. The infarct size was measured as a ratio of infarction to the circumference of the left ventricle, resulting in a mean value of 34.3±1.4% in the MI. There was no difference in body weight between the sham (465.3±22.9 g, $n$=4) and the MI (442.8±5.7 g, $n$=4), but the mean heart-to-body weight ratio was significantly higher in the MI (4.7±0.1 g/kg, $P$<0.05, Figure 1B) than in the sham (3.7±0.1 g/kg). A similar infarct size and heart weight increase have been described to be associated with the common hemodynamic characteristics observed in chronic HF in a rat model (Zhu et al., 2004).

### *Distribution of CTB-labeled, PVN-RVLM neurons*

Retrograde tracing was performed to identify the RVLM-projecting PVN neurons. The PVN-RVLM neurons were widely but differentially distributed along the rostrocaudal axis of the PVN. This differential distribution of the PVN-RVLM neurons was found to be associated with the location of the posterior magnocellular (pm) subdivision. Based on this, the PVN was classified into three distinct levels (Stocker et al., 2004). Level 1 (Figure 2, top), where the pm locates in the ventral

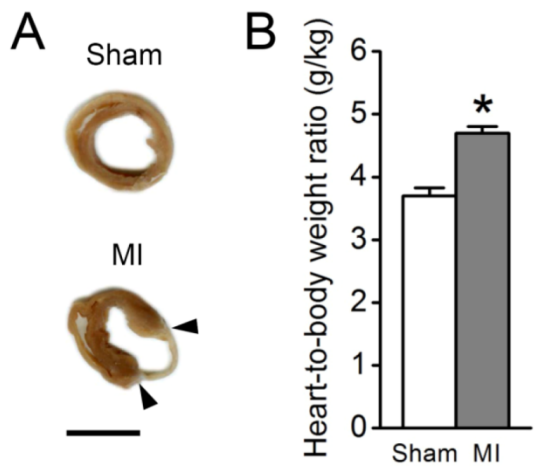


**Figure 1. Confirmation of the rat myocardial infarction model. A,** Examples of transverse sections of hearts from the sham and the myocardial infarction (MI). Arrowheads indicate the infarct area; scale bar=10 mm. **B,** Comparison of heart-to-body weight ratio (g/kg) between the sham and the MI. The heart weight increased in the MI compared to the sham (*$P$<0.05 by unpaired $t$-test).

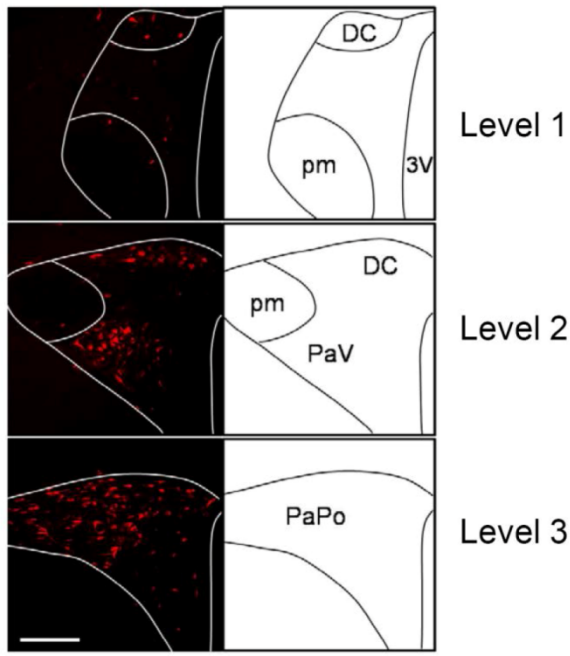


**Figure 2. Distribution of PVN-RVLM neurons.** Representative fluorescent photomicrographs show CTB-labeled PVN-RVLM neurons (left) at distinctive levels throughout the rostro-caudal extension. Level 1 is the most rostral and level 3 is the most caudal. PVN-RVLM neurons are prominently found in the three PVN subdivisions: the dorsal cap (DC), the ventral parvocellular (PaV), and the posterior parvocellular (PaPo), as indicated in the schematic drawings of the PVN (right). Scale bar= 0.2 mm; 3V, third ventricle; pm, posterior magnocellular subdivision.

aspect of the PVN, is the most rostral and had a few CTB-positive cells in the dorsal cap (DC) subdivision. Level 2 (Figure 2, middle), where the pm is in the mediolateral aspect, displayed a number of CTB-positive cells in the DC and the ventral parvocelluar (PaV) subdivision, which are exclusively segregated by the pm. Level 3 (Figure 2, bottom), where the pm is absent, contained a large amount of CTB-positive cells in the posterior parvocellular (PaPo) subdivision. The predominant distribution of the CTB-labeled cells in the specific subdivisions (DC, PaV, and PaPo) corresponds to the distributions of PVN-RVLM neurons shown previously (Stern and Zhang, 2003).

### *Expression of Kv4.2 and Kv4.3 in PVN-RVLM neurons*

To examine protein expressions of Kv4.2 and Kv4.3 in the PVN-RVLM neurons, an immunohistochemical study was performed on hypothalamic sections of a rat brain subjected to retrograde tracing. Figure 3A illustrates representative fluorescent images showing CTB-labeled PVN-RVLM neurons (red) and Kv4.2 immunoreactivity (Kv4.2-ir, green) in the PVN at the three distinct levels. To clearly examine fluorescent signals in a single PVN neuron, PVN subdivisions were magnified at a higher resolution (Figure 3B) to show CTB-labeling (top), Kv4.2-ir (middle), and the co-localization of the two fluorescent signals (bottom). Figure 4A illustrates representative fluorescent images showing CTB-labeled PVN-RVLM neurons (red) and Kv4.3 immunoreactivity (Kv4.3-ir, green) in the PVN at the three distinct levels. The magnified images (Figure 4B) more clearly show CTB-labeling (top), Kv4.3-ir (middle), and the co-localization of the two fluorescent signals (bottom) in a single PVN neuron.

**Figure 3. Expression of Kv4.2 in PVN-RVLM neurons. A,** Representative fluorescent photomicrographs of the PVN at the three distinctive levels show CTB-labeled PVN-RVLM neurons (red) and Kv4.2 immunoreactivities (green) in an MI rat. Scale bar= 0.2 mm; 3V, third ventricle. **B,** At each level, PVN subdivisions (box area in [a]) are magnified at a higher resolution to more clearly depict CTB-Kv4.2 doubly labeled neurons. CTB-labeled PVN-RVLM neurons are shown at the top, and Kv4.2-immunoreactive cells are shown in the middle. Both photographs are merged in the bottom. Arrows point to CTB-Kv4.2 doubly labeled neurons; scale bar= 0.1 mm.

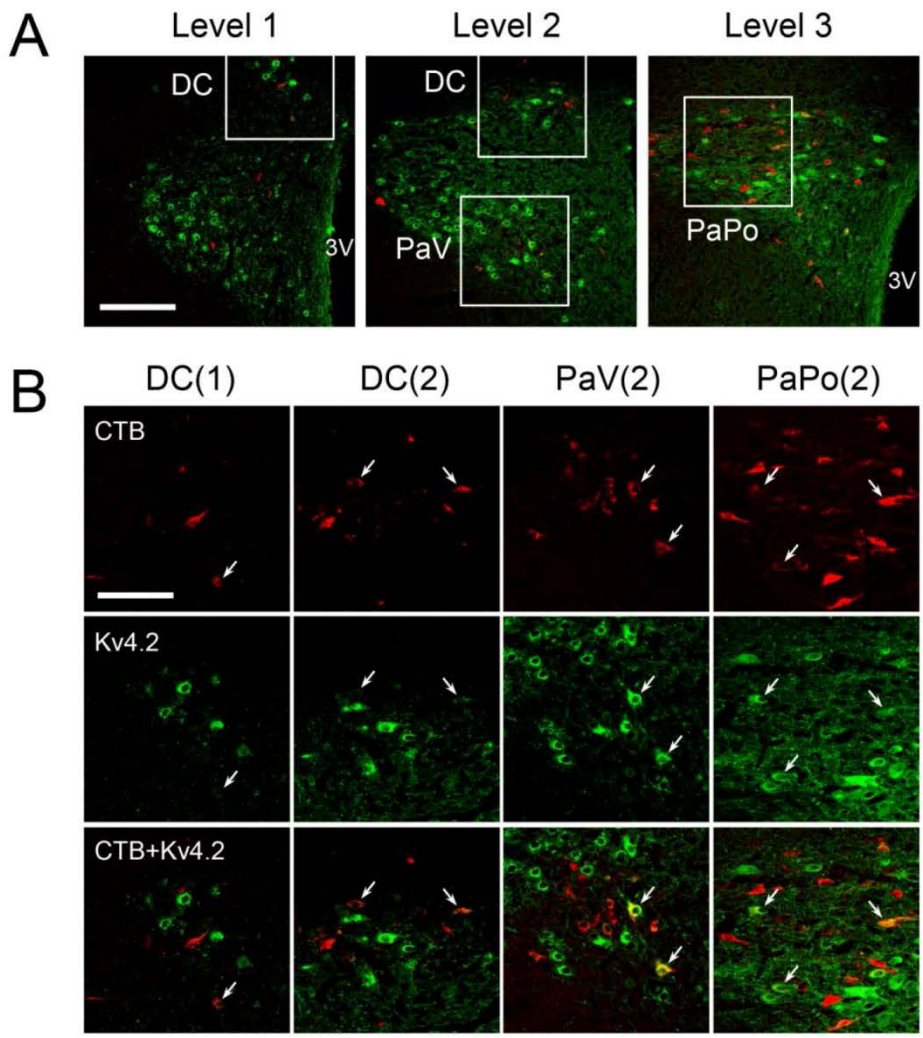
A
Level 1
Level 2
Level 3
DC
DC
PaV
PaPo
3V
3V
B
DC(1)
DC(2)
PaV(2)
PaPo(2)
CTB
Kv4.2
CTB+Kv4.2

**Figure 4. Expression of Kv4.3 in PVN-RVLM neurons. A,** Representative fluorescent photomicrographs of the PVN at three distinctive levels show CTB-labeled PVN-RVLM neurons (red) and Kv4.3 immunoreactivities (green) in a sham rat. Scale bar= 0.2 mm; 3V, third ventricle. **B,** At each level, PVN subdivisions (box area in [a]) are magnified at a higher resolution to more clearly depict CTB-Kv4.3 doubly labeled neurons. CTB-labeled PVN-RVLM neurons are shown at the top and Kv4.3-immunoreactive cells are shown in the middle. Both photographs are merged in the bottom. Arrows point to CTB-Kv4.3 doubly labeled cells; scale bar= 0.1 mm.

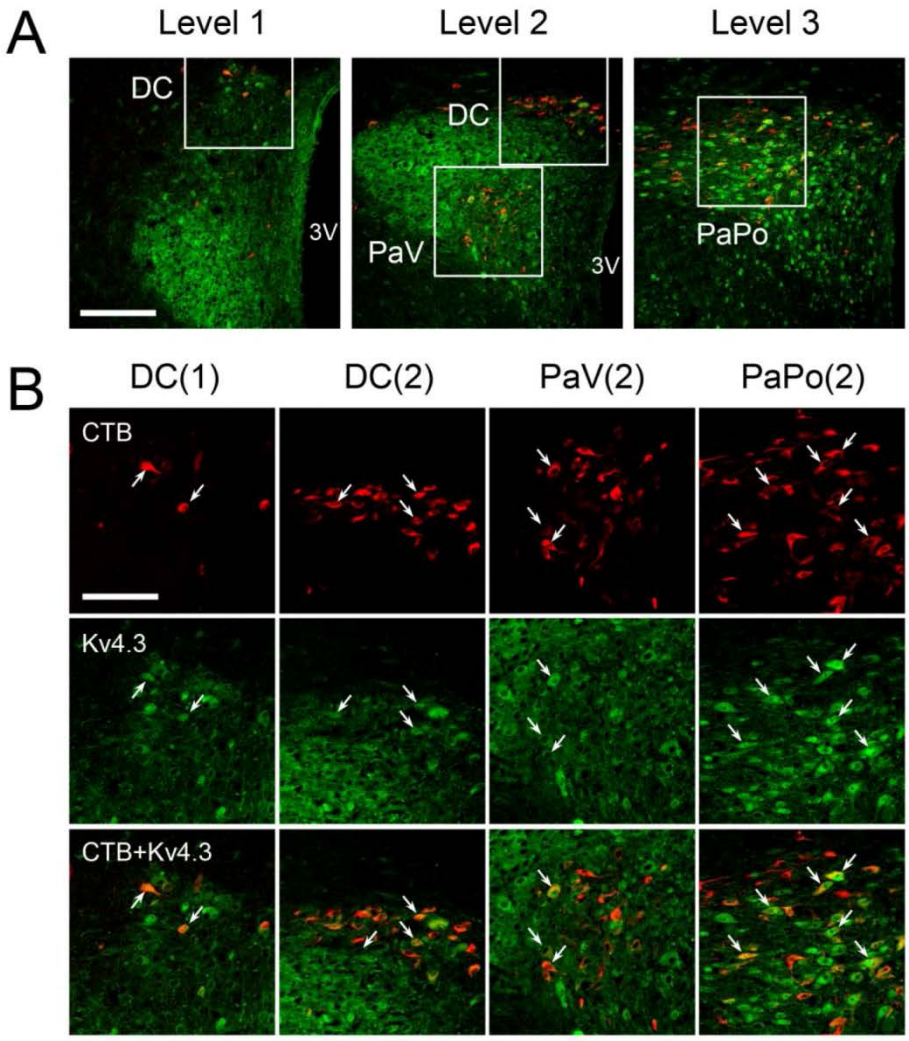
A
Level 1
Level 2
Level 3
DC
3V
DC
PaV
3V
PaPo
B
DC(1)
DC(2)
PaV(2)
PaPo(2)
CTB
Kv4.3
CTB+Kv4.3

### *MI-induced regulation of Kv4.2 and Kv4.3 in PVN-RVLM neurons*

To compare Kv4.2 protein expressions in the PVN-RVLM neurons between the sham and the MI, the proportion of Kv4.2-CTB doubly labeled cells in the CTB-labeled neurons was measured (Figure 5). Almost one-third of the PVN-RVLM neurons (29% [240/815]) expressed Kv4.2 in the sham, while nearly one-half of PVN-RVLM neurons (45% [524/1167]) did so in the MI, showing a significant increase in the MI. For each of the major subdivisions where the PVN-RVLM neurons were dominantly distributed, the MI showed a higher expression of Kv4.2 in the PVN-RVLM neurons compared to the sham (DC at level 2 [DC(2)], sham 24% [35/147] and MI 39% [88/136]; PaV, sham 26% [88/338] and MI 45% [198/444]; PaPo, sham 38% [108/284] and MI 48% [232/483]) except for DC at level 1 (DC(1), sham 20% [9/46] and MI 37.5% [6/16]). Additionally, I analyzed differences in Kv4.2 expression between subdivisions in each of the sham and the MI. For the sham, the Kv4.2 expression was significantly higher in the PVN-RVLM neurons of the PaPo(3) compared to the DC(1), DC(2), and PaV(2) ($P$<0.05). However, for the MI, this specific difference was not observed.

The differences in the proportion of the PVN-RVLM neurons expressing Kv4.3 between the sham and the MI are summarized in Figure 6. Kv4.3 was observed in over three-fourths of the PVN-RVLM neurons (73% [837/1153]) in the sham but only in two-fifths of the PVN-RVLM neurons (39% [340/869]) in the MI, showing a significant decrease in the MI. For each of the subdivisions, Kv4.3 expression by the PVN-RVLM neurons was significantly decreased in the MI compared to the sham (DC(1), sham 77% [83/64] and MI 39% [9/23]; DC(2), sham 75% [164/197] and MI 42% [104/247]; PaV, sham 68% [271/401] and MI 32%

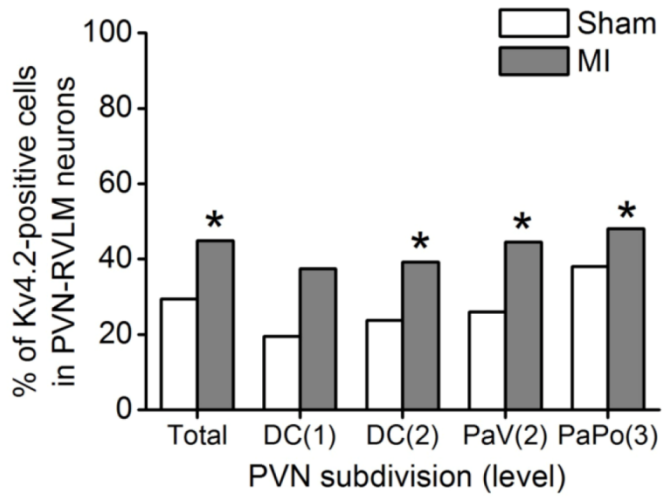


**Figure 5. MI-induced modulation of Kv4.2 in PVN-RVLM neurons.** Bar graphs indicate he proportion of CTB-Kv4.2 doubly labeled cells in the CTB-labeled neurons. The proportion between the sham and the MI was compared for the PVN overall and for each of the subdivisions. Kv4.2 expression was significantly increased in the MI compared to the sham; *$P$<0.05 for sham vs. MI (chi-squared test). DC(1) and DC(2), dorsal cap at level 1 and level 2, respectively; PaV(2), ventral parvocellular subdivision at level 2; PaPo(3), posterior parvocellular subdivision at level 3.

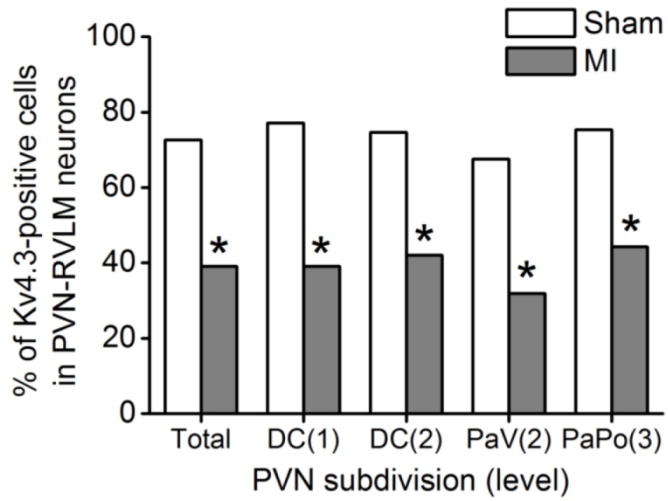


**Figure 6. MI-induced modulation of Kv4.3 in PVN-RVLM neurons.** Bar graphs indicate the proportion of CTB-Kv4.3 doubly labeled cells in the CTB-labeled neurons. The proportion between the sham and the MI was compared for the PVN overall and for each of the subdivisions. Kv4.3 expression was significantly decreased in the MI compared to the sham; *$P$<0.05 for sham vs. MI by (chi-squared test). DC(1) and DC(2), dorsal cap at level 1 and level 2, respectively; PaV(2), ventral parvocellular subdivision at level 2; PaPo(3), posterior parvocellular subdivision at level 3.

[99/310]; PaPo, sham 75% [305/405] and MI 44% [128/289]). Additionally, I analyzed the difference in Kv4.3 expression between subdivisions for each of the sham and the MI. For the MI, Kv4.3 expression was significantly lower in the PVN-RVLM neurons of the PaV(2) compared to the DC(2) and PaPo(3) ($P<0.05$). However, for the sham, this specific difference was not observed.

# DISCUSSION

The immunohistochemical experiment combined with retrograde tracing revealed that Kv4.2 and Kv4.3 proteins are expressed in the PVN-RVLM neurons. The majority (73%) of the PVN-RVLM neurons expressed Kv4.3, whereas fewer cells (29%) expressed Kv4.2, thus showing a predominant expression of Kv4.3 compared to Kv4.2. Following HF, both Kv4.2 and Kv4.3 were regulated, but Kv4.2 increased and Kv4.3 decreased, by which the large difference between Kv4.2 and Kv4.3 expressions observed in the sham was remarkably reduced in the MI (45% for Kv4.2 and 39% for Kv4.3). This type of change was observed in each of the subdivisions for the PVN-RVLM neurons.

A modulation of Kv4.2 and Kv4.3 by HF has been demonstrated mostly in the heart and brain. In cardiac myocytes obtained from post-infarction, both Kv4.2 and Kv4.3 were down-regulated, and $I_A$ concomitantly decreased, suggesting that the reduction in Kv4.2- and Kv4.3-mediated $I_A$ alters the action potential waveform, which contributes to the cardiac hypertrophy generally observed in a failing heart (Kaprielian et al., 1999; Li et al., 2008). In the rat brain, the RVLM, an important center for cardiovascular sympathetic regulation, displayed a down-regulation of Kv4.3 during HF, suggesting that its reduction is correlated with sympathoexcitation of MI rats (Gao et al., 2010). A recent study showed the modulation of Kv4.3 in the PVN-RVLM neurons in a hypertensive state in which Kv4.3 was down-regulated with $I_A$ diminished and neuronal excitability increased, suggesting that this subunit contributes to blunted $I_A$ functions during hypertension

(Sonner et al., 2011). Although direct evidence on the modulation of $I_A$ in the PVN-RVLM neurons under an HF condition has not been reported, studies have shown elevated neuronal excitability of the PVN-RVLM neurons as an apparent consequence following HF (Han et al., 2010; Xu et al., 2012). Accordingly, it is expected that in HF, as in hypertension, Kv4.3, possibly in association with $I_A$ functions, may be one of the major molecular components contributing to the increase in neuronal excitability of the PVN-RVLM neurons. However, further study is required to confirm this speculation.

In contrast to Kv4.3, Kv4.2 was unexpectedly up-regulated in the PVN-RVLM neurons during HF. From the perspective that Kv4.2 and Kv4.3 are members of the same subfamily underlying $I_A$ in the brain, Kv4.2 would be expected to be down-regulated in the same fashion as Kv4.3 in the PVN-RVLM neurons, as shown in cardiac myocytes (Kaprielian et al., 1999; Li et al., 2008). However, the investigation of Kv4 channel subunits in presympathetic neurons related to cardiovascular disorders has been confined to Kv4.3 (Gao et al., 2010; Sonner et al., 2011). To date, little is known about Kv4.2 modulation in presympathetic neurons, which may be due to less or rare detection of Kv4.2 in these neuronal populations in a normal state (Sonner and Stern, 2007). In agreement with this, results in this study also showed a lower detection of Kv4.2 compared to Kv4.3. Furthermore, Kv channel subunits showed differential regulation among each other even though they are members of the same subfamily. Following postnatal ages, Kv1 subunits were differentially regulated in ventricular myocytes - Kv1.2 and Kv1.5 increased whereas Kv1.4 decreased (Xu et al., 1996). This differential regulation is possibly attributed to the distinct current

characteristic of Kv1.4 from the other members of the Kv1 subfamily, which is similar to Kv4-mediated $I_A$ (Po et al., 1993). Nevertheless, the regulation pattern of Kv1.4 is not necessarily consistent with that of the Kv4 channels (Kaprielian et al., 1999; Xu et al., 1996). Therefore, Kv channel subunits are not uniformly but rather diversely regulated dependent on cell types where they are expressed or on physiological traits so that the differential regulation of Kv4.2 and Kv4.3 in the PVN-RVLM neurons in HF is conceivable.

This differential regulation of Kv4.2 and Kv4.3 suggests different functional roles of the two subunits. It is possible that Kv4.3 is the primary component for $I_A$ functions in the PVN-RVLM neurons and Kv4.2 is the secondary component that plays a compensatory role for $I_A$ loss in altered physiological conditions, such as hypertension. Research has previously demonstrated the compensatory roles of Kv channels to maintain neuronal firing properties when a specific functional Kv subunit was deleted (Nerbonne et al., 2008). In addition, Kv4.2 and Kv4.3 have shown different expressions temporally during neuronal development (Huang et al., 2006). Therefore, the up-regulation of Kv4.2 may be a compensatory action in response to the decrease of Kv4.3 in HF, finally preventing the elevation of neuronal excitability of the PVN-RVLM neurons following HF. The protective role of Kv4.2 against cell death by increasing neuronal excitability has been suggested (Huang et al., 2006). The results presented here that dominantly expressed Kv4.3 decreased and the relatively less expressed Kv4.2 increased during HF support such a functional possibility of Kv4.2 and Kv4.3 in the PVN-RVLM neurons.

It is possible that Kv4.2 and Kv4.3 are differentially regulated

independently of each other according to their specific functions. Recent studies have demonstrated the distinct roles of the two subunits in shaping the action potential waveform and in regulating neuronal excitability and have suggested their functional independency in cortical pyramidal neurons (Carrasquillo et al., 2012; Norris and Nerbonne, 2010). Therefore, Kv4.2 and Kv4.3 could play distinct roles in determining neuronal excitability of the PVN-RVLM neurons, and could be differentially regulated in independent ways suitable for their individual functions. In this view, the increase in Kv4.2 expression in HF is notable because it suggests that the contribution of Kv4.2 in the PVN-RVLM neurons was strengthened to a similar or slightly higher level of the remains of Kv4.3. However, the functional effects on the PVN-RVLM neurons by the increase in Kv4.2 expression and the decrease in Kv4.3 expression remain to be confirmed.

# CONCLUSIONS

The present study provides the first evidence of the regulation of Kv4.2 in the presympathetic PVN neurons in HF and the differential regulation of Kv4.2 and Kv4.3 in opposing directions. This differential regulation was consistent for all subdivisions. The finding that differentially expressed Kv4 subunits are differentially regulated in HF suggests the possibility of distinct functions of Kv4 subunits and of molecular dissection of Kv currents encoded by different subunits in the PVN-RVLM neurons. This study provides important evidence to be used in further research of neuronal functions and modulations in the hypothalamic presympathetic neurons related to cardiovascular pathology.

# CHAPTER III

# Selective regulation of Kv channels in rat presympathetic PVN neurons by estrogen replacement

# ABSTRACT

The hypothalamic paraventricular nucleus (PVN) is an important site in the regulation of the autonomic nervous system. Specifically, PVN neurons projecting to the rostral ventrolateral medulla (PVN-RVLM) play a regulatory role in the determination of the sympathetic outflow in the cardiovascular system. In the PVN-RVLM neurons, the estrogen receptor β is expressed. However, to date, the effects of estrogen on the PVN-RVLM neurons have not been reported. The present study investigated estrogen-mediated modulation of the two Kv channel subunits, Kv4.2 and Kv4.3, which are expressed predominantly in PVN neurons, and $I_A$, the functional current of Kv4.2 and Kv4.3. Single-cell real-time RT-PCR analysis showed that 17β-estradiol (E2) replacement (once daily for 4 days) selectively down-regulated Kv4.2 mRNA levels in the PVN-RVLM neurons of ovariectomized female rats. There was no change in Kv4.3 levels. Whole-cell patch-clamp recordings demonstrated that E2 also diminished $I_A$ density. Interestingly, these effects were most apparent in the dorsal cap parvocellular subdivision of the PVN. E2 also reduced a delay in the excitation of the PVN-RVLM neurons. These findings demonstrate that E2 exerts an inhibitory effect on the functions of $I_A$, potentially by selectively down-regulating Kv4.2 but not Kv4.3 in the PVN-RVLM neurons distributed in a specific parvocellular subdivision.

# INTRODUCTION

The hypothalamic paraventricular nucleus (PVN) is an important site of neuroendocrine and autonomic control and has distinct subpopulations with different morphological and anatomical characteristics. The magnocellular cells project to the pituitary gland, and the parvocellular cells project to the median eminence, brain stem, and spinal cord (Swanson and Kuypers, 1980). Within the parvocellular cells, the presympathetic neurons project directly to the intermediolateral column in the spinal cord where the sympathetic preganglionic nuclei are concentrated or project indirectly via the rostral ventrolateral medulla (RVLM) to influence cardiovascular sympathetic outflows (Pyner and Coote, 2000). The RVLM contains vasomotor neurons, which regulate tonic and phasic vasomotor tone (Dampney, 1994). Several previous studies have revealed the important role of PVN-RVLM pathways in the regulation of the cardiovascular system (Badoer, 2001; Chen and Toney, 2010; Yang and Coote, 1998).

Estrogen, a typical ovarian hormone, influences homeostatic function, reproduction, and the immune system (Clegg, 2012; Grossman, 1985). Estrogen regulates gene transcription by binding the nuclear estrogen receptor, which contains two subtypes, α (ER-α) and β (ER-β) (Nilsson et al., 2001). The two different subtypes have been shown to be expressed widely in rat brain and distributed differentially across different regions of the brain, of which PVN exclusively expresses ER-β (Shughrue et al., 1997). The distributional pattern of ER-β in the PVN is similar to that of the parvocellular cells projecting to the brain

stem or spinal cord (Alves et al., 1998; Hrabovszky et al., 1998). This similarity was confirmed by the observation that the PVN-RVLM neurons identified by retrograde tracing expressed ER-β (Stern and Zhang, 2003). The aforementioned studies potentially indicate that the PVN-RVLM neurons could be major target cells for estrogen within the PVN (Alves et al., 1998; Hrabovszky et al., 1998; Shughrue et al., 1997; Stern and Zhang, 2003). However, the effects of estrogen on this specific cell population have not been studied.

Similar to other neurons, $K^+$ channels control the firing activity of the PVN-RVLM neurons (Chen and Toney, 2009; Sonner and Stern, 2007). Studies have demonstrated that $I_A$ plays an important role in controlling the membrane excitability and firing discharge of the PVN-RVLM neurons and that it contributes to remodeling neuronal excitation under pathological conditions (Sonner and Stern, 2007; Sonner et al., 2008). $I_A$ is encoded by homomultimeric or heteromultimeric complexes of Kv channel subunits within identical subfamilies (Covarrubias et al., 1991; Serodio et al., 1996). Among those, Kv1.4 and Kv4.3 have been suggested to be molecular correlates of $I_A$ in the PVN-RVLM neurons based on their strong immunoreactivities (Sonner and Stern, 2007). The recent observation that Kv4.3 mRNA expression decreased coincident to diminished $I_A$ in hypertensive rats (Sonner et al., 2011) supports the correlation of Kv4.3 and $I_A$ in the PVN-RVLM neurons. The previous study showed that Kv4.2 and Kv4.3 mRNAs were abundant in PVN neurons and that the differential expression of Kv4.2 and Kv4.3 was parallel to the differences in the delay in the onset of the first action potential (Lee et al., 2012) that is known to be associated with $I_A$ in the PVN neurons (Luther and Tasker, 2000). This suggests that these subunits are closely related to $I_A$ in the PVN

neurons. Taken together, Kv4.2 and Kv4.3 are most likely molecular components underlying $I_A$ in the PVN, including the PVN-RVLM neurons.

Several studies have reported estrogenic regulation of Kv4.2 or Kv4.3 transcript levels in tissues from distinct organs, such as the heart (Eghbali et al., 2005; Saito et al., 2009) and uterus (Song et al., 2001), as well as in a hormone-producing brain cell line (Farkas et al., 2007), indicating that Kv4.2 and Kv4.3 are widely expressed target molecules that are modulated by estrogen. Furthermore, these studies have shown that alternations in transcript levels of these subunits coincide with changes in $I_A$.

Hence, I hypothesized that estrogen would modify Kv4.2 and Kv4.3 transcript levels in the PVN-RVLM neurons and investigated changes in the mRNA levels of these subunits in the PVN-RVLM neurons of ovariectomized female rats (OVX-rat) by 17β-estradiol (E2) replacement, using single cell real-time RT-PCR. Additionally, the study examined alternations in the current density and kinetic properties (activation and inactivation) of $I_A$ using whole cell patch-clamp recording.

# MATERIALS AND METHODS

## *Animals*

Sprague-Dawley female rats (*n*=36, 7 wks old) were used (Orient Bio Inc., Kyonggi-do, Korea). The rats were maintained under a 12-hr light/dark cycle (lights on at 9:00 A.M.) and given free access to food and water until sacrifice. Anesthesia was induced by an intraperitoneal injection of Zoletil (25 mg/kg) and xylazine (10 mg/kg) for the surgical procedure. Animals were bilaterally ovariectomized (OVX). Every effort was made to minimize the number of animals and their suffering. The experimental protocols were performed in accordance with the guidelines of the Institutional Animal Care and Use Committee of Seoul National University and were approved by the Institute of Laboratory Animal Resources of Seoul National University (SNU-100917-1).

## *Retrograde tracing*

One week after OVX, the retrograde-transported fluorescent tracer (FluoSphere-Red; Molecular Probes, Eugene, OR, USA), was injected into the RVLM of OVX-rats to identify PVN-RVLM neurons, as previously described (Han et al., 2010). The injection point was, on average, 12.5 mm caudal, 1.7 mm lateral, and 8.0 mm ventral from bregma. To verify that dye was injected into the RVLM, serial medulla slices (100 μm thicknesses) of all animals subjected to retrograde tracing were examined after sacrifice.

### *E2 treatment*

Treatments began on the fourth day after the retrograde tracing process. Rats were divided into two groups: the oil-treated group (oil-group) and the 17β-estradiol-treated group (E2-group). The treatments were given once daily for four consecutive days prior to sacrifice and brain slice preparation; subcutaneous injections of corn coil (0.1 ml; Sigma-Aldrich, St. Louis, MO, USA) and 17β-estradiol-3-benzoate (25 μg/kg in 0.1 ml corn oil; Sigma-Aldrich) were administered to the oil-group and the E2-group, respectively. The quality of treatments was assessed by comparing serum E2 concentrations, body weight gain rates, and uterus weights between the two groups. Serum E2 concentrations were measured using the Estradiol ELISA kit (Labor Diagnostika Nord GmbH & Co. KG, Nordhorn, Germany; sensitivity, 10 pg/ml) according to the manufacture's manual. Blood samples were collected from the abdominal vein of rats before sacrifice, allowed to cluster for 30-40 min at room temperature, and centrifuged for 25 min at 4 °C. The serum layers were removed carefully into new tubes, and stored in -70 °C until used for the ELISA assay. Body weight was measured before every treatment for all animals. The ratio of increased body weight on each day to the weight on the first day of treatment was used for the body weight gain rate. Uteri were isolated after sacrifice, weighed, and normalized to body weights on the day of sacrifice.

### *Hypothalamic slice preparation*

Hypothalamic brain slices were prepared within 2 hrs after the fourth treatment as previously described (Han et al., 2010) and used for single cell real-time RT-PCR

or electrophysiological recording. After anesthesia, a rat was perfused transcardially with the ice-cold sucrose-rich ACSF containing (in mM) 210 sucrose, 26 $NaHCO_3$, 5 KCl, 1.2 $NaH_2PO_4$, 1.2 $CaCl_2$, 2.4 $MgCl_2$, and 10 glucose. The brains were briefly removed and dissected to two or three coronal slices (300 μm), including PVN regions, using a vibrating tissue slicer (Vibratome 1000 plus, Vibratome Company, St. Louis, MO, USA). The slices were incubated in an oxygenated normal ACSF containing (in mM) 126 NaCl, 26 $NaHCO_3$, 5 KCl, 1.2 $NaH_2PO_4$, 2.4 $CaCl_2$, 1.2 $MgCl_2$, and 10 glucose for 1 hr at 30 °C until used.

### *Single-cell real-time RT-PCR*

To gain RNAs of the PVN-RVLM neurons for real-time RT-PCR, the hypothalamic brain slice was transferred to the same recording chamber as that used for electrophysiological recording, perfused continuously with an oxygenated ACSF (4-5 ml/min), and maintained at 30-32 °C. The fluorescent-labeled PVN-RVLM neurons were visualized by combining differential interference contrast video microscopy with a fluorescence microscope installed with a green filter cube (WG, Olympus, Tokyo, Japan). The cells were approached with patch pipettes, using a micromanipulator (MP-225, Sutter instruments, Novato, CA, USA), that were pulled from borosilicate glass capillaries (1.7 mm diameter and 0.5 mm wall thickness) and filled with nuclease-free water (Qiagen). After the whole cell configuration was achieved, a slight negative pressure was applied to pull the cytoplasm contents of each cell into the pipette, taking care to avoid including the nucleus. Each mixture of cytoplasm and water was immediately removed into a prepared microtube containing (μl) 4 of nuclease free water (Qiagen) and 1 of

RNase Inhibitor (Applied Biosystems). Reverse transcription for single-cell cDNA preparations was carried out using High Capacity cDNA Reverse Transcription Kits (Applied Biosystems) according to the manufacturer's instructions.

PCR amplification was induced with a fraction of the single cell cDNA using the StepOnePlus System (Applied Biosystems) with SYBR Green detection for Kv4.2 and Kv4.3. SYBR Green detection was carried out as previously described with a minor modification (Lee et al., 2012). The primer sequences used for real-time RT-PCR were listed in Table 1. The real-time PCR reactions were prepared by mixing (in μl) 2 of the cDNA template, 0.2 each of 10 μM forward and reverse primers, 0.4 of 50x Rox dye, 10 of 2x SYBR master mix (SYBR premix Ex Taq, Takara Bio Inc.), and nuclease free water. The total volume was 20 μl. The thermal protocol was as follows: pre-denaturation at 95 °C for 10 sec, 50 cycles of denaturation at 95 °C for 5 sec and annealing at 60 °C for 25 sec, and the melt curve step to verify the specificity of the PCR products. All samples were run in duplicate. Negative controls were assessed by running RT without the reverse transcript. Kv4.2 and Kv4.3 mRNA expression was compared between the oil-group and the E2-group using relative quantitative analysis (Livak and Schmittgen, 2001). The threshold cycle (Ct) value of Kv4.2 and Kv4.3 was normalized to that of a reference gene, β-actin, in identical cells. Final values were expressed as the n-fold of Kv4.2 or Kv4.3 transcript levels in the E2-group to those in the oil-group. Primer efficiencies for each target and reference gene were calculated from the formula $E=10^{[-1/slope]}$ (Pfaffl, 2001), where slope was obtained from the relationship between serial cDNA dilutions and Ct values, resulting in 98% for Kv4.2, 101% for Kv4.3, and 98% for β-actin. The Ct values of β-actin were similar across the cells (coefficient of variation=3%), between the groups, and among plates.

**Table 1. Primer sequences for single cell real-time RT-PCR.**

| Target (Acc. No.) | Sequence | Product size (bp) |
|---|---|---|
| Kv4.2 (NM_031730) | 5'-ACAAACGAAGGGCACAGAAGA-3'<br>5'-CATGTAGGCATTTGCACTTCCA-3' | 77 |
| Kv4.3 (NM_031739) | 5'-AACGCAGGGCACAGAAGAAG-3'<br>5'-GGCATTGGAGCTCCCTGTT-3' | 68 |
| β-actin (NM_031144) | 5'-CATTGCTGACAGGATGCAGAA-3'<br>5'-AGAGCCACCAATCCACACAGA-3' | 109 |

### *Electrophysiological recording*

A brain slice was placed in a recording chamber and perfused, and the fluorescent-labeled PVN-RVLM neurons were visualized as describe above (see single-cell real-time RT-PCR). Patch pipettes were prepared from the same glass capillaries as above, but filled with the internal solution containing (in mM) 135 K-gluconate, 5 KCl, 20 HEPES, 0.5 $CaCl_2$, 5 EGTA, and 5 MgATP (The pH was adjusted to 7.2 with KOH). The open resistance of the pipette ranged from 3 to 7 MΩ. The Axoclamp 2B amplifier (Molecular Devices, Foster City, CA, USA) was used for whole cell recordings. The signals were filtered at 1 kHz and digitized at 10 kHz using an analog-digital converter (Digidata 1320A, Molecular Devices) and pClamp software (Version 9.0, Molecular Devices). The liquid junction potential (~14.3 mV) was corrected for further analysis.

$I_A$ recordings were obtained in voltage clamp mode. To isolate $I_A$, the modified ACSF was used, containing (in mM) 109 NaCl, 26 $NaHCO_3$, 5 KCl, 1.2 $NaH_2PO_4$, 3.6 $MgCl_2$, and 10 glucose plus 0.2 $CdCl_2$, 3 EGTA, 30 tetraethylammonium (TEA), and 0.5 μM tetrodotoxin (TTX) to block $Ca^{2+}$ channels, delayed rectifier $K^+$ channels, and voltage-gated $Na^+$ channels. The protocols consisted of depolarizing step pulses, ranging from -70 mV to +25 mV for 400 ms in 5 mV increments, from conditioning pulse to -90 mV or to -40 mV for 340 ms, as described previously (Sonner and Stern, 2007). Currents obtained from two different conditioning pulses were subtracted digitally using pClamp software. To verify that the obtained $K^+$ current was $I_A$, 4-aminopyridine (4-AP; 5 mM) was applied at the end of the recording. $I_A$ amplitudes were used for the subsequent analysis of activation characteristics and current densities. Activation

curves were plotted with normalized chord conductance, versus step potentials, obtained by dividing the current amplitude by differences between each step potential and reversal potential of $K^+$ ions (obtained from the Nernst equation; -87.04 mV); they were then fitted with the Boltzmann equation using OriginPro 8 (OriginLab Corporation, Northampton, MA, USA). Current densities were calculated by dividing $I_A$ amplitudes by cell capacitances. Inactivation characteristics of $I_A$ were analyzed using the protocol of conditioning step pulses, ranging from -120 mV to -35 mV for 50 ms in 5 mV increments, and successive depolarizing pulses to -10 mV for $I_A$ activation, as described previously (Sonner and Stern, 2007). Inactivation curves were plotted with normalized current amplitudes versus conditioning step potentials, and fitted with the Boltzmann equation. Differences in voltage dependences of $I_A$ activation and inactivation between the oil-group and the E2-group were analyzed by comparing the half-activation potential ($V_{1/2}$, at which half of the $I_A$ is activated), the slope factor obtained from the activation curve, the half-inactivation potential ($V_{1/2}$, at which half of the $I_A$ is inactivated), and slope factor obtained from the inactivation curve.

To investigate the effects of E2 on the membrane excitability of the PVN-RVLM neurons, delays to action potential generation was examined in current-clamp mode for both the oil- and E2-groups. The cells were hyperpolarized to near -90 mV, and depolarized by injecting a +45 pA current. The delay time was determined by measuring the duration from the point initiating depolarization to the peak of the first action potential. All drugs were obtained from Sigma-Aldrich except TTX (Tocris Bioscience, Bristol, UK).

### *Statistical analysis*

All values were expressed as means ± S.E.M. Comparisons between the oil-group and the E2-group were analyzed using an unpaired *t*-test. When necessary, analyses included two-way ANOVAs with fisher LSD *post hoc* test. Differences were considered significant at $P<0.05$. All statistical analyses were conducted using OriginPro 8 (OriginLab) or SPSS Statistics 20 (IBM Corporation, Armonk, NY, USA).

# RESULTS

### *The effects of E2 treatments on OVX-rats*

The mean serum E2 concentration measured after sacrifice was 25±4 pg/ml in the oil-group ($n$=9) and 59±11 pg/ml in the E2-group ($n$=9) and was significantly different between the two groups ($P$<0.05). Suppression in body weight gain by the E2 treatment appeared significantly on the third day (6.14±0.42% [$n$=14] for the oil-group and 2.01±0.52% [$n$=10] for the E2-group, $P$<0.05); a larger effect was evident on the fourth day (8.37±0.91% [$n$=16] for the oil group and 1.39±1.02 [$n$=12] for the E2 group, $P$<0.05), as shown in Figure 1A. Uteri were isolated after sacrifice and normalized to body weights (uterus/body, mg/g). The mean normalized uterus weight was larger in the E2-group (4.15±0.33 mg/g [$n$=12], $P$ <0.05) than in the oil-group (0.51±0.02 mg/g [$n$=16]), as shown in Figure 1B.

### *Retrograde labeling of PVN-RVLM neurons*

To identify the PVN-RVLM neurons for recording and single-cell real-time RT-PCR, fluorescent tracer was injected into the RVLM of OVX-rats. After the animals were sacrificed, the serial medulla slices (100 μm thicknesses) were examined to determine that the dye was injected into the RVLM. A representative image of the medulla slice, including the RVLM, is illustrated in Figure 2A. A dye spot is present within the triangle frame, made by the nucleus ambiguus, the spinal trigeminal nucleus, and the pyramidal tracts, which was suggested as the guideline for RVLM location (Stocker et al., 2004). Figure 2B illustrates the fluorescent-

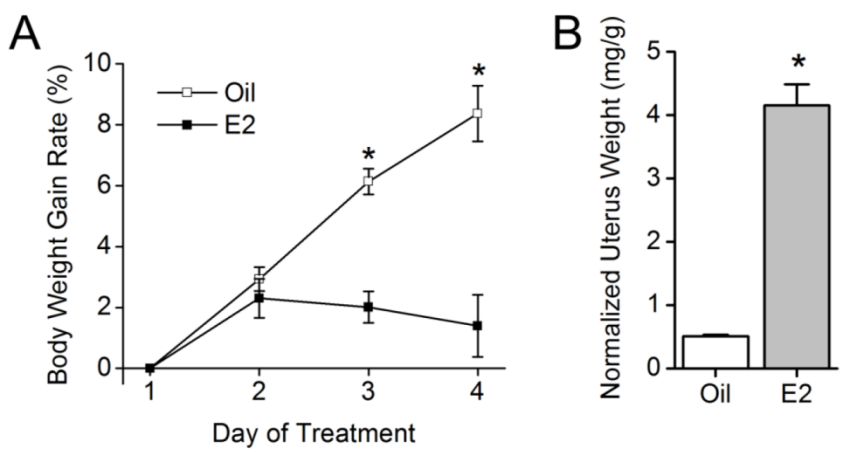


**Figure 1. Effects of E2 treatments on OVX rats.** OVX rats were treated with vehicle (corn oil, 0.1 ml) and 17β-estradiol-3-benzoate (25 μg/kg in 0.1 ml corn oil) for the oil-group and the E2-group, respectively. **A,** The body weight-gain rate was compared between the two groups by calculating the ratio of body weight increase each day to the weight on the first day of treatment. A significant difference appeared on the third and the fourth days (*$P$<0.05). **B,** The mean uterus weight was compared between the two groups. Uteri were isolated after sacrifice and weighed. The weight was normalized to the body weight on the day of sacrifice. E2 treatment significantly increased uterus weight (*$P$<0.05).

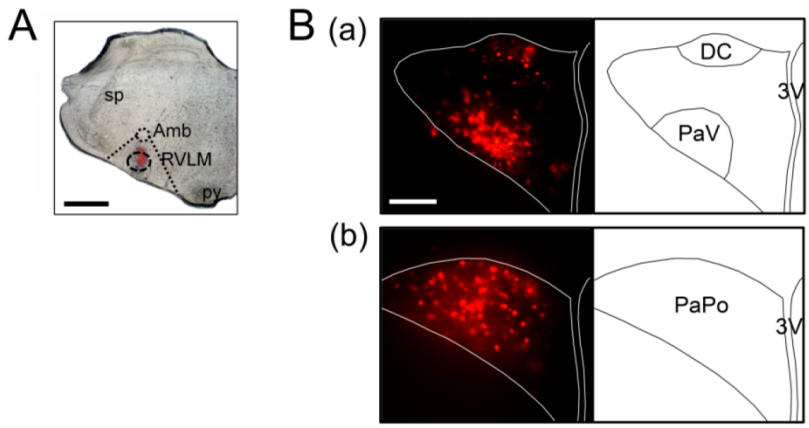


**Figure 2. Retrograde labeling of PVN-RVLM neurons. A,** RVLM injection site was verified with serial medulla slices including the RVLM (100 μm thickness). The representative image shows that a fluorescent spot was confined to the triangular frame defined as RVLM (Stocker et al., 2004). Amb, nucleus ambiguus; sp, spinal trigeminal nucleus; py, pyramidal tracts; scale bar= 1 mm. **B,** The fluorescent image illustrates that the labeled PVN-RVLM neurons were located in the medial region (a) and in the posterior region (b) of the PVN in the hypothalamic brain slices (300 μm thickness). The PVN-RVLM neurons are evident primarily in the dorsal cap (DC), the ventral parvocellular (PaV), and the posterior parvocellular (PaPo) subdivisions. 3V, third ventricle; scale bar= 200 μm.

labeled PVN-RVLM neurons in a rat hypothalamic brain slice. The PVN-RVLM neurons were located primarily in the three main PVN subdivisions: the dorsal cap (DC), the ventral parvocellular (PaV), and the posterior parvocellular (PaPo), which was consistent with the previous report (Stern and Zhang, 2003).

### *E2 effects on the mRNA expression density of Kv4.2 and Kv4.3 in single PVN-RVLM neurons*

To investigate the effect of E2 on the mRNA expression of Kv4.2 and Kv4.3 in rat PVN-RVLM neurons, single-cell real-time RT-PCR was performed. The mRNA expression density of Kv4.2 and Kv4.3 of the PVN-RVLM neurons was compared between the oil-group and the E2-group for the PVN-RVLM overall and for each subdivision. The PVN-RVLM neurons used in each subdivision are illustrated in Figure 3A. The mRNA expression density of Kv4.2 (Figure 3B) and Kv4.3 (Figure 3C) was analyzed using the $2^{-\Delta\Delta Ct}$ method. Kv4.2 decreased 0.54±0.06 fold in the E2-group ($n$=21; $P$<0.05) compared to that of the oil-group ($n$=19; Figure 3B). However, there was no significant difference in Kv4.3 expression between the oil-group ($n$=23) and the E2-group (1.00±0.18 fold, $n$=31; Figure 3C). For each subdivision, Kv4.2 decreased more prominently in the DC by E2 (0.29±0.05 fold, $n$=8 in the E2-group and $n$=4 in the oil group; $P$<0.05) compared to other subdivisions (in the PaV, 0.89±0.15 fold, $n$=8 in the E2-group and $n$=6 in the oil group; in the PaPo, 0.51±0.09 fold, $n$=5 in the E2-group and $n$=9 in the oil-group; Figure 3B). In contrast, as shown in Figure 3C, Kv4.3 mRNA expression densities exhibited the smallest differences in the DC (0.87±0.15 fold, $n$=12 in the E2-group; $n$=9 in the oil group). In the PaV, Kv4.3 decreased 0.56±0.15 fold in the E2-group

**Figure 3. E2 effects on mRNA expression density of Kv4.2 and Kv4.3 in single PVN-RVLN neurons.** For relative quantification of Kv4.2 and Kv4.3 mRNA expression in the PVN-RVLM neurons between the oil- and the E2- groups, single-cell real-time RT-PCR was performed. **A,** Images show the locations of the PVN-RVLM neurons used for single-cell real-time RT-PCR in each subdivision. DC, dorsal cap subdivision; PaV, ventral parvocellular subdivision; PaPo, posterior parvocellular subdivision. **B,** The mRNA density of Kv4.2 was analyzed for the PVN-RVLM neurons overall and for each subdivision using the $2^{-\Delta\Delta Ct}$ method, and was finally expressed as n-fold that of the oil-group. The Kv4.2 significantly decreased, 0.54±0.06 fold, in the E2-group ($n$=21, *$P$<0.05) compared to that of the oil-group ($n$=19). For each subdivision, only in the DC, Kv4.2 significantly decreased in the E2 group compared to that of the oil group. This decrease was more dominant than that in the overall PVN-RVLM neurons. **C,** Kv4.3 mRNA expression in the PVN-RVLM neurons was compared between the oil-group and the E2-group using the same method as for Kv4.2. However, there was no significant difference in Kv4.3 expression between the two groups either for the overall PVN-RVLM neurons or for each subdivision.

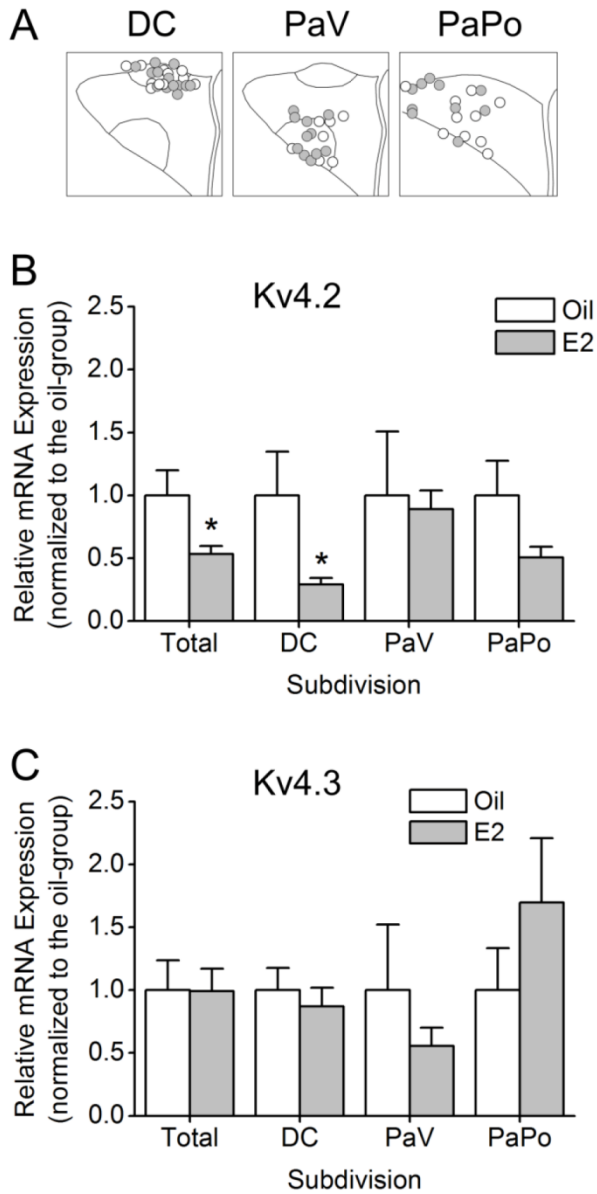
A
DC
PaV
PaPo
B
Kv4.2
Oil
E2
Relative mRNA Expression
(normalized to the oil-group)
2.5
2.0
1.5
1.0
0.5
0.0
*
*
Total
DC
PaV
PaPo
Subdivision
C
Kv4.3
Oil
E2
Relative mRNA Expression
(normalized to the oil-group)
2.5
2.0
1.5
1.0
0.5
0.0
Total
DC
PaV
PaPo
Subdivision

(*n*=9) compared to that of the oil group (*n*=8), while in the PaPo, Kv4.3 increased 1.70±0.51 fold in the E2-group (*n*=10) compared to that of the oil group (*n*=6), but the differences were not significant.

### *E2 effects on $I_A$ in PVN-RVLM neurons*

To examine a change in electrophysiological properties of the PVN-RVLM neurons as a result of E2, a whole cell clamp recording was performed with 67 PVN-RVLM neurons, 36 cells from the oil-group and 31 cells from the E2-group. The resting membrane potential (RMP), the input resistance ($R_{in}$), and the membrane capacitance ($C_m$) showed no differences between the two groups (RMP, -60.55±0.67 mV in the oil-group and -60.36±0.92 mV in the E2-group; $R_{in}$, 492.89±47.10 MΩ in the oil-group and 500.08±42.73 MΩ in the E2-group; $C_m$, 35.23±2.16 pF in the oil-group and 36.19±1.92 pF in the E2-group).

The study investigated possible $I_A$ modulation by E2. To verify that the current recorded in this experiment was $I_A$, 4-AP, the blocker of $I_A$, was applied to the bath solution at the end of recording. When 30 cells were tested, 68% of $I_A$ peak amplitudes were blocked by 5 mM 4-AP (Figure 4A, *inset* on right). The $I_A$ current densities (the normalized current amplitude to cell capacitance) significantly decreased in the E2-group compared to those of the oil-group (Figure 4B, $P<0.05$). However, the voltage-dependence of $I_A$ activation and inactivation was not different between the two groups (Figure 4C: for activation, $V_{1/2}$ -18.84±0.92 mV, slope factor 11.79±0.38 (*n*=36) in the oil-group and $V_{1/2}$ -16.69±1.04 mV, slope factor 11.22±0.45 (*n*=31) in the E2-group; for inactivation, $V_{1/2}$ -69.14±1.19 mV, slope factor 10.92±0.41 (*n*=33) in the oil-group and $V_{1/2}$ -

**Figure 4. E2 effect on $I_A$ in PVN-RVLM neurons. A,** Representative images illustrate $I_A$ isolated in PVN-RVLM neurons from the oil-group (left) and the E2-group (right). The left *inset* indicates the voltage protocol used to isolate $I_A$. The right *inset* indicates the reduction in $I_A$ by 4-aminopyridine (4-AP), the blocker of $I_A$. **B,** Plots of $I_A$ current densities versus command step potentials. The current density was calculated by dividing the current amplitude of $I_A$ by cell capacitance. The E2 group (filled squares) displayed significant reductions in current densities of $I_A$, compared to the oil-group (open squares). *$P$<0.05. **C,** Activation curve plotted with the mean normalized chord conductance (open squares for the oil-group and filled squares for the E2-group) and inactivation curve plotted with the mean normalized amplitude (open circles for the oil-group and filled circles for the E2-group). The curves were fitted with the Boltzmann equation. There were no significant differences in either the activation or the inactivation properties of $I_A$.

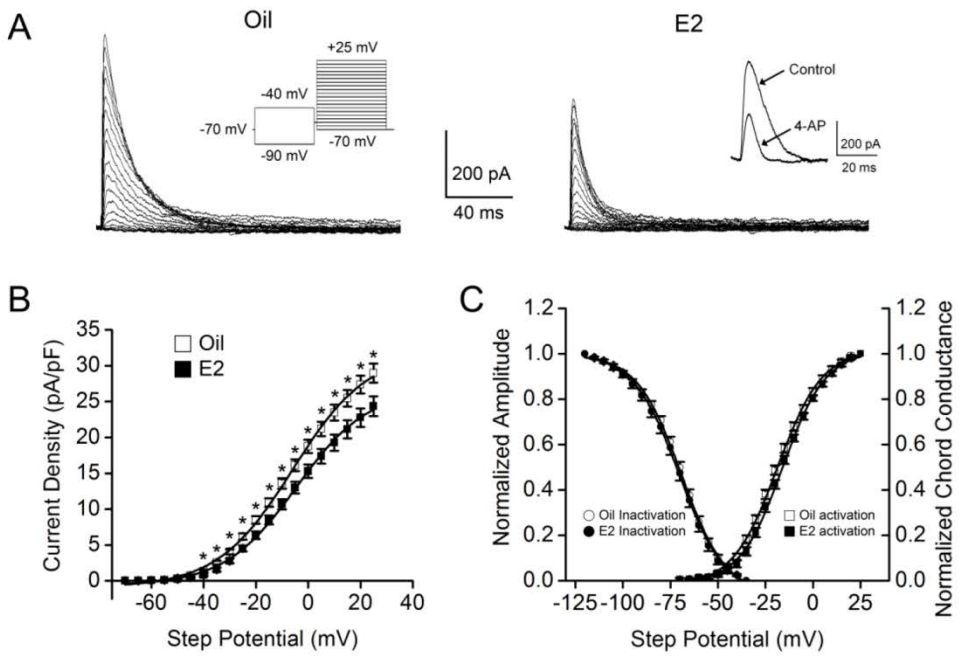
A
Oil
E2
+25 mV
-40 mV
-70 mV
-90 mV
-70 mV
200 pA
40 ms
Control
4-AP
200 pA
20 ms
B
Oil
E2
Current Density (pA/pF)
Step Potential (mV)
C
Normalized Amplitude
Normalized Chord Conductance
Oil Inactivation
E2 Inactivation
Oil activation
E2 activation
Step Potential (mV)

71.24±1.71 mV, slope factor 10.84±0.47 (*n*=28) in the E2-group).

When the maximal current density of $I_A$ (at +25 mV step potential) was compared between the oil-group and the E2-group for the PVN-RVLM neurons overall, the E2-group expressed significantly smaller current densities than those of the oil-group (24.3±1.39 pA/pF for the E2 group and 29.0±1.33 pA/pF for the oil-group, Figure 5B, $P<0.05$). The differential modulation in $I_A$ current density by E2 was examined according to the different subdivisions, as shown in the mRNA expression analysis. The locations of the PVN-RVLM neurons used for whole cell patch-clamp recording were illustrated in Figure 5A. A significant reduction in $I_A$ current density occurred only in the DC (22.23±2.04 pA/pF [*n*=9] for the E2-group; 28.33±1.79 pA/pF [*n*=16] for the oil-group; Figure 5B, $P<0.05$); other subdivisions did not have similar significant changes (in the PaV, 25.20±2.75 pA/pF [*n*=9] in the E2-group and 28.03±4.52 pA/pF [*n*=6] in the oil-group; in the PaPo, 25.22±2.38 pA/pF [*n*=13] in the E2-group and 30.07±2.11 pA/pF [*n*=14] in the oil-group).

### *E2 effects on delay of excitation in PVN-RVLM neurons*

The study investigated E2 modulation of the membrane excitability of the PVN-RVLM neurons by comparing delays in the onset of the first action potential between the oil-group and the E2-group. When hyperpolarized to near -90 mV and depolarized by injecting a +45 pA current, most cells generated action potentials. However, delay durations to the onset of the first action potential were different between the oil-group and the E2-group (Figure 6A). Delays significantly shortened in the E2-group (22.41±2.37 ms [*n*=17]; $P<0.05$) compared to that of the oil-group (35.35±5.10 ms [*n*=23]; Figure 6B). As the extent of hyperpolarization

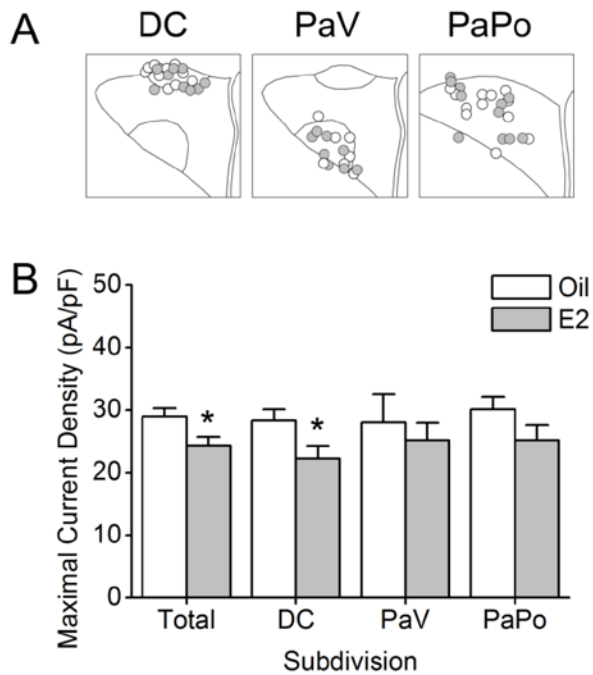


**Figure 5. E2 effect on $I_A$ density in PVN-RVLM neurons for each subdivision.** **A**, Images show locations of PVN-RVLM neurons used for whole cell patch-clamp recording. DC, dorsal cap subdivision; PaV, ventral parvocellular subdivision; PaPo, posterior parvocellular subdivision. **B,** The maximal current density (at +25 mV step potential) was compared between the oil group and the E2 group. In the E2-group, the maximal current density of $I_A$ significantly decreased, compared to that of the oil-group. When the differences between the two groups were compared according to subdivisions, a significant difference was detected only in the DC, not in either the PaV or the PaPo. *$P$<0.05.

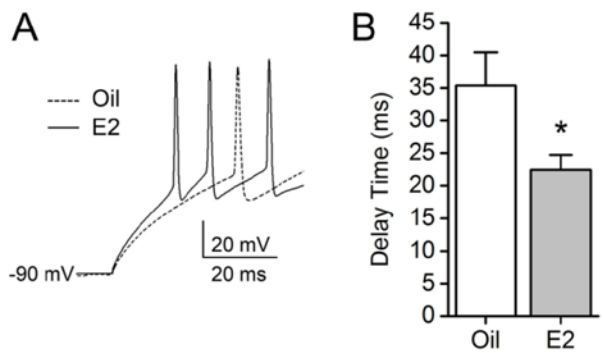


**Figure 6. E2 effects on delay of excitation in PVN-RVLM neurons. A,** A representative image shows a delay in the onset of the first action potential expressed in the PVN-RVLM neurons from the oil-group (dashed line) and the E2-group (solid line). The cells were hyperpolarized to near -90 mV to remove $I_A$ inactivation and depolarized by injecting a +45 pA current. **B,** The bar graph summarizes the differences in delay in the onset of the first action potential between the oil-group and the E2-group. The mean delay time of the E2-group significantly decreased, compared to that of the oil-group (*$P$<0.05).

for removing $I_A$ inactivation may influence delay durations, hyperpolarizations were compared between the two groups. There was no difference between the groups (-89.64±0.64 mV in the oil group and 88.50±1.05 mV in the E2-group).

# DISCUSSION

The biophysical and pharmacological properties of the PVN-RVLM neurons, known as presympathetic neurons, have been extensively studied in physiological and pathological conditions (Li et al., 2006; Sonner and Stern, 2007; Sonner et al., 2011). It has also been demonstrated that ER, especially ER-β, is substantially expressed in the PVN-RVLM neurons (Stern and Zhang, 2003), suggesting specific roles of E2 in the PVN-RVLM neurons. However, the effects of E2 on the cellular properties of the PVN-RVLM neurons remain unknown. The present study investigated differences in the cellular properties of the PVN-RVLM neurons between estrogen-deficient rats (the oil-group) and estrogen-replaced rats (the E2-group) following E2 treatment in vivo after ovariectomy. The investigation focused on Kv channel subunit expression and its functional current, $I_A$, because $I_A$ is one of the major currents expressed in the PVN-RVLM neurons, and Kv channel subunits are modulated by altered physiological conditions (Sonner and Stern, 2007; Sonner et al., 2011). The results showed that E2 significantly down-regulated the mRNA expression of Kv4.2, but not that of Kv4.3, and diminished $I_A$ density. Interestingly, this effect was only observed in the DC among three subdivisions (DC, PaV, and PaPO). E2 also shortened the delay in the onset of the first action potential that is known to be associated with $I_A$ in PVN neurons (Luther and Tasker, 2000). These results suggest that E2 exerts an inhibitory effect on the function of $I_A$, potentially by selectively down-regulating the transcript levels of Kv4.2 but not Kv4.3 in the PVN-RVLM neurons distributed in the specific subdivision. However,

some limitations should be considered in the present study. First, the electrophysiological recording and single cell real-time RT-PCR were performed in different cells rather than in the same cells due to the poor quality of the RNA samples following a long recording time and continuous exposure of the cells to multiple ion channel blockers. Therefore, a direct correlation between $I_A$ and Kv4.2 in E2-mediated regulation cannot be confirmed. However, the observation that the down-regulation by E2 of the mRNA expression of Kv4.2 and the density of $I_A$ appeared consistent indicates that Kv4.2 and $I_A$ are closely related/associated in the cellular modulation of the PVN-RVLM neurons. Second, the mechanism underlying E2-mediated regulation of Kv4.2 and $I_A$ remains unclear. Future studies are warranted to confirm whether ER-β located in the PVN-RVLM neurons mediates the transcriptional regulation of Kv4.2. Third, the possibility that non-genomic actions of E2 contributed to Kv4.2 and $I_A$ modulation in the PVN-RVLM neurons cannot be excluded because it has been shown that acute application of E2 in bath solution inhibits outward $K^+$ currents, including $I_A$ (Fatehi et al., 2006). E2 induces non-genomic events via membrane estrogen receptor or other E2-binding proteins, which activate second messenger cascades, including adenylate cyclase, phospholipase C, extracellular-signal-regulated kinase, and mitogen-activated protein kinase (Deroo and Buensuceso, 2010; Levin, 1999). It was reported that inhibition of the $I_A$ density by E2 replacement is reversed by application of a kinase inhibitor in gonadotropin-releasing hormone neurons of OVX-mice (DeFazio and Moenter, 2002).

In spite of these limitations, this study is noteworthy because it is the first to reveal estrogenic modulation of cellular properties of the PVN-RVLM neurons,

particularly its target gene selectivity, for example, for Kv4.2 but not Kv4.3, and its regional selectivity in the DC subdivision. The selectivity for Kv4.2 is interesting because the major potential subunit for $I_A$, to date, in the PVN-RVLM neurons has been considered to be Kv4.3 (Sonner and Stern, 2007; Sonner et al., 2011) because the latter is predominantly expressed in the PVN-RVLM neurons (Sonner and Stern, 2007). However, the previous study found that Kv4.2 may also contribute to $I_A$ in PVN neurons, despite its lower detection frequency compared to Kv4.3 (Lee et al., 2012). The selective modulation of Kv4.2 by E2 suggests that even less dominantly expressed subunits could be involved in the cellular modulation or the functions of PVN-RVLM neurons and that gene modulation is not necessarily parallel to preponderance in the gene expression level. The target selectivity of E2 in the modulation of Kv4.2 and Kv4.3 is evident in distinct cell types. In heart cells, Kv4.3 was regulated by E2, whereas Kv4.2 was not (Eghbali et al., 2005; Saito et al., 2009). In uterus cells, Kv4.2 and Kv4.3 were both regulated simultaneously by E2 during pregnancy (Song et al., 2001; Suzuki and Takimoto, 2005). In a GT1-7 cell line producing gonadotropin-releasing hormones, Kv4.2 was regulated by E2 (Farkas et al., 2007). Kv4.1 was regulated by E2 in the hypothalamic arcuate nucleus (Roepke et al., 2007). Therefore, estrogenic regulation has specific selectivity in molecular targeting, depending on distinct tissues or cells. This selectivity may be related to the differential expression of ER subtypes in distinct tissues. In the uterus and the heart, the expression of ER-α is greater than that of ER-β, which is uncommon in the PVN-RVLM neurons.

Regional selectivity in E2-induced modulation of Kv4.2 mRNA expression suggests that the effect of E2 on the PVN-RVLM neurons is likely to be

different on each subdivision. E2 significantly down-regulated Kv4.2 only in the DC. This finding is consistent with the recording data in which the $I_A$ density was significantly down-regulated in the same division by E2, indicating that E2 modulation of the PVN-RVLM neurons almost reflects the effects of E2 in the DC. From this result, I speculate that heterogeneous cells that have different sensitivities and responses to E2 exist in the PVN-RVLM neurons and that these cells are clustered in a specific region. In this regard, the DC subdivision is likely to be the specific region where E2 exerts inhibitory effects on $I_A$ functions of the PVN-RVLM neurons, potentially by down-regulating Kv4.2. The specific modulation of E2 in the DC subdivision may be due to distinct properties of the PVN-RVLM neurons distributed in this subdivision. For example, biochemical differences among subdivisions could account for this specific modulation. It has been reported that spinally-projecting PVN neurons which are distributed in similar regions to the PVN-RVLM neurons have different neurochemical characteristics according to subdivisions (Hallbeck et al., 2001). Dynorphin and oxytocin were detected in all subdivisions, but the expression of enkephalin and vasopressin was considerably lower in the DC, compared to other subdivisions. Immunohistochemical studies showed that ER-β was abundantly double-labeled with oxytocin, whereas it was not with vasopressin or corticotropin-releasing hormone in PVN neurons (Alves et al., 1998; Simonian and Herbison, 1997). Although such neurochemical differences have not been reported in the PVN-RVLM neurons, the differences may be closely related to the regional-specific modulation by E2 in these neurons.

This study investigated the effects of E2 on the membrane excitability of

the PVN-RVLM neurons by observing changes in the delay of the onset of the first action potential between the oil-group and the E2-group, because $I_A$ is known to exert a hyperpolarizing effect on membrane discharge to delay membrane excitation (Rogawski, 1985). In agreement with E2-mediated down-regulation of $I_A$, the results showed that the delay was shortened in the E2-group. The delay has been referred to as a representative characteristic of magnocellular PVN neurons because these neurons apparently express a stronger $I_A$, coincidentally associated with a longer delay, than parvocellular PVN neurons (Luther and Tasker, 2000). Although the parvocellular PVN-RVLM neurons displayed much smaller delays than the magnocellular neurons, the delays are regulated to a significant extent by E2, and these are probably associated with the regulation of $I_A$. This suggests that reductions in $I_A$ and in the delay of the onset of the action potential by E2 influence the functions of the PVN-RVLM neurons. However, the neuronal properties of the PVN-RVLM neurons are determined not only by $I_A$, but also by a variety of other factors. Regarding the intrinsic membrane property, other ionic currents besides $I_A$, including voltage-gated $Ca^{2+}$ channels and small conductance $Ca^{2+}$-activated $K^+$ channels, participate in determining the excitability of the PVN-RVLM neurons (Chen and Toney, 2009; Lee et al., 2008). Studies have reported that E2 modulates these channels in other neuronal cells within the brain (Bosch et al., 2002; Bosch et al., 2009; Qiu et al., 2006). Research has also shown that neuronal activity is governed not only by intrinsic membrane properties, but also by the synaptic inputs of excitatory and inhibitory signals (Li et al., 2006). In addition, studies have demonstrated that receptors underlying the excitatory and inhibitory synaptic signals are also influenced by E2 in other brain regions (McEwen, 2001; Parducz et

al., 1993).

The aforementioned raises the question of how E2-induced cellular modulation of the PVN-RVLM neurons influences cardiovascular regulation. Studies have demonstrated that estrogen plays protective roles in the pathological development of, and the incidence of, cardiovascular disorders (Beer et al., 2007; Kannel et al., 1976; Mendelsohn and Karas, 1999). Accumulating evidence shows that the neuronal activity of the PVN-RVLM neurons is elevated by enhancing the intrinsic membrane activity or by eliminating inhibitory synaptic inputs in cardiovascular diseases, such as hypertension and chronic myocardial infarction (Chen et al., 2010; Han et al., 2010; Sonner et al., 2008). Therefore, the E2-mediated modulation of the PVN-RVLM neurons shown in this study (i.e., the diminution in $I_A$ density and the likely enhancement of membrane excitability) seems to be controversial with respect to the protective effects of E2 on the cardiovascular system because the modified pattern is more likely to reinforce the increase in neuronal excitability induced by abnormal cardiovascular conditions. However, it should be noted that E2 exerts different effects, depending on differing cardiovascular conditions. For instance, increased E2 levels during pregnancy induce hypertrophy, but E2 also attenuates the development of pressure-overload hypertrophy (Eghbali et al., 2005; van Eickels et al., 2001). As the present study investigated E2-mediated modulation under normal conditions, different results can be expected under pathological conditions. This expectation is supported by the fact that different molecular targets were employed in the modulation of $I_A$ in the PVN-RVLM neurons, depending on the modulating sources involved. A reduction in $I_A$ in the PVN-RVLM neurons resulted from E2 replacement or artificial

hypertension in a similar manner. Nevertheless, E2 down-regulated Kv4.2 mRNA levels, whereas hypertension down-regulated Kv4.3 (Sonner et al., 2011). Therefore, Kv4.2, as the target of E2 actions, could be modulated in different ways in the PVN-RVLM neurons, according to normal or pathological conditions. Estrogenic effects on the PVN-RVLM neurons modified by cardiovascular disorders remain to be determined.

# CONCLUSIONS

This study demonstrated that E2 modified the cellular properties of the PVN-RVLM neurons. E2 played an inhibitory role in the $I_A$ function in the PVN-RVLM neurons and selectively down-regulated the mRNA expression of Kv4.2 but not that of Kv4.3. The finding that this modulation occurred predominantly in the DC subdivision suggests that functionally-discrete PVN-RVLM neurons may be distributed in specific subdivisions, indicating that these subdivisions deserve the important consideration in researching PVN-RVLM neurons. This study provides the first evidence of estrogenic modulation of the PVN-RVLM neurons.

# CHAPTER IV

# Differential distributions of neuropeptides in rat presympathetic PVN neurons

# ABSTRACT

The hypothalamic paraventricular nucleus (PVN) plays major regulatory roles in the endocrine and the autonomic system. It has anatomically and functionally distinct cell populations. Among those, the presympathetic cells that project to the rostral ventrolateral medulla (PVN-RVLM) participate in the sympathetic regulation of the cardiovascular system. To investigate expression and distribution of peptides in the PVN-RVLM neurons of rats, single cell RT-PCR was employed in combination with retrograde tracing. Approximately 80% of the PVN-RVLM neurons expressed oxytocin and 60% expressed dynorphin. Differential distribution of peptides was found between the subdivisions of the PVN-RVLM neurons. Oxytocin was predominant in the posterior parvocellular subdivision. Vasopressin appeared significantly less distributed in the dorsal cap subdivision than in other subdivisions. In addition, the PVN-RVLM neurons preponderantly co-expressed multiple peptides. These results support that peptides may contribute to elaborate responses of PVN to various stimuli.

# INTRODUCTION

Hypothalamic paraventricular nucleus (PVN) is an important integrating site for endocrine and autonomic regulation (Swanson and Sawchenko, 1980). It consists of the magnocellular and the parvocellular cell group. The former projects to the posterior pituitary gland and is responsible for secretions of oxytocin (OT) and vasopressin (VP). Some of the latter project to the median eminence to regulate secretions of several hormones, and others of the latter cell group project to the brain stem or the spinal cord, regulating the autonomic functions (Armstrong et al., 1980; Swanson and Sawchenko, 1980). Within the autonomic-related cell group, specifically those involved in sympathetic control, two subgroups were characterized by their different projecting sites. One group projects directly to sympathetic centers in the spinal cord, and the other gives rise to indirect connections via relays in the rostral ventrolateral medulla (RVLM) (Badoer, 2001; Pyner and Coote, 2000). The critical role of the PVN neurons projecting to the RVLM (PVN-RVLM) in the regulation of cardiovascular sympathetic outflows has been well demonstrated (Allen, 2002; Coote et al., 1998; Dampney, 1994).

Peptides functions, as a neurotransmitter, in the nervous system are well known (Kandel et al., 2000). In the PVN, peptides, including OT and VP, were detected not only in the magnocellular and parvocellular cells associated with endocrine functions, but also in the parvocellular neurons with long descending projections to the autonomic centers in the brain- stem and the spinal cord (Swanson and Sawchenko, 1980). Subsequently, accumulating evidence has

indicated that more peptides exist in the PVN and that they are differentially distributed according to functionally or anatomically distinct cell groups within the PVN (Hallbeck et al., 2001; Sawchenko and Swanson, 1982; Simmons and Swanson, 2009). However, such information remains unknown for the PVN-RVLM neurons.

The present study aimed to investigate expression and distribution of peptides in the PVN-RVLM neurons. For detection of peptides, single cell RT-PCR was performed, as it is able to detect multiple targets in a single cell simultaneously but independently. Eight representative peptides known to be prominent in the PVN were selected: dynorphin (Dyn), enkephalin (Enk), somatostatin (Sst), growth hormone-releasing hormone (GHRH), corticotropin-releasing hormone (CRH), thyrotropin-releasing hormone (TRH), oxytocin (OT), and vasopressin (VP).

# MATERIALS AND METHODS

### *Animals*

Male Sprague-Dawley rats (*n*= 4, 7wks old) were used (Orient Bio Inc., Kyonggi-do, Korea). The rats were maintained under a 12 hr light/dark cycle (lights on at 9:00 A.M.) and given free access to food and water until sacrifice. All surgical procedures were performed after anesthesia induced by an intraperitoneal injection of Zoletil (25 mg/kg) and xylazine (10 mg/kg). Every effort was made to minimize the number of animals and their suffering. The experimental protocols were performed in accordance with the guidelines set by the Institutional Animal Care and Use Committee of Seoul National University and were approved by the Institute of Laboratory Animal Resources of Seoul National University (SNU-130722-2).

### *Retrograde tracing*

The retrograde-transported fluorescent tracer (FluoSphere-Red; Molecular Probes) was injected into the RVLM of rats to identify PVN-RVLM neurons as previously described (Han et al., 2010). The injection point was, on average, 12.3 mm caudal, 1.7 mm lateral, and 8.0 mm ventral from bregma. Verification of the RVLM injection site was assessed by examining serial medulla slices (100 μm thickness) of all animals after sacrifice. Injections were located ventral to the nucleus ambiguus, within ~1 mm caudal of the facial nucleus.

### *Hypothalamic slice preparation*

Hypothalamic brain slices were prepared according to the methods described previously (Han et al., 2010). After anesthesia, the rat was transcardially perfused with an ice- cold sucrose-rich ACSF containing (in mM) 210 Sucrose, 26 $NaHCO_3$, 5 KCl, 1.2 $NaH_2PO_4$, 1.2 $CaCl_2$, 2.4 $MgCl_2$, and 10 glucose. The brains were briefly removed and dissected into two or three coronal slices (300 μm thickness) including PVN regions, using a vibrating tissue slicer (Vibratome 1000 plus; Vibratome Company). The slices were incubated in an oxygenated normal ACSF containing (in mM) 126 NaCl, 26 $NaHCO_3$, 5 KCl, 1.2 $NaH_2PO_4$, 2.4 $CaCl_2$, 1.2 $MgCl_2$, and 10 glucose for 1 hr at 30 ºC until used.

### *Single cell RT-PCR*

To gain RNAs from single PVN-RVLM neurons for RT-PCR, the hypothalamic brain slice was transferred to the recording chamber used for electrophysiological recording, perfused continuously with an oxygenated ACSF (4-5 ml/min), and maintained at 30~32 ºC. Fluorescent-labeled PVN-RVLM neurons were visualized by combining differential interference contrast video microscopy with fluorescence microscope equipped with a green filter cube (WG, Olympus, Tokyo, Japan). The healthy cells that had apparent boundaries shaped by fluorescent dots and were located within three subdivisions of the PVN, including the dorsal cap (DC), the ventral parvocellular (PaV), and the posterior parvocellular (PaPo) (Stern and Zhang, 2003) (Figure. 2A), were chosen. The cells were approached with micropipettes pulled from borosilicate glass capillaries (1.7 mm diameter and 0.5

mm wall thickness) and filled with nuclease-free water (Qiagen) using a micromanipulator (MP-225; Sutter Instruments). After the tip of the micropipettes attached to a cell, a slight negative pressure was applied to pull the cytoplasmic contents out of the cells into the pipette, taking care to avoid including the nucleus. A mixture of cytoplasm and water was immediately removed into the tube containing (μl) 4 of nuclease free water (Qiagen) and 1 Rnase Inhibitor (Applied Biosystems).

Reverse transcription for single cell cDNA preparations was carried out using High Capacity cDNA Reverse Transcription Kits (Applied Biosystems), according to the manufacturer's instructions. PCR was performed using a thermal cycler (the GeneAmp® PCR System 9700, Applied Biosystems). Primers used to amplify the target cDNAs are listed in Table 1. Primers were designed using Primer 3 software (Rozen and Skaletsky, 2000) but those for CRH and VP were adapted from a previous report (Glasgow et al., 1999). To amplify the target cDNA, the PCR reactions were prepared by mixing (μl) 2 of cDNA template, 1 each of 10 μM forward and reverse primers, 10 of 2x Taq polymerase master mix (GoTaq Green Master Mix; Promega, Madison, WI, USA), and 6 μl of nuclease free water. PCR conditions were as follows: pre-denaturation at 94 ℃ for 5 min, 50 cycles of denaturation at 94 ℃ for 40 sec, annealing at 60 ℃ for 40 sec, extension at 72 ℃ for 1 min, and a final extension at 72 ℃ for 7 min. PCR product was electrophoresized in 1.6% agarose gel containing ethidium bromide to visualize its band. Negative controls for checking contamination from the genomic DNA were ascertained by running RT without the reverse transcriptase for every set.

**Table 1. Primer sequences for single cell RT-PCR.**

| Target (Acc. No.) | Sequence | Product size (bp) |
|---|---|---|
| Dynorphin (NM_019374) | 5'-CCTGTCCTTGTGTTCCCTGT-3'<br>5'-AGAGGCAGTCAGGGTGAGAA-3' | 157 |
| Enkephalin (NM_017139) | 5'-AAGATTGTCCCTGCTGGTCC-3'<br>5'-GGCTAGCAAGTGGCTCTCAT-3' | 406 |
| Somatostatin (NM_012659) | 5'-TGGCAGAACTGCTGTCTGAG-3'<br>5'-GGATCAGAGGTCTGGCTGAG-3' | 229 |
| Growth hormone-releasing hormone (NM_031577) | 5'-ATTATATGCCCGCAAACTGC-3'<br>5'-GCTGAAAGCTTCATCCTTGG-3' | 126 |
| Corticotropin-releasing hormone (NM_031019) | 5'-AACTCAGAGCCCAAGTACGTTGAG-3'<br>5'-TCACCCATGCGGATCAGAATC-3' | 354 |
| Thyrotropin-releasing hormone (NM_013046) | 5'-GGTGCTGCCTTAGACTCCTG-3'<br>5'-TTCTTCCCAGCTTCTTTGGA-3' | 372 |
| Oxytocin (NM_012996) | 5'-CTTGGCCTACTGGCTCTGAC-3'<br>5'-GGGCAGGTAGTTCTCCTCCT-3' | 216 |
| Vasopressin (NM_016992) | 5'-CCTCACCTCTGCCTGCTACTT-3'<br>5'-GGGGGCGATGGCTCAGTAGAC-3' | 463 |

# RESULTS

### *Expressions of various peptides in PVN-RVLM neurons*

All peptides targeted were detected in the PVN-RVLM neurons (Figure 1A). Expression frequency of OT among the peptides was most high (79%, 34/43), and followed by Dyn (63%, 27/43), CRH (30%, 13/43), and VP (28%, 12/43), as shown in Figure 1B. Enk, Sst, GHRH, and TRH were detected in fewer than 20% of the cells. The PVN-RVLM neurons were prominent in three regionally discrete subdivisions: DC, PaV, and PaPo (Figure 2A). For the four peptides that were predominantly detected (Dyn, CRH, OT, and VP), differences in their distributions among subdivisions were analyzed (Figure 2B; DC, $n$=13; PaV, $n$=15; PaPo, $n$=15). Dyn and CRH were similarly distributed among the subdivisions. However, OT and VP were differently distributed; all of the PVN-RVLM neurons in the PaPo expressed OT (100%, 15/15), whereas significantly fewer in the DC did (54%, 7/13; $P$<0.05 by a chi-squared test), and very few neurons in the DC expressed VP (8%, 1/13) compared to the PaV (40%, 6/15; $P$<0.05).

### *Co-expression of peptides in PVN-RVLM neurons*

All of the PVN-RVLM neurons expressed at least one peptide (100%, 43/43). The majority of the neurons displayed co-expression of different peptides (84%, 36/43). The co-expression of two different peptides was most frequently detected (47%, 20/43). Co-expression of three different peptides (28%, 12/43), of four different peptides (5%, 2/43), and of five different peptides (5%, 2/43) followed in that order

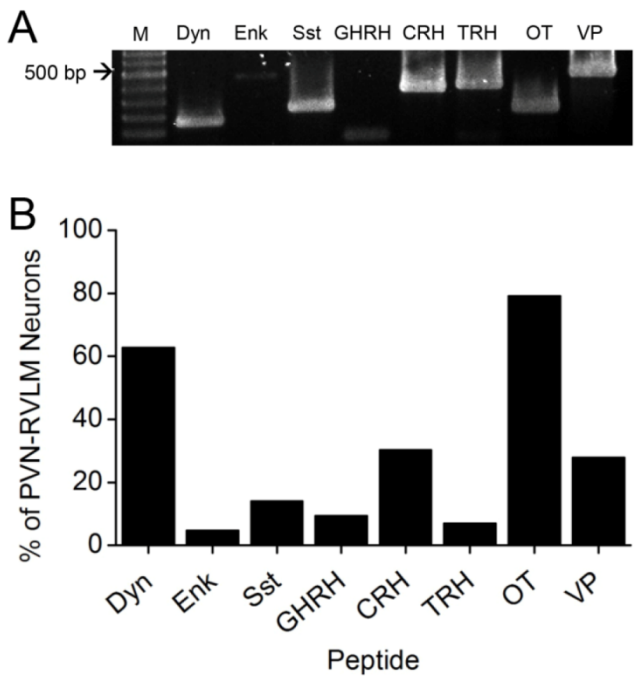


**Figure 1. Expression of various peptides in PVN-RVLM neurons. A,** A representative gel image indicates expression of Dyn, Enk, Sst, GHRH, CRH, TRH, OT, and VP in PVN-RVLM neurons **B,** Percentages of cells expressing each peptide in PVN-RVLM neurons were summarized. OT and Dyn were predominantly detected in the largest number of PVN-RVLM neurons, and CRH and VP were detected in the intermediate number.

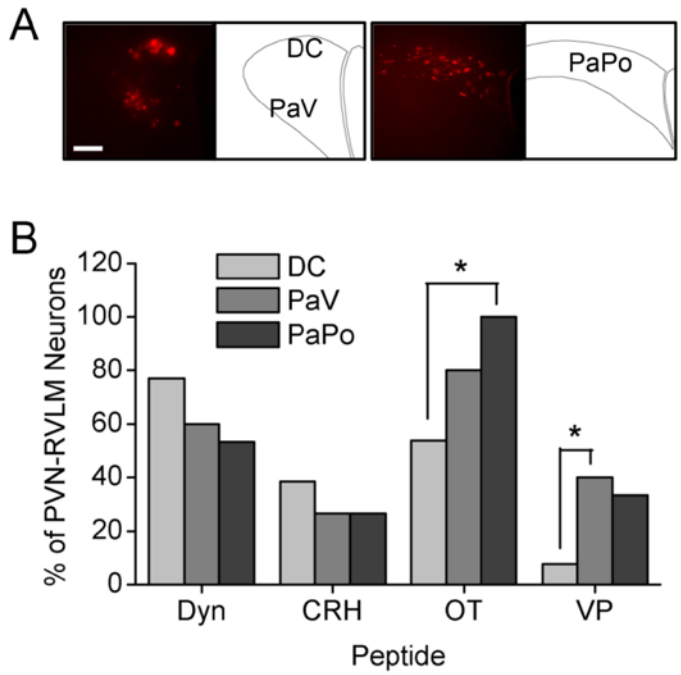


**Figure 2. Differential distribution of peptides in PVN-RVLM neurons. A,** Representative fluorescent images show retrograde-labeled PVN-RVLM neurons. The PVN-RVLM neurons are preponderantly distributed in three subdivisions: the dorsal cap (DC), the ventral parvocellular (PaV), and the posterior parvocellular (PaPo). Scale bar=0.2mm. **B,** Bar graphs represent percentages of cells expressing Dyn, CRH, OT, and VP in each subdivision. The OT-expressing cells and the VP-expressing cells are distributed differently among subdivisions (*$P$<0.05 by a chi-squared test).

(Figure 3A). Figure 3B illustrates representative single PVN-RVLM neurons expressing one peptide (cell ID: 24) or co-expressing more than two different peptides (cell ID: 25, 23, 44, and 43). For the cells that expressed Dyn, CRH, OT, or VP, I analyzed the proportion that expressed one, two, three, four, or five peptides (Figure 3C). Most of the cells displayed co-expressions. Only a few showed solo-expression of one type of peptides, and these cells were restricted to either the Dyn- or the CRH-containing neurons (19% [5/27] and 15% [2/13], respectively). OT- and VP-containing cells invariably showed co-expressions with other peptides.

### *Co-expression of peptides in the OT- or the VP-expressing PVN-RVLM neurons*

As co-expression of either OT or VP with other peptides was predominant, expression frequencies of peptides were analyzed in the OT- or VP-positive PVN-RVLM neurons. In the OT-positive cells, Dyn was found most frequently (58%, 21/34); however, other peptides were found: Enk (6%, 2/34), Sst (15%, 5/34), GHRH (12%, 4/34), CRH (29%, 10/34), TRH (9%, 3/34), and VP (29%, 10/34; Figure 4A). In the VP-positive cells, OT was most frequently expressed (83%, 10/12); however, and other peptides, except for Enk and GHRH, were found: Dyn (33%, 4/12), Sst (33%, 4/12), CRH (33%, 4/12), and TRH (8%, 1/12; Figure 4B). Additionally, to determine whether each peptide was specifically expressed with either VP or OT, distributions for each peptide were compared between positive and negative cells for either OT or VP. Between the OT-positive and the OT-

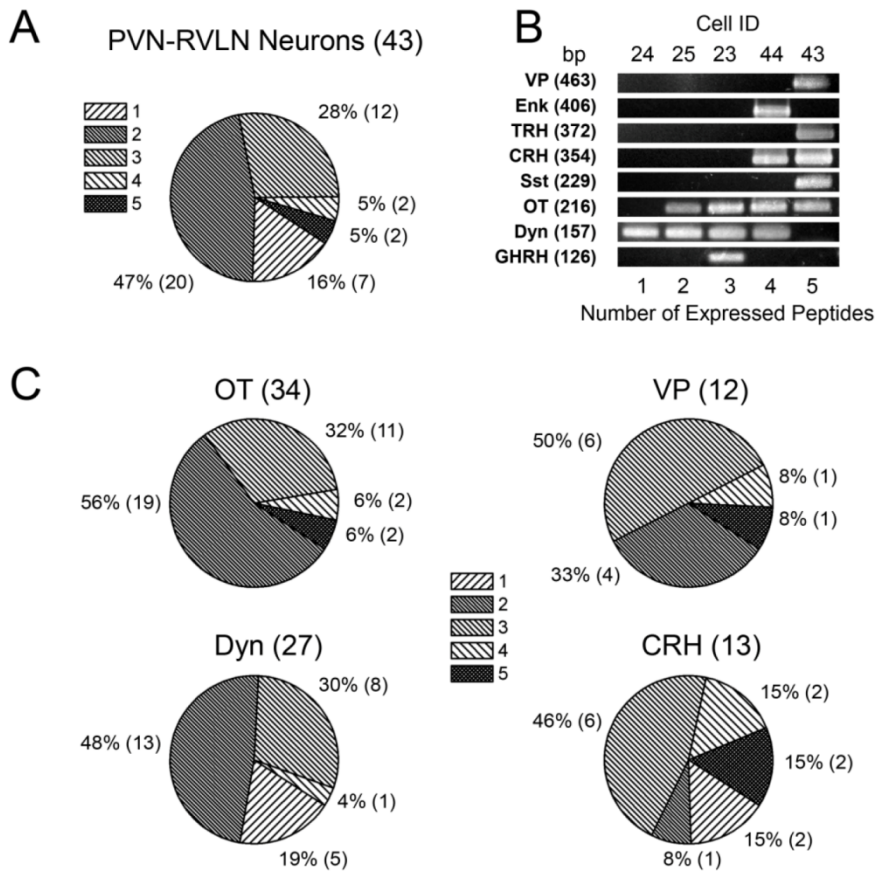


**Figure 3. Co-expression of peptides in PVN-RVLM neurons. A,** A pie graph representing the proportion of cells expressing one peptide, or two, three, four, or five different peptides in the PVN-RVLM neurons. **B,** Gel images of representative cells expressing one peptide or two, three, four, or five different peptides (cell ID: 24, 25, 23, 44, and 43, respectively). The number on the side of each peptide indicates the PCR product size (bp) for each peptide. **C,** Each pie graph represents the proportion of cells expressing one, two, three, four, or five peptides in peptide-positive neurons for OT, VP, Dyn, and CRH. Note that OT-neurons and VP-neurons always co-expressed other peptides. The number in parentheses (A and C) indicates the number of positive cells.

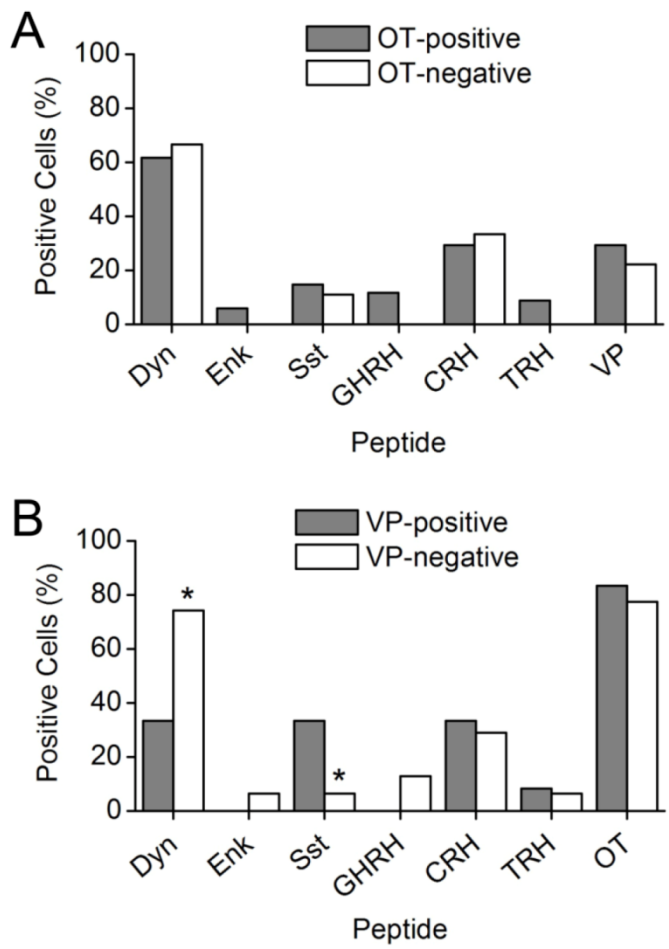


**Figure 4. Co-expression of peptides in the OT- and the VP-positive PVN-RVLM neurons. A,** Percentages of cells expressing each peptide in the OT-positive or the OT-negative cells. Dyn was most frequently detected in the OT-positive cells. Enk, Sst, GHRH, CRH, TRH, and VP were also expressed in the OT-positive cells. **B,** Percentages of cells expressing each peptide in the VP-positive or the VP-negative cells. OT was most frequently expressed by the VP-positive cells. Dyn, Sst, CRH, and TRH, except for Enk and GHRH, were detected in the VP-positive cells. Note that Dyn or Sst were differentially distributed between the VP-positive and the VP-negative cells (*$P$<0.05 by a chi-squared test).

negative cells, there were no significant differences for any of the peptides (Figure 4A). On the other hand, between the VP-positive and the VP-negative cells, there were significant differences for Dyn and Sst (Figure 4B, $P<0.05$ by a chi-squared test). Sst was more frequent in the VP-positive cells (33%, 4/12) than in the VP-negative cells (6%, 2/31). Conversely, Dyn was more frequently expressed in the VP-negative cells (74%, 23/31) than in the VP-positive cells (33%, 4/12).

# DISCUSSION

The PVN-RVLM neurons expressed several peptides. Among them, the large majority expressed OT (79%) and Dyn (63%). The PVN-RVLM neurons appeared to be dominantly distributed in the DC, the PaV, and the PaPo subdivisions (Stern and Zhang, 2003; Stocker et al., 2004). Each subdivision displayed distinct distributions for some peptides. The DC showed very rare VP expression compared to the other subdivisions, whereas the PaPo displayed very abundant OT expression. Such distributional characteristics of peptides were comparable to those examined from another autonomic-related PVN cell group that projects to the spinal cord (PVN-spinal) (Hallbeck et al., 2001). The PVN-spinal neurons showed expression for OT that was approximately twice lower (PVN-spinal: 38%, PVN-RVLM: 79%) and expression for Enk that was four times higher (PVN-spinal: 20%, PVN-RVLM: 5%) with respect to the percentage of cells positive for each peptide compared to the PVN-RVLM neurons. These differences between the PVN-RVLM neurons and the PVN-spinal neurons suggest that OT and Enk could be a biochemical specificity that distinguishes the two different cell populations, although there have been methodological differences that may account for these variations. On the other hand, the distributional patterns examined differentially among the subdivisions of the PVN-spinal neurons (Hallbeck et al., 2001) were similar to those of the PVN-RVLM neurons; there was greater expression of OT in the PaPo and extremely less expression of VP in the DC.

In addition to the distributional differences of peptides, most PVN-RVLM

neurons co-expressed multiple peptides. The possibility of co-expression of different peptides in autonomic-related PVN neurons has previously arisen (Hallbeck et al., 2001), but a direct observation has not yet been made. This study is the first study to examine co-expressions of multiple peptides in identified PVN-RVLM neurons directly by using analysis of single cells. Most PVN-RVLM neurons co-expressed multiple peptides rather than showed expression of only one peptide. Some of the cells co-expressed up to five different peptides, among the eight peptides examined. Such co-expression of multiple peptides is a general characteristic for hypothalamic endocrine neurons, including those in the PVN (Glasgow et al., 1999; Lee et al., 2012). This could be extended to the autonomic-related PVN neurons through the present study. Interestingly, some peptides prefer or avoid co-expression with a specific peptide in the PVN-RVLM neurons. For example, Sst was expressed more in the VP-positive neurons than in the VP-negative neurons. In contrast, Dyn was expressed significantly more in the VP-negative neurons than in the VP-positive neurons. However, the implication of these co-expressions needs to be investigated.

Accumulating reports have demonstrated that various peptides participate in the central regulation of cardiovascular and respiratory functions through the PVN-RVLM pathway. Administration of OT into the RVLM has been found to increase cardiovascular and respiratory activities; additionally, the blockade of OT receptors in the RVLM has been found to abolish PVN-induced cardiorespiratory activation (Mack et al., 2002; Mack et al., 2007). VP also has been found to mediate PVN-induced RVLM activities, and increased VP transmission in the PVN-RVLM pathway contributes to augmented cardiorespiratory outflows after

exposure to chronic intermittent hypoxia (Kc et al., 2010; Yang et al., 2001; Yang and Coote, 2003). A microinjection of CRH into the RVLM increased the arterial pressure, and CRH-like immunoreactive-terminals present in the RVLM have been shown to originate predominantly from the PVN (Milner et al., 1993). Administration of Dyn into the RVLM has been found to induce a decrease in blood pressure and heart rate (Punnen and Sapru, 1986), but, unlike OT, VP, and CRH, it is still unclear where the origin of active Dyn in the RVLM is. At this point, the observation regarding the prominent expression of prodynorphin mRNAs in the PVN-RVLM suggests that at least prodynorphin-derived peptides released on the RVLM are possible from the PVN. Enk's inhibitory effects on the activity of the RVLM have also been described previously (Hayar and Guyenet, 1998; Sun and Guyenet, 1989). The main source of this Enk is likely to be nuclei other than PVN, potentially the nucleus of the solitary tract that is responsible for the baroreflex responses (Morilak et al., 1989). The result presented here indicates that very few PVN-RVLM neurons express Enk, supporting this possibility. From this evidence, I speculated that each different opioid peptide might be employed as a specific signal mediator by different input into the RVLM, constituting a distinct signal pathway. Altogether, the peptides present in the PVN-RVLM neurons play a role as excitatory or inhibitory neurotransmitters in central regulatory signaling via the PVN-RVLM pathway that is involved in the cardiovascular and the respiratory system. In this regard, the observation that various peptides are present in the PVN-RVLM neurons, distributed differentially according to subdivisions, and co-expressed with different combinations from cell to cell suggests that peptides in the PVN-RVLM neurons contribute to specific and selective responses of the PVN to

various stimuli (Hallbeck et al., 2001), including water deprivation (Stocker et al., 2004), hypoxia (Kc et al., 2010), and hot temperatures (Cham and Badoer, 2008). As such, this could enable the PVN to maintain finer control of the regulation of cardiovascular and respiratory outflows.

# CONCLUSIONS

Several peptides are expressed in the PVN-RVLM neurons. Most PVN-RVLM neurons are oxytocinergic. OT and VP have differential distributions among subdivisions of the PVN-RVLM neurons, indicating that distinct peptide-coded PVN-RVLM neurons could be regionally segregated. The PVN-RVLM neurons preferred co-expression of multiple peptides to solo-expression, showing distinct peptidergic compositions from cell to cell. The PVN-RVLM neurons containing OT showed co-expression with Dyn, Enk, Sst, GHRH, CRH, TRH, and VP. The neurons containing VP displayed co-expression with Dyn, Sst, CRH, TRH, and OT. These differential expressions of various peptides among subdivisions of the PVN-RVLM neurons and among the cells may contribute to the specific and selective responses of the PVN to various stimuli, allowing fine control of cardiorespiratory outflows.

# GENERAL CONCLUSIONS

The PVN is an integrating site in the regulation of the endocrine and autonomic systems so that it is composed of heterogeneous cells that are functionally different. Because of such complex cell populations, single cell analysis is required for examination of gene expressions in specific PVN neurons, which were electrophysiologically or anatomically characterized. The PVN neurons express or co-express several Kv channel subunits and peptides. Among the Kv channel subunits, Kv4.2 and Kv4.3 are the most potential subunits responsible for the determination of electrophysiological characteristics of different cell types and involved in neuronal modulations occurred under pathophysiological or hormonal states. In addition, Kv4.2 and Kv4.3 are differentially or selectively regulated following heart failure or estrogen replacement, which suggests that $I_A$ can be molecularly dissected and that Kv4.2 and Kv4.3 play independent roles for $I_A$ under each specific regulatory mechanism. The regional selectivity shown in the estrogen-induced regulation of Kv4.2 suggests that the PVN may employ regionally clustered cells potentially participating in a specific peptide signaling, in response to a specific stimulus. Taken together, Kv4.2 and Kv4.3 are likely to cooperatively but differentially contribute to $I_A$ in the PVN, thereby participating in the coordination of specific and selective responses of the PVN to various types of stimuli.

To more clearly understand the physiological roles of the PVN comprising heterogeneous cells, it is important to classify PVN neurons according to their

functions and identify the neuronal properties and specificity. In this regard, the present study provides important evidence of the identification of the critical molecular components responsible for the neuronal properties and modulations in the single PVN neurons specified by electrophysiological or anatomical properties, which is helpful for more deeply understanding the functional roles of the PVN.

# REFERENCES


Akaishi, T., Sakuma, Y., 1985. Estrogen excites oxytocinergic, but not vasopressinergic cells in the paraventricular nucleus of female rat hypothalamus. Brain Res. 335**,** 302-5.

Allen, A.M., 2002. Inhibition of the hypothalamic paraventricular nucleus in spontaneously hypertensive rats dramatically reduces sympathetic vasomotor tone. Hypertension. 39**,** 275-80.

Alves, S.E., Lopez, V., McEwen, B.S., Weiland, N.G., 1998. Differential colocalization of estrogen receptor beta (ERbeta) with oxytocin and vasopressin in the paraventricular and supraoptic nuclei of the female rat brain: an immunocytochemical study. Proc Natl Acad Sci U S A. 95**,** 3281-6.

Anderson, D., Mehaffey, W.H., Iftinca, M., Rehak, R., Engbers, J.D., Hameed, S., Zamponi, G.W., Turner, R.W., 2010. Regulation of neuronal activity by Cav3-Kv4 channel signaling complexes. Nat Neurosci. 13**,** 333-7.

Armstrong, W.E., Warach, S., Hatton, G.I., McNeill, T.H., 1980. Subnuclei in the rat hypothalamic paraventricular nucleus: a cytoarchitectural, horseradish peroxidase and immunocytochemical analysis. Neuroscience. 5**,** 1931-58.

Armstrong, W.E., Stern, J.E., Teruyama, R., 2002. Plasticity in the electrophysiological properties of oxytocin neurons. Microsc Res Tech. 56**,** 73-80.

Arroyo, A., Kim, B.S., Biehl, A., Yeh, J., Bett, G.C., 2011. Expression of Kv4. 3 Voltage-Gated Potassium Channels in Rat Gonadotrophin-Releasing Hormone (GnRH) Neurons During the Estrous Cycle. Reprod Sci. 18**,** 136-144.

Badoer, E., 2001. Hypothalamic paraventricular nucleus and cardiovascular regulation. Clin Exp Pharmacol Physiol. 28**,** 95-9.

Baldwin, T.J., Tsaur, M.L., Lopez, G.A., Jan, Y.N., Jan, L.Y., 1991. Characterization of a mammalian cDNA for an inactivating voltage-

sensitive K+ channel. Neuron. 7**,** 471-83.

Baxter, D., Byrne, J., 1991. Ionic conductance mechanisms contributing to the electrophysiological properties of neurons. Curr Opin Neurobiol. 1**,** 105-112.

Beer, S., Reincke, M., Kral, M., Callies, F., Stromer, H., Dienesch, C., Steinhauer, S., Ertl, G., Allolio, B., Neubauer, S., 2007. High-dose 17beta-estradiol treatment prevents development of heart failure post-myocardial infarction in the rat. Basic Res Cardiol. 102**,** 9-18.

Bicknell, R.J., Leng, G., 1981. Relative efficiency of neural firing patterns for vasopressin release in vitro. Neuroendocrinology. 33**,** 295-9.

Birnbaum, S., Varga, A., Yuan, L., Anderson, A., Sweatt, J., Schrader, L., 2004. Structure and function of Kv4-family transient potassium channels. Physiol Rev. 84**,** 803.

Blair, M.L., Piekut, D., Want, A., Olschowka, J.A., 1996. Role of the hypothalamic paraventricular nucleus in cardiovascular regulation. Clin Exp Pharmacol Physiol. 23**,** 161-5.

Bosch, M.A., Kelly, M.J., Ronnekleiv, O.K., 2002. Distribution, neuronal colocalization, and 17beta-E2 modulation of small conductance calcium-activated K(+) channel (SK3) mRNA in the guinea pig brain. Endocrinology. 143**,** 1097-107.

Bosch, M.A., Hou, J., Fang, Y., Kelly, M.J., Ronnekleiv, O.K., 2009. 17Beta-estradiol regulation of the mRNA expression of T-type calcium channel subunits: role of estrogen receptor alpha and estrogen receptor beta. J Comp Neurol. 512**,** 347-58.

Buller, K.M., Day, T.A., 2000. Opposite effects of short and continuous oestradiol replacement on CNS responses to hypoxic stress. Neuroreport. 11**,** 2243-2246.

Carrasquillo, Y., Burkhalter, A., Nerbonne, J.M., 2012. A-type K+ channels encoded by Kv4.2, Kv4.3 and Kv1.4 differentially regulate intrinsic excitability of cortical pyramidal neurons. J Physiol. 590**,** 3877-3890.

Carrasquillo, Y., Nerbonne, J.M., 2013. IA Channels: Diverse Regulatory Mechanisms. Neuroscientist.

Cham, J.L., Badoer, E., 2008. Exposure to a hot environment can activate rostral ventrolateral medulla-projecting neurones in the hypothalamic paraventricular nucleus in conscious rats. Exp Physiol. 93**,** 64-74.

Chen, Q.H., Toney, G.M., 2009. Excitability of paraventricular nucleus neurones that project to the rostral ventrolateral medulla is regulated by small-conductance Ca2+-activated K+ channels. J Physiol. 587**,** 4235-47.

Chen, Q.H., Andrade, M.A., Calderon, A.S., Toney, G.M., 2010. Hypertension induced by angiotensin II and a high salt diet involves reduced SK current and increased excitability of RVLM projecting PVN neurons. J Neurophysiol. 104**,** 2329-37.

Chen, Q.H., Toney, G.M., 2010. In vivo discharge properties of hypothalamic paraventricular nucleus neurons with axonal projections to the rostral ventrolateral medulla. J Neurophysiol. 103**,** 4-15.

Christie, M.J., North, R.A., Osborne, P.B., Douglass, J., Adelman, J.P., 1990. Heteropolymeric potassium channels expressed in Xenopus oocytes from cloned subunits. Neuron. 4**,** 405-11.

Chung, Y.H., Kim, H.S., Shin, C.M., Kim, M.J., Cha, C.I., 2001. Immunohistochemical study on the distribution of voltage-gated K(+) channels in rat brain following transient focal ischemia. Neurosci Lett. 308**,** 157-60.

Clegg, D.J., 2012. Minireview: The Year in Review of Estrogen Regulation of Metabolism. Mol Endocrinol. 26**,** 1957-1960.

Coetzee, W.A., Amarillo, Y., Chiu, J., Chow, A., Lau, D., McCormack, T., Moreno, H., Nadal, M.S., Ozaita, A., Pountney, D., Saganich, M., Vega-Saenz de Miera, E., Rudy, B., 1999. Molecular diversity of K+ channels. Ann N Y Acad Sci. 868**,** 233-85.

Coote, J.H., 1995. Cardiovascular function of the paraventricular nucleus of the hypothalamus. Biol Signals. 4**,** 142-9.

Coote, J.H., Yang, Z., Pyner, S., Deering, J., 1998. Control of sympathetic outflows by the hypothalamic paraventricular nucleus. Clin Exp Pharmacol Physiol. 25**,** 461-3.

Covarrubias, M., Wei, A.A., Salkoff, L., 1991. Shaker, Shal, Shab, and Shaw

express independent K+ current systems. Neuron. 7**,** 763-73.

Dampney, R.A., 1994. Functional organization of central pathways regulating the cardiovascular system. Physiol Rev. 74**,** 323-64.

DeFazio, R., Moenter, S., 2002. Estradiol feedback alters potassium currents and firing properties of gonadotropin-releasing hormone neurons. Mol Endocrinol. 16**,** 2255.

Deroo, B.J., Buensuceso, A.V., 2010. Minireview: Estrogen receptor-beta: mechanistic insights from recent studies. Mol Endocrinol. 24**,** 1703-14.

Di, S., Malcher-Lopes, R., Halmos, K.C., Tasker, J.G., 2003. Nongenomic glucocorticoid inhibition via endocannabinoid release in the hypothalamus: a fast feedback mechanism. J Neurosci. 23**,** 4850-7.

Dutton, A., Dyball, R.E., 1979. Phasic firing enhances vasopressin release from the rat neurohypophysis. J Physiol. 290**,** 433-40.

Eghbali, M., Deva, R., Alioua, A., Minosyan, T.Y., Ruan, H., Wang, Y., Toro, L., Stefani, E., 2005. Molecular and functional signature of heart hypertrophy during pregnancy. Circ Res. 96**,** 1208-16.

Farkas, I., Varju, P., Liposits, Z., 2007. Estrogen modulates potassium currents and expression of the Kv4.2 subunit in GT1-7 cells. Neurochem Int. 50**,** 619-27.

Fatehi, M., Zidichouski, J.A., Kombian, S.B., Saleh, T.M., 2006. 17beta-estradiol attenuates excitatory neurotransmission and enhances the excitability of rat parabrachial neurons in vitro. J Neurosci Res. 84**,** 666-74.

Gao, L., Li, Y., Schultz, H.D., Wang, W.Z., Wang, W., Finch, M., Smith, L.M., Zucker, I.H., 2010. Downregulated Kv4.3 expression in the RVLM as a potential mechanism for sympathoexcitation in rats with chronic heart failure. Am J Physiol Heart Circ Physiol. 298**,** H945-55.

Gerrits, M., Grootkarijn, A., Bekkering, B.F., Bruinsma, M., Den Boer, J.A., Ter Horst, G.J., 2005. Cyclic estradiol replacement attenuates stress-induced c-Fos expression in the PVN of ovariectomized rats. Brain Res Bull. 67**,** 147-55.

Glasgow, E., Kusano, K., Chin, H., Mezey, E., Young, W.S., 3rd., Gainer, H., 1999. Single cell reverse transcription-polymerase chain reaction analysis of rat supraoptic magnocellular neurons: neuropeptide phenotypes and high

voltage-gated calcium channel subtypes. Endocrinology. 140, 5391-401.

Griffith, W.H., Han, S.-H., McCool, B.A., Murchison, D., 2006. Molecules and membrane activity: single-cell RT-PCR and patch-clamp recording from central neurons. In Neuroanatomical Tract-Tracing 3. Vol., ed.^eds. Springer, pp. 142-174.

Grossman, C.J., 1985. Interactions between the gonadal steroids and the immune system. Science. 227, 257-261.

Guan, D., Lee, J.C., Tkatch, T., Surmeier, D.J., Armstrong, W.E., Foehring, R.C., 2006. Expression and biophysical properties of Kv1 channels in supragranular neocortical pyramidal neurones. J Physiol. 571, 371-89.

Gutman, G.A., Chandy, K.G., Grissmer, S., Lazdunski, M., Mckinnon, D., Pardo, L.A., Robertson, G.A., Rudy, B., Sanguinetti, M.C., Stühmer, W., 2005. International Union of Pharmacology. LIII. Nomenclature and molecular relationships of voltage-gated potassium channels. Pharmacol Rev. 57, 473-508.

Hallbeck, M., Larhammar, D., Blomqvist, A., 2001. Neuropeptide expression in rat paraventricular hypothalamic neurons that project to the spinal cord. J Comp Neurol. 433, 222-38.

Han, S.K., Chong, W., Li, L.H., Lee, I.S., Murase, K., Ryu, P.D., 2002. Noradrenaline excites and inhibits GABAergic transmission in parvocellular neurons of rat hypothalamic paraventricular nucleus. J Neurophysiol. 87, 2287-96.

Han, T.H., Lee, K., Park, J.B., Ahn, D., Park, J.H., Kim, D.Y., Stern, J.E., Lee, S.Y., Ryu, P.D., 2010. Reduction in synaptic GABA release contributes to target-selective elevation of PVN neuronal activity in rats with myocardial infarction. Am J Physiol Regul Integr Comp Physiol. 299, R129-139.

Hayar, A., Guyenet, P.G., 1998. Pre- and postsynaptic inhibitory actions of methionine-enkephalin on identified bulbospinal neurons of the rat RVL. J Neurophysiol. 80, 2003-14.

Heinemann, S.H., Rettig, J., Graack, H.R., Pongs, O., 1996. Functional characterization of Kv channel beta-subunits from rat brain. J Physiol. 493 ( Pt 3), 625-33.

Hille, B., 2001. Ion channels of excitable membranes. Vol. 507, Sinauer Sunderland, MA.

Hoffman, N.W., Tasker, J.G., Dudek, F.E., 1991. Immunohistochemical differentiation of electrophysiologically defined neuronal populations in the region of the rat hypothalamic paraventricular nucleus. J Comp Neurol. 307**,** 405-16.

Hrabovszky, E., Kallo, I., Hajszan, T., Shughrue, P.J., Merchenthaler, I., Liposits, Z., 1998. Expression of estrogen receptor-beta messenger ribonucleic acid in oxytocin and vasopressin neurons of the rat supraoptic and paraventricular nuclei. Endocrinology. 139**,** 2600-4.

Huang, H.Y., Liao, C.W., Chen, P.H., Tsaur, M.L., 2006. Transient expression of A-type K channel alpha subunits Kv4.2 and Kv4.3 in rat spinal neurons during development. Eur J Neurosci. 23**,** 1142-50.

Jerng, H., Pfaffinger, P., Covarrubias, M., 2004. Molecular physiology and modulation of somatodendritic A-type potassium channels. Mol Cell Neurosci. 27**,** 343-369.

Kandel, E.R., Schwartz, J.H., Jessell, T.M., 2000. Principles of Neural Science. Vol., McGraw-Hill, New York.

Kannan, H., Niijima, A., Yamashita, H., 1988. Effects of stimulation of the hypothalamic paraventricular nucleus on blood pressure and renal sympathetic nerve activity. Brain Res Bull. 20**,** 779-83.

Kannel, W.B., Hjortland, M.C., McNamara, P.M., Gordon, T., 1976. Menopause and risk of cardiovascular disease: the Framingham study. Ann Intern Med. 85**,** 447-52.

Kaprielian, R., Wickenden, A.D., Kassiri, Z., Parker, T.G., Liu, P.P., Backx, P.H., 1999. Relationship between K+ channel down-regulation and [Ca2+]i in rat ventricular myocytes following myocardial infarction. J Physiol. 517 ( Pt 1)**,** 229-45.

Kc, P., Balan, K.V., Tjoe, S.S., Martin, R.J., Lamanna, J.C., Haxhiu, M.A., Dick, T.E., 2010. Increased vasopressin transmission from the paraventricular nucleus to the rostral medulla augments cardiorespiratory outflow in chronic intermittent hypoxia-conditioned rats. J Physiol. 588**,** 725-40.

Kisley, L.R., Sakai, R.R., Flanagan-Cato, L.M., Fluharty, S.J., 2000. Estrogen increases angiotensin II-induced c-Fos expression in the vasopressinergic neurons of the paraventricular nucleus in the female rat. Neuroendocrinology. 72**,** 306-17.

Lee, S., Han, T.H., Sonner, P.M., Stern, J.E., Ryu, P.D., Lee, S.Y., 2008. Molecular characterization of T-type Ca(2+) channels responsible for low threshold spikes in hypothalamic paraventricular nucleus neurons. Neuroscience. 155**,** 1195-203.

Lee, S.K., Lee, S., Shin, S.Y., Ryu, P.D., Lee, S.Y., 2012. Single cell analysis of voltage-gated potassium channels that determines neuronal types of rat hypothalamic paraventricular nucleus neurons. Neuroscience. 205**,** 49-62.

Lee, S.K., Ryu, P.D., Lee, S.Y., 2013a. Estrogen replacement modulates voltage-gated potassium channels in rat presympathetic paraventricular nucleus neurons. BMC neuroscience. 14**,** 134.

Lee, S.K., Ryu, P.D., Lee, S.Y., 2013b. Differential distributions of neuropeptides in hypothalamic paraventricular nucleus neurons projecting to the rostral ventrolateral medulla in the rat. Neuroscience Letters. 556**,** 160-165.

Levin, E.R., 1999. Cellular Functions of the Plasma Membrane Estrogen Receptor. Trends Endocrinol Metab. 10**,** 374-377.

Levitan, E., Takimoto, K., 1998. Dynamic regulation of K+ channel gene expression in differentiated cells. J Neurobiol. 37**,** 60-68.

Li, X., Tang, K., Xie, B., Li, S., Rozanski, G.J., 2008. Regulation of Kv4 channel expression in failing rat heart by the thioredoxin system. Am J Physiol Heart Circ Physiol. 295**,** H416-24.

Li, Y.F., Jackson, K.L., Stern, J.E., Rabeler, B., Patel, K.P., 2006. Interaction between glutamate and GABA systems in the integration of sympathetic outflow by the paraventricular nucleus of the hypothalamus. Am J Physiol Heart Circ Physiol. 291**,** H2847-56.

Li, Z., Ferguson, A.V., 1996. Electrophysiological properties of paraventricular magnocellular neurons in rat brain slices: modulation of IA by angiotensin II. Neuroscience. 71**,** 133-45.

Liss, B., Bruns, R., Roeper, J., 1999. Alternative sulfonylurea receptor expression

defines metabolic sensitivity of K-ATP channels in dopaminergic midbrain neurons. EMBO J. 18**,** 833-846.

Liss, B., Franz, O., Sewing, S., Bruns, R., Neuhoff, H., Roeper, J., 2001. Tuning pacemaker frequency of individual dopaminergic neurons by Kv4.3L and KChip3.1 transcription. EMBO J. 20**,** 5715-24.

Liss, B., 2002. Improved quantitative real-time RT–PCR for expression profiling of individual cells. Nucleic Acids Res. 30**,** e89-e89.

Livak, K.J., Schmittgen, T.D., 2001. Analysis of Relative Gene Expression Data Using Real-Time Quantitative PCR and the 2-[Delta][Delta]CT Method. Methods. 25**,** 402-408.

Llinas, R., 1988. The intrinsic electrophysiological properties of mammalian neurons: insights into central nervous system function. Science. 242**,** 1654-1664.

Luther, J.A., Halmos, K.C., Tasker, J.G., 2000. A slow transient potassium current expressed in a subset of neurosecretory neurons of the hypothalamic paraventricular nucleus. J Neurophysiol. 84**,** 1814-25.

Luther, J.A., Tasker, J.G., 2000. Voltage-gated currents distinguish parvocellular from magnocellular neurones in the rat hypothalamic paraventricular nucleus. J Physiol. 523**,** 193-209.

Luther, J.A., Daftary, S.S., Boudaba, C., Gould, G.C., Halmos, K.C., Tasker, J.G., 2002. Neurosecretory and non-neurosecretory parvocellular neurones of the hypothalamic paraventricular nucleus express distinct electrophysiological properties. J Neuroendocrinol. 14**,** 929-32.

Mack, S.O., Kc, P., Wu, M., Coleman, B.R., Tolentino-Silva, F.P., Haxhiu, M.A., 2002. Paraventricular oxytocin neurons are involved in neural modulation of breathing. J Appl Physiol. 92**,** 826-34.

Mack, S.O., Wu, M., Kc, P., Haxhiu, M.A., 2007. Stimulation of the hypothalamic paraventricular nucleus modulates cardiorespiratory responses via oxytocinergic innervation of neurons in pre-Botzinger complex. J Appl Physiol. 102**,** 189-99.

MacKinnon, R., 1991. Determination of the subunit stoichiometry of a voltage-

activated potassium channel. Nature. 350, 232-5.

McEwen, B.S., 2001. Invited review: Estrogens effects on the brain: multiple sites and molecular mechanisms. J Appl Physiol. 91, 2785-801.

Mendelsohn, M.E., Karas, R.H., 1999. The protective effects of estrogen on the cardiovascular system. N Engl J Med. 340, 1801-11.

Milner, T.A., Reis, D.J., Pickel, V.M., Aicher, S.A., Giuliano, R., 1993. Ultrastructural localization and afferent sources of corticotropin-releasing factor in the rat rostral ventrolateral medulla: implications for central cardiovascular regulation. J Comp Neurol. 333, 151-67.

Morilak, D.A., Somogyi, P., McIlhinney, R.A., Chalmers, J., 1989. An enkephalin-containing pathway from nucleus tractus solitarius to the pressor area of the rostral ventrolateral medulla of the rabbit. Neuroscience. 31, 187-94.

Nerbonne, J.M., Gerber, B.R., Norris, A., Burkhalter, A., 2008. Electrical remodelling maintains firing properties in cortical pyramidal neurons lacking KCND2-encoded A-type K+ currents. J Physiol. 586, 1565-79.

Nilsson, S., Makela, S., Treuter, E., Tujague, M., Thomsen, J., Andersson, G., Enmark, E., Pettersson, K., Warner, M., Gustafsson, J.A., 2001. Mechanisms of estrogen action. Physiol Rev. 81, 1535-65.

Nishiyama, A., Kambe, F., Kamiya, K., Seo, H., Toyama, J., 1998. Effects of thyroid status on expression of voltage-gated potassium channels in rat left ventricle. Cardiovasc Res. 40, 343-351.

Norris, A.J., Nerbonne, J.M., 2010. Molecular dissection of I(A) in cortical pyramidal neurons reveals three distinct components encoded by Kv4.2, Kv4.3, and Kv1.4 alpha-subunits. J Neurosci. 30, 5092-101.

Ohbuchi, T., Yokoyama, T., Saito, T., Suzuki, H., Fujihara, H., Katoh, A., Otsubo, H., Ishikura, T., Ueta, Y., 2010. Modulators of BK and SK channels alter electrical activity in vitro in single vasopressin neurons isolated from the rat supraoptic nucleus. Neurosci Lett. 484, 26-9.

Parducz, A., Perez, J., Garcia-Segura, L.M., 1993. Estradiol induces plasticity of gabaergic synapses in the hypothalamus. Neuroscience. 53, 395-401.

Patel, K.P., Zhang, K., 1996. Neurohumoral activation in heart failure: role of paraventricular nucleus. Clin Exp Pharmacol Physiol. 23, 722-6.

Pfaffl, M.W., 2001. A new mathematical model for relative quantification in real-time RT-PCR. Nucleic Acids Res. 29**,** e45-50.

Po, S., Roberds, S., Snyders, D.J., Tamkun, M.M., Bennett, P.B., 1993. Heteromultimeric assembly of human potassium channels. Molecular basis of a transient outward current? Circ Res. 72**,** 1326-36.

Porter, J.P., Brody, M.J., 1985. Neural projections from paraventricular nucleus that subserve vasomotor functions. Am J Physiol. 248**,** R271-81.

Porter, J.P., Brody, M.J., 1986. A comparison of the hemodynamic effects produced by electrical stimulation of subnuclei of the paraventricular nucleus. Brain Res. 375**,** 20-9.

Poulain, D.A., Wakerley, J.B., 1982. Electrophysiology of hypothalamic magnocellular neurones secreting oxytocin and vasopressin. Neuroscience. 7**,** 773-808.

Punnen, S., Sapru, H.N., 1986. Cardiovascular responses to medullary microinjections of opiate agonists in urethane-anesthetized rats. J Cardiovasc Pharmacol. 8**,** 950-956.

Pyner, S., Coote, J.H., 2000. Identification of branching paraventricular neurons of the hypothalamus that project to the rostroventrolateral medulla and spinal cord. Neuroscience. 100**,** 549-56.

Qiu, J., Bosch, M.A., Jamali, K., Xue, C., Kelly, M.J., Ronnekleiv, O.K., 2006. Estrogen upregulates T-type calcium channels in the hypothalamus and pituitary. J Neurosci. 26**,** 11072-82.

Rettig, J., Heinemann, S.H., Wunder, F., Lorra, C., Parcej, D.N., Dolly, J.O., Pongs, O., 1994. Inactivation properties of voltage-gated K+ channels altered by presence of beta-subunit. Nature. 369**,** 289-94.

Roepke, T., Malyala, A., Bosch, M., Kelly, M., Ronnekleiv, O., 2007. Estrogen regulation of genes important for K+ channel signaling in the arcuate nucleus. Endocrinology. 148**,** 4937-4951.

Rogawski, M.A., 1985. The A-current: how ubiquitous a feature of excitable cells is it? Trends in Neurosciences. 8**,** 214-219.

Rozen, S., Skaletsky, H., 2000. Primer3 on the WWW for general users and for biologist programmers. Methods Mol Biol. 132**,** 365-86.

Rudy, B., 1988. Diversity and ubiquity of K channels. Neuroscience. 25**,** 729-49.

Rudy, B., Hoger, J.H., Lester, H.A., Davidson, N., 1988. At least two mRNA species contribute to the properties of rat brain A-type potassium channels expressed in Xenopus oocytes. Neuron. 1**,** 649-58.

Saito, T., Ciobotaru, A., Bopassa, J.C., Toro, L., Stefani, E., Eghbali, M., 2009. Estrogen contributes to gender differences in mouse ventricular repolarization. Circ Res. 105**,** 343-52.

Sawchenko, P.E., Swanson, L.W., 1982. Immunohistochemical identification of neurons in the paraventricular nucleus of the hypothalamus that project to the medulla or to the spinal cord in the rat. J Comp Neurol. 205**,** 260-72.

Schrader, L.A., Tasker, J.G., 1997. Modulation of multiple potassium currents by metabotropic glutamate receptors in neurons of the hypothalamic supraoptic nucleus. J Neurophysiol. 78**,** 3428-37.

Serodio, P., Kentros, C., Rudy, B., 1994. Identification of molecular components of A-type channels activating at subthreshold potentials. J Neurophysiol. 72**,** 1516.

Serodio, P., Vega-Saenz de Miera, E., Rudy, B., 1996. Cloning of a novel component of A-type K+ channels operating at subthreshold potentials with unique expression in heart and brain. J Neurophysiol. 75**,** 2174-9.

Serodio, P., Rudy, B., 1998. Differential expression of Kv4 K+ channel subunits mediating subthreshold transient K+ (A-type) currents in rat brain. J Neurophysiol. 79**,** 1081-91.

Shibata, R., Nakahira, K., Shibasaki, K., Wakazono, Y., Imoto, K., Ikenaka, K., 2000. A-type K+ current mediated by the Kv4 channel regulates the generation of action potential in developing cerebellar granule cells. J Neurosci. 20**,** 4145-4155.

Shughrue, P.J., Lane, M.V., Merchenthaler, I., 1997. Comparative distribution of estrogen receptor-alpha and -beta mRNA in the rat central nervous system. J Comp Neurol. 388**,** 507-25.

Simmons, D.M., Swanson, L.W., 2009. Comparison of the spatial distribution of seven types of neuroendocrine neurons in the rat paraventricular nucleus: toward a global 3D model. J Comp Neurol. 516**,** 423-41.

Simonian, S.X., Herbison, A.E., 1997. Differential expression of estrogen receptor alpha and beta immunoreactivity by oxytocin neurons of rat paraventricular nucleus. J Neuroendocrinol. 9**,** 803-6.

Song, M., Helguera, G., Eghbali, M., Zhu, N., Zarei, M.M., Olcese, R., Toro, L., Stefani, E., 2001. Remodeling of Kv4.3 potassium channel gene expression under the control of sex hormones. J Biol Chem. 276**,** 31883-90.

Sonner, P.M., Stern, J.E., 2007. Functional role of A-type potassium currents in rat presympathetic PVN neurones. J Physiol. 582**,** 1219-38.

Sonner, P.M., Filosa, J.A., Stern, J.E., 2008. Diminished A-type potassium current and altered firing properties in presympathetic PVN neurones in renovascular hypertensive rats. J Physiol. 586**,** 1605-22.

Sonner, P.M., Lee, S., Ryu, P.D., Lee, S.Y., Stern, J.E., 2011. Imbalanced K+ and Ca2+ subthreshold interactions contribute to increased hypothalamic presympathetic neuronal excitability in hypertensive rats. J Physiol. 589**,** 667-83.

Stern, J.E., 2001. Electrophysiological and morphological properties of pre-autonomic neurones in the rat hypothalamic paraventricular nucleus. J Physiol. 537**,** 161-77.

Stern, J.E., Zhang, W., 2003. Preautonomic neurons in the paraventricular nucleus of the hypothalamus contain estrogen receptor beta. Brain Res. 975**,** 99-109.

Stocker, S.D., Cunningham, J.T., Toney, G.M., 2004. Water deprivation increases Fos immunoreactivity in PVN autonomic neurons with projections to the spinal cord and rostral ventrolateral medulla. Am J Physiol Regul Integr Comp Physiol. 287**,** R1172-83.

Sun, M.K., Guyenet, P.G., 1989. Effects of vasopressin and other neuropeptides on rostral medullary sympathoexcitatory neurons 'in vitro'. Brain Res. 492**,** 261-70.

Suzuki, T., Takimoto, K., 2005. Differential expression of Kv4 pore-forming and KChIP auxiliary subunits in rat uterus during pregnancy. Am J Physiol Endocrinol Metab. 288**,** E335-E341.

Swanson, L.W., Kuypers, H.G., 1980. The paraventricular nucleus of the

hypothalamus: cytoarchitectonic subdivisions and organization of projections to the pituitary, dorsal vagal complex, and spinal cord as demonstrated by retrograde fluorescence double-labeling methods. J Comp Neurol. 194**,** 555-70.

Swanson, L.W., Sawchenko, P.E., 1980. Paraventricular nucleus: a site for the integration of neuroendocrine and autonomic mechanisms. Neuroendocrinology. 31**,** 410-7.

Swanson, L.W., Sawchenko, P.E., 1983. Hypothalamic integration: organization of the paraventricular and supraoptic nuclei. Annu Rev Neurosci. 6**,** 269-324.

Tasker, J.G., Dudek, F.E., 1991. Electrophysiological properties of neurones in the region of the paraventricular nucleus in slices of rat hypothalamus. J Physiol. 434**,** 271-93.

Timpe, L.C., Jan, Y.N., Jan, L.Y., 1988. Four cDNA clones from the Shaker locus of Drosophila induce kinetically distinct A-type potassium currents in Xenopus oocytes. Neuron. 1**,** 659-67.

van Eickels, M., Grohe, C., Cleutjens, J.P., Janssen, B.J., Wellens, H.J., Doevendans, P.A., 2001. 17beta-estradiol attenuates the development of pressure-overload hypertrophy. Circulation. 104**,** 1419-23.

Wamsteeker, J.I., Bains, J.S., 2010. A synaptocentric view of the neuroendocrine response to stress. Eur J Neurosci. 32**,** 2011-21.

Xu, B., Zheng, H., Patel, K.P., 2012. Enhanced activation of RVLM-projecting PVN neurons in rats with chronic heart failure. Am J Physiol Heart Circ Physiol. 302**,** H1700-11.

Xu, H., Dixon, J.E., Barry, D.M., Trimmer, J.S., Merlie, J.P., McKinnon, D., Nerbonne, J.M., 1996. Developmental analysis reveals mismatches in the expression of K+ channel alpha subunits and voltage-gated K+ channel currents in rat ventricular myocytes. J Gen Physiol. 108**,** 405-19.

Yang, Z., Coote, J.H., 1998. Influence of the hypothalamic paraventricular nucleus on cardiovascular neurones in the rostral ventrolateral medulla of the rat. J Physiol. 513 (Pt 2)**,** 521-30.

Yang, Z., Bertram, D., Coote, J.H., 2001. The role of glutamate and vasopressin in the excitation of RVL neurones by paraventricular neurones. Brain Res.

908, 99-103.

Yang, Z., Coote, J.H., 2003. The influence of vasopressin on tonic activity of cardiovascular neurones in the ventrolateral medulla of the hypertensive rat. Auton Neurosci. 104, 83-7.

Zhang, C., Bosch, M.A., Rick, E.A., Kelly, M.J., Ronnekleiv, O.K., 2009. 17Beta-estradiol regulation of T-type calcium channels in gonadotropin-releasing hormone neurons. J Neurosci. 29, 10552-62.

Zhang, T.T., Takimoto, K., Stewart, A.F., Zhu, C., Levitan, E.S., 2001. Independent regulation of cardiac Kv4.3 potassium channel expression by angiotensin II and phenylephrine. Circ Res. 88, 476-82.

Zhu, G.Q., Gao, L., Patel, K.P., Zucker, I.H., Wang, W., 2004. ANG II in the paraventricular nucleus potentiates the cardiac sympathetic afferent reflex in rats with heart failure. J Appl Physiol. 97, 1746-54.

# ABSTRACT IN KOREAN

## 국문초록

# 시상하부 뇌실곁핵 세포의 전기생리학적 활성을 조절하는 전압의존성 $K^+$ 통로의 분자생물학적 특성


**이 슬 기**

**서울대학교 대학원**

**협동과정 뇌과학전공**

**(지도교수: 류판동)**



시상하부에 존재하는 뇌실곁핵(hypothalamic paraventricular nucleus; PVN)은 구조적으로 또는 기능적으로 구별되는 이질적인 세포들로 이루어져 있다. 이들 세포들의 전기생리학적 특성과 A-type $K^+$ 전류($I_A$)의 관련성은 잘 알려져 있지만, 그 분자적 특성에 대해서는 밝혀진 바가 없다. 따라서, 본 연구에서는 $I_A$를 인코딩하는 전압의존성 $K^+$ 통로(voltage-gated $K^+$ channel; Kv 통로)가 PVN의 전리생리학적인 특성에 관여할 것이라고 가정하고, 성격이 다른 세포 형태(type I, type II)에서의 Kv 통로 발현차이와, 심부전이나 에스트로겐에 의해 그 활성이 변화하는 교감신경조절세포에서의 Kv 통로 발현변화를 살펴보고자 하였다. PVN에서 특정 세포에서의 분자적 정보를 얻기 위해, 단일세포 역전사-중합효소연쇄반응법(single cell reverse transcription-polymerase chain reaction; single cell RT-PCR) 또는 단일세포 실시간 역전사-중합효소연쇄반응법 (single cell real-time RT-PCR)을 실시하였다.

그 결과, type I, type II 모두에서 다양한 Kv 채널 subunit들의

발현이 관찰되었는데 그 중, Kv4.2와 Kv4.3은 그 발현 정도에 있어서 type II에서보다 type I에서 유의적으로 높게 나타났다. 교감신경조절세포에서도 Kv4.2와 Kv4.3의 발현이 관찰되었는데, 심부전 유발에 따라 그 발현이 다르게 조절되었다. Kv4.2는 증가되고 Kv4.3은 감소되었다. 반면 에스트로겐에 의해서는 Kv4.2만이 선택적으로 감소되었으며 Kv4.3은 변화가 없었다. 또한 $I_A$ 의 감소도 함께 관찰되었다. 이러한 에스트로겐의 영향은 바소프레신이 특이적으로 적게 분포되어 있는 dorsal cap 영역에서만 관찰되었다.

위의 연구결과는 Kv4.2와 Kv4.3이 PVN의 type I, type II를 구별하고 교감신경조절세포의 전기생리학적 활성을 조절하는 데 주요하게 작용하며, 질병이나 호르몬 변화에 의해 서로 독립적으로 조절되고 있음을 보여준다. 따라서, Kv 통로는 자율신경계와 내분비계의 기능 이상에 따른 PVN의 신경전달 변화에 참여하는 하나의 기전으로 여겨진다.

---

주요어: 단일세포분석, 시상하부 뇌실곁핵, 전압의존성 $K^+$ 통로, A-type $K^+$ 전류, 전기생리학적 활성, 유전자 발현

**학번: 2008-20475**